



University of Salerno

Department of Civil Engineering

PhD Course in

Risk and Sustainability in Civil, Architecture and Environmental Engineering Systems
Advanced technologies, Infrastructures and territorial sustainable development

XXXIII Cycle

A.A. 2020/2021

How Sustainable Drainage Systems may improve city resilience: Experimental insights, Urban design modeling and performance assessment at the catchment scale

Candidate:

Roberta D'Ambrosio

Handwritten signature of Roberta D'Ambrosio in black ink.

Supervisor:

Professor Antonia Longobardi

Handwritten signature of Antonia Longobardi in black ink.

PhD course Coordinator:

Professor Fernando Fraternali

Handwritten signature of Fernando Fraternali in black ink.

The research project has been funded by the National Research and Innovation Operational Program 2014-2020, European Social Fund, Action I.1 "Innovative Doctorates with Industrial Characterization"



Unione europea
Fondo sociale europeo



MINISTERO DELL'ISTRUZIONE,
DELL'UNIVERSITÀ E DELLA RICERCA



Index

- Premise 6

- 1. Overview..... 11**
 - Growing cities and related issues 12
 - Traditional strategies for stormwater managing 18
 - SuDS: a new approach to urban flooding 20
 - Suds Typologies 22
 - What are the benefits of SuDS? 27
 - Examples of projects and approaches 28
 - Research Objectives and Partnerships..... 34

- 2. Green Roofs: trials and insights 38**
 - Details concerning Green Roofs 40
 - Experimental Study: Predicting Stormwater Retention Capacity of Green
Roofs 42
 - The experimental site and the monitoring system 44
 - Evaluation of GRs evolution impact on substrate soil water content by FDR sensors
calibration 46
 - Long term and event scale climate characterization..... 50
 - Methodology 51
 - Results 52
 - Assessing Green Roofs performance under controlled conditions: Set up of

indoor GRs test site	60
Assessment of GRs retrofitting surface to counteract land use changes effects: the case study of Mercato San Severino (SA).....	64
SAR images elaboration for the detection of variation in build-up area	65
Estimation of hydraulic and hydrological variations of the catchment between 1995 and 2016.....	66
Results	67
Final discussions	70
3. Re-think urban drainage with SuDS	74
SuDS implementation in urban catchments: the case study of Sesto Ulteriano (MI)	76
The case study	78
SuDS Scenarios and hydrological-hydraulic modelling	79
Rainfall dataset analysis	82
Output analysis and definition of key parameters	84
Hydrological and Hydraulic analysis results	85
Centralized and diffuse storage in urban areas: the case study of Sesto Ulteriano (MI)	96
The case study: central storage vs diffuse storage approach	102
The project of detention tanks in the “Central-Storage” scenario	103
Sensitivity Analysis Low Impact Development modules: rain barrels, drainage trenches and pervious pavements	103
LID implementation at the catchment scale aiming at a “Diffuse-Storage” scenario	110
Results	112
Final Discussions	136

4. Historical precipitations analysis	140
Historical rainfall in the Sesto Ulteriano urban area	142
Interpolation methodology for obtaining historical rainfall data	142
Inverse distance weighting method and results verification	144
Analysis of rainfall data of Sesto Ulteriano obtained from interpolation	145
Analysis and detection of the most significant precipitation scenarios of the last 10 years	146
SuDS performance under historical rainfall	148
5. SuDS adaptation to Climate Change	150
SuDS as an adaptation strategy to climate change consequences: A methodological approach experienced for Sesto Ulteriano urban catchment	152
Hard-technology versus SuDS scenario	156
Historical rainfall statistical analysis and climate scenarios	156
Identification of potential rainfall scenarios at 2050	162
Climate Change Analysis Results: assessing SWMM ₅ drainage models performance focusing on climate change effects	165
Drainage Network Analysis Results: comparing under the same climate condition different SWMM ₅ drainage models	166
Results discussion	168
6. Discussion and Conclusions	170
Epilogue	174
References	176

Premise

Water resources, essential for human beings and nature itself, has always been one of the key elements for the development of urban agglomerations. History teaches us that the first inhabited centres, small villages, rural settlements and large metropolis were born and expanded nearby seas or rivers, once used as main sources for water supply and as transportation networks. The need for a constant supply of water resources, for different purposes, led to the construction of different types of infrastructures capable of allowing a correct management of demand, even during periods of drought, and reducing risk levels throughout cyclical flood phenomena. Over time, in parallel with an evolution of the cities and the needs of its inhabitants, it was recognized that these traditional infrastructures were, in many contexts, inadequate and unable to implement sustainable water management strategies. In particular, the several criticalities observed in the more urbanized realities revealed the impossibility of these infrastructures to carry out their function in compliance with the environmental limits of water and energy resources exploitation and pollution. In 1987, the United Nations Brundtland Commission defined sustainable development as “development which meets the needs of the present without compromising the ability of future generations to meet their own needs.” In the context of management of limited resources, the issues that revolve around Water Sciences can be certainly considered fundamental tools for identifying objectives and strategies capable of guaranteeing the respect and sustainable use of an essential resource for human beings. Even nowadays, punctual and constant supplies are a mirage for developing countries, while increasingly extreme urbanization dynamics make industrialized countries more vulnerable and less resilient to urban flooding problems. Furthermore, the effects of the ongoing



Alessandro D'Ambrosio - MARINA DI CAMEROTA (IT)

climate change seem to contribute globally to a further intensification of the aforementioned conditions: increase in periods of drought and intensification of rainfall events. Sustainability, respect for limited resources, climate change, resilience towards negative impacts are increasingly topical issues. We wonder about how it seems fairer to intervene, what are the most effective strategies to support an aware and environmentally conscious development, to solve the hydraulic and hydrological criticalities encountered in urbanized contexts, to encourage water re-use strategies, to make cities more resilient and resistant against urban flooding, to prevent widespread pollution of our waterways, of the seas. These issues, extremely relevant worldwide, are all examined by the 2030 Agenda for Sustainable Development, an action program for people, the planet and prosperity, signed in September 2015 by the governments of the 193 member countries of the Organization of the United Nations. This program incorporates 17 Sustainable Development Goals, SDGs - into a large action program for 169 'targets' or milestones. The official launch of the Sustainable Development Goals coincided with the beginning of 2016, leading the world on the way to go over the next 15 years: the countries, in fact, are committed to achieving them by 2030. The Development Goals follow up on the outcomes of the Millennium Development Goals that preceded them, and represent common goals on a set of important development issues: the fight against poverty, the eradication of hunger, the realization of sustainable cities and society, avoid water waist and climate change adaptation, to name but a few. These goals are meant to be "common" because they concern all countries and all individuals; no one is excluded, nor should be left behind on the path necessary to design a sustainable world.





Chapter I

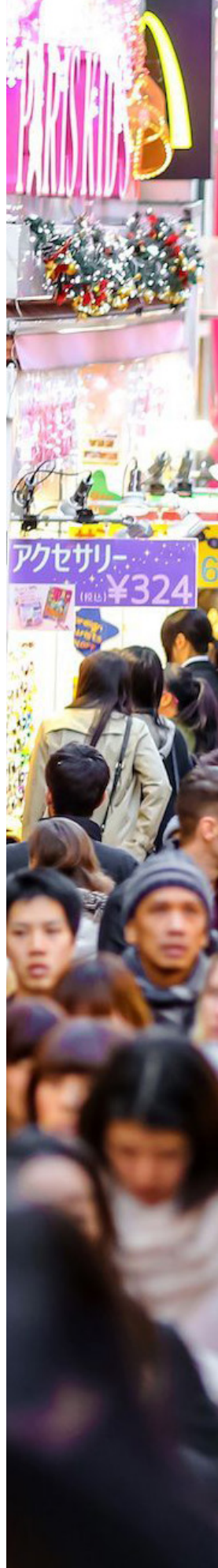
Overview

Growing cities and related issues

In recent years, particularly invasive Urban Planning strategies gradually transformed the structure of our territory. These dynamics are mainly justified by the needs of a population increasingly driven by social and economic motivations to live in large urban areas (Tutino & Melosi, 2019; Galea et al., 2019). The intensive urbanization, mainly linked to an increase in the built-up area and annexed works, led to a substantial increase in the impermeable surface and a reduction in "natural" soils. In recent years, we have even talked about alteration of the hydrological cycle following the observation of phenomena such as the reduction of infiltration, evapotranspiration and groundwater recharge (Zhang & Chui, 2019; Huang, 2019; McDaniel & O'Donnell, 2019).



Illustration - Chad Crowe





Pola Damonte - National Geographic
TOKYO (JP)



Scott Olson - National Geographic
YAZOO RIVER-VICKSBURG-MISSISSIPPI (USA)



The direct consequence of this is certainly the growing phenomenon of urban flooding, increasingly frequent in different regions of the Italian territory characterized by rapid development and by administrations not always careful to implement urban planning strategies capable of compensating and balancing the inevitable construction with targeted interventions to restore or relocate natural permeable areas (Luino et al., 2012; Brandolini et al., 2012; Albano et al., 2014; Pistocchi et al., 2015; Recanatesi & Petroselli, 2020; Galuppini et al., 2020; Palermo et al., 2020). The precipitations runoff, therefore, constitute in these contexts an increasingly serious problem to be managed by the administrations. The presence of an almost totally impervious territory, in fact, doesn't completely allow the infiltration of stormwater that inevitably has to be managed by traditional urban drainage systems. The sewers, however, are now under-sized and are therefore no longer able to manage stormwater in a truly sustainable manner. Crisis events that make them the cause of widespread water pollution phenomena are increasingly frequent (Luino et al., 2012; Guzzetti et al., 2013; Mazzoleni et al., 2014; Faccini et al., 2016; Sperotto et al., 2016; Apollonio et al., 2016; Viero et al., 2019). Moreover, the situation just presented cannot but worsen due to the effects of climate change that will see the Mediterranean climate regions being hit by increasingly intense meteorological phenomena as well as long periods of droughts (D'Ambrosio & Longobardi, in press).



Didarul Alan Chy - National Geographic
FLOODING IN BANGLADESH

First, in Italy, the Lombardia region, with the law n.4 of March 15th 2016, proposed a revision of the regional legislation related to soil protection, prevention and mitigation of hydrological risk and management of natural drainage networks. In particular, this law, specifically in article 7, introduced the respect of the principles of hydraulic and hydrological invariance in the case of new urban planning interventions. The principle of hydraulic invariance implies that the runoff flow rates from the newly urbanized area must not exceed those generated before the intervention. The principle of hydrological invariance, on the other hand, imposes not only a restriction in terms of flow rate but also in terms of volume between the scenario before and after the urbanization works. This strategy, useful for putting a brake on unsustainable planning that are still used in other contexts, allows to ensure high levels of hydraulic and environmental protection (Regional Law 15 March 2016, n. 4, Review of regional legislation on soil protection, prevention and mitigation of hydrogeological risk and management of water courses, BURL n. 11, supplement of 18 March 2016). What has just been said, however, applies to the containment of future actions and does not help us to understand how to intervene on urban context in order to mitigate the negative impact of the massive planning activity that has affected the territory in recent years. In this regard, however, there are two different approaches to the problem: the first is the traditional approach involving hard-engineering, the second can instead be defined “integrated” implementing, along with the mentioned traditional drainage systems, also Sustainable Drainage Infrastructures (D’Ambrosio et al., 2019).





Manuel Silvestri- National Geographic
VENICE SPECIAL FLOODING (IT)

Traditional strategies for stormwater managing

Traditional strategies include those interventions commonly deployed for urban runoff management thanks to their effectiveness, handiness and cost. The sewer, emblem of traditional drainage infrastructures called “hard engineering”, is responsible for collecting and conveying, as quickly as possible, stormwater into the water treatment plant and water bodies. These infrastructures are dimensioned in order to ensure full effectiveness within fixed risk levels but urban expansion and climate change make these systems even more fragile. Increasingly common phenomena are surface water floods, sewer floods following the over-loading of underground pipes, river flood or erosion and diffuse pollution. The modification and modernization of the entire sewerage system would entail a considerable cost for the administration, therefore, the “legislative” approach essentially involves the possibility of enhancing the system’s response capacity through the reconfiguration of elements that are part of the existing traditional network. For example though the installation of flood control and treatment artifacts such as spillways, rainwater storage tanks and first flush treatment tanks. These





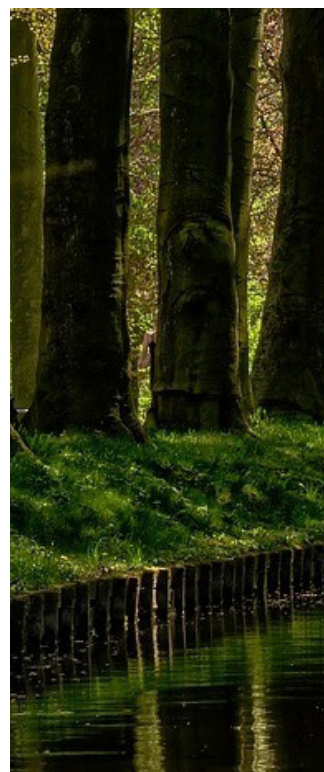
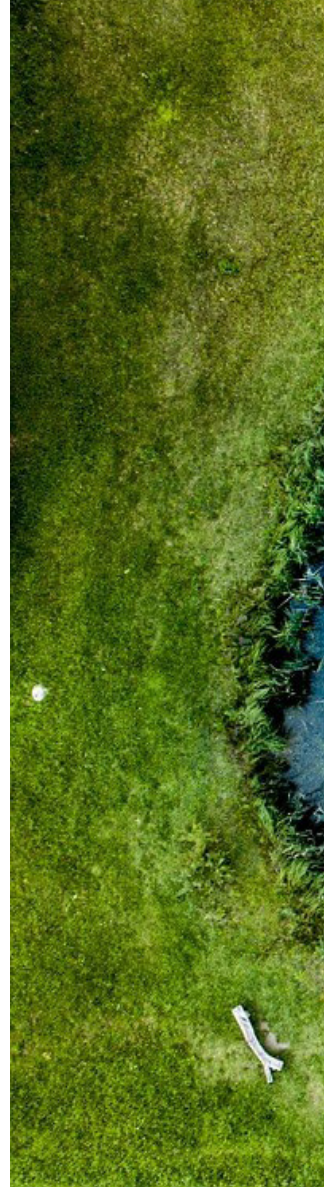
KING'S SCHOLARS' POND SEWER, LONDON (UK)
(Picture from the web of Adam Powell)

infrastructures are usually located in strategic points downstream of the catchment and are capable of accommodating large volumes of water coming from the waterproofed surrounding areas. The problem linked to the implementation of a strategy of this type mainly consists in the fact that, although it is able to reduce the load that the traditional drainage network must handle, it is not able to implement a sustainable management of precipitation runoff and to deploy land restoration strategies. It is considered absolutely essential, today more than ever, to begin to tackle the problems related to the progressive soil sealing of increasingly large urban agglomerations in a more structured, systematic and responsible manner. The effects, over the years, of definitely unsustainable administrative policies or, in any case, not very attentive to the consequences of massive building interventions, are unfortunately now very visible and can no longer be postponed (Fahy & Chang, 2019). It is true that it is certainly not possible to stop the development of the cities but, with some precautions, it is possible, today, to make them more and more resilient towards climatological and hydrological risks.

SuDS: a new approach to urban flooding

Therefore, a new, integrated approach is taking hold, in which sustainable technologies come into play, capable of reducing the flow introduced into the network and bringing numerous benefits to the territory in which they are installed (Larsen et al., 2016; Kabisch et al., 2017). Such solutions are known in the scientific literature with several acronyms, defined by different groups of researchers from different countries (Fletcher et al., 2015). The following are the best known: LID (Low Impact Development), BMP (Best Management Practices), WSUD (Water Sensitive Urban Design) and SuDS (Sustainable Drainage Systems). The term low impact development (LID), commonly used in North America and New Zealand, appeared for the first time in 1977 in a report on land use planning in Vermont, USA. This approach focused on minimizing costs of stormwater management, achieving a “natural” hydrology with the implementation of integrated control measures. Best management practice (BMP) is a term coined in 1972 within the first draft of the Clean Water Act and it is used in the USA and Canada to describe a type of practice or structured approach to prevent pollution in the management of wastewater treatment processes. The term water sensitive urban design (WSUD) began to be used in the 1990s in Australia with reference to the implementation of measures able to manage water balance, enhance water quality and water conservation and maintain water-related environmental and recreational opportunities. In UK, the term SuDS identify a range of technologies and techniques used to drain stormwater more sustainably than conventional solutions. They are able to partially restore the permeable surface and allow the territory to return to the drainage configuration prior to massive edification (Fletcher et al., 2015; Lashford et al., 2019).

In the following text, this term will be frequently used to describe this kind of drainage measures. Surely these infrastructures, well known for their water retention, holding and filtering capacities (Johannessen et al., 2018; Ghofrani et al., 2019), cannot completely manage the problem of runoff but, if used in combination with traditional drainage systems, they are able to support the pre-existing network, contributing also to the generation of numerous additional benefits for human beings and the environment. SuDS, although all capable of reproducing the “natural” drainage configuration, differ in construction technology and in their different locations in urban contexts (Woods Ballard et al., 2015). Basins of bio-retention and detention, rain gardens, draining trenches, green roofs and permeable parking lots are just some of the types of Sustainable Urban Drainage Systems that are spreading, a little at a time, also in Italy. SuDS are scalable to various sized projects and land-use types.





Suds Typologies

SuDS differ for the level of treatment service (quality) as well as the level of volume reduction (quantity). Flow control devices offer the least amount of treatment services while constructed wetland offers the most. However, these systems, if combined, can satisfy better performance requirements. Selection of the optimum sustainable drainage facility or combination of facilities for a project or site depends on the desired hydrologic outcomes. At first, an evaluation of site opportunities and constraints such as the characteristics of the soil, groundwater and bedrock depth, climate variables, drainage area and slope is necessary. Then, a definition of hydrologic controls required (flow control, detention, retention, filtration, infiltration and treatment) is recommended. Moreover,

maintenance and management protocols, community acceptance and cost should be also taken into account.

Oversized pipes are subsurface pipe systems sized larger than required to reduce peak flow rates, especially during larger storm events.

Flow control devices are used to reduce peak discharge, attenuating stormwater runoff before its discharge into the drainage network.

Dry swales are open grassed conveyance channel that filters, collect, and detains stormwater runoff.

Underground detention systems retain and detain stormwater runoff prior to its conveyance into the local drainage system.

Detention ponds are stormwater basins designed to intercept stormwater runoff, reducing peak flows that cause downstream scouring and loss of aquatic habitat.



Wet vaults are subterranean structures that provides runoff volume control, peak discharge reduction, sediment control, and harvesting potential.

Rainwater harvesting involves collection, storage, and reuse of runoff from roofs. It reduces runoff volume and peak flows.

Retention ponds are constructed stormwater ponds that retains permanently water and removes pollutants through biological uptake processes and sedimentation.

Filter strips with their slope attenuates stormwater runoff by converting it into sheet flow and it is typically located parallel to an impervious surface such as a parking lot, driveway, or roadway.

Underground sand filters are system that pre-treats, filters, and temporarily stores the first flush of stormwater runoff. They are mainly intended for quality control.

Surface sand filters settle out heavier solids of the first flush and then, through the sand, filters pollutants. They also reduce peak discharge by collecting and slowing runoff velocity as water flows through the filter.

Vegetated walls can be a passive or active system. The first category address air quality while the second water quality, and thus is more applicable to SuDS. They harvest water to reduce stormwater runoff and provide additional thermal insulation.

Vegetated roofs are garden installed at the top of the buildings. They collect rainwater at its source, slow its release, reduce its volume through evapotranspiration from plants and regulate building's temperature.

Permeable pavements allows water to vertically flow through surfaces used for pedestrian and vehicular traffic, reducing and distributing stormwater volume and encouraging groundwater infiltration.



Diane Cook and Len Jenshel - National Geographic
JUSTIN BERE'S NEW HOME, LONDON (UK)

Infiltration trenches are laminated systems used to increase runoff infiltration and to filter particulates.

Tree box filters treat and collect stormwater runoff captured from the street into the box filter. An underdrain carries treated runoff to either a surface discharge location or a larger retention system for secondary treatment.

Rain gardens are planted depression designed to infiltrate stormwater runoff, but not to hold it. Stormwater pollutant mitigation is accomplished through phytoremediation processes as runoff passes through its layers.

A riparian buffer is a strip of hydric soil with facultative vegetation along the banks of a river or stream that protect and improve water quality through local plant communities.

Bioswales are open, sloped, vegetated channel designed for treatment and conveyance of stormwater runoff. Pollutant mitigation occurs through phytoremediation by facultative vegetation.

Infiltration basins are areas with highly permeable soils designed to temporarily detain and infiltrate stormwater runoff. They do not retain a permanent pool of water. These facilities filter pollutants from stormwater runoff and recharge groundwater supply.

Constructed wetlands are artificial swamps with permanent standing water that able to treat water pollution and bringing different ecosystem services.







Pierluigi Palazzi -
BOSCO VERTICALE,
ARCH. STEFANO BOERI, QUARTIERE ISOLA - MILANO (IT)



What Are The Benefits Of Suds?

SuDS deliver high quality drainage while supporting urban areas in the management of stormwater. They also help counteract the impact of increased urbanization on waters cycle, improving infiltration and groundwater recharge. SuDS can enhance the quality of life in the cities making them more beautiful, resilient to change and sustainable, by improving air quality, regulating building temperatures, and reducing noise and delivering recreation and education opportunities. The community for sustainable drainage (susdrain), created by the Construction Industry Research and Information Association -CIRIA-, is a neutral, independent and not-for-profit organization that provides guidance, information, case studies, videos, and photos that help to support planning, design, approval, construction and maintenance of SuDS. On the independent and authoritative platform "www.susdrain.org" benefits of these systems were specified as follow: Flood risk and water quality management, Biodiversity & ecology, Amenity, Air quality, Building temperature, Carbon reduction & sequestration, Crime, Economic growth, Education, Enabling development, Climate change adaptation, Groundwater recharge, Health & wellbeing, Pumping wastewater, Rainwater harvesting, Recreation, Tourism, Traffic calming, Treating wastewater. CIRIA has produced also "Benefits of SuDS Tool (BeST)" to assist with the assessment of SuDS easier. It provides a structured approach to the assessment of the mentioned benefits, often based on the drainage performance.

Examples of projects and approaches in Italy...

ForestaMi is the research project undertaken by the Politecnico di Milano and financed by the Falk Foundation with the support of the Ferrovie dello Stato Italiane Group through the FS Urban Systems. The study identifies the areas of the Metropolitan City where to open spaces for forestation, investigating in particular the areas most affected by the effects of climate change, mitigating the heat island effect and reducing the risks from floods through new ecosystem services. Already in 2018, as part of ForestaMi, 85,000 trees were planted by the Municipalities of the Metropolitan City thanks to the support of associations, local authorities and of citizens. Wetlands, forestation, environmental compensation and depaving of parking lots are some of the interventions carried out, which actively work to improve the quality of the landscape and air in the Metropolitan City.

Milano, november 21st, 2019

THE FORESTAMI FOUND
WAS SET UP TO ENSURE 3
MILLIONS OF TREES IN THE
CITY OF MILAN BY THE 2030



"Moltiplicare il numero degli alberi e delle altre piante presenti nelle città del mondo, sostituire con superfici verdi migliaia di ettari di asfalto e di lamiera (le macchine parcheggiate che spesso non usiamo), portare la natura vivente non solo nelle corti e lungo i viali ma anche sulle facciate e sui tetti delle case, delle scuole, dei musei, dei centri commerciali. Tutti questi non sono più solamente gesti di sana ecologia, ma scelte necessarie e urgenti. Dobbiamo piantare migliaia di alberi se vogliamo che le nostre città, da principali responsabili del cambiamento climatico nel nostro pianeta diventino le protagoniste di una sfida che ogni giorno diventa più difficile, ma che è ancora aperta: quella di provare, se non a fermare, almeno a rallentare il riscaldamento del pianeta. Con ForestaMi, Milano raccoglie questa sfida e si candida a diventarne una delle più attive protagoniste."

"Multiply the number of trees and other plants in the cities of the world, replace thousands of hectares of asphalt and sheet metal with green surfaces (the parked cars that we often don't use), bring living nature not only into the courtyards and along the avenues but also on the facades and roofs of houses, schools, museums, shopping centers. All these are no longer just gestures of healthy ecology, but necessary and urgent choices. We must plant thousands of trees if we want our cities, from being the main responsible for climate change on our planet to become the protagonists of a challenge that becomes more difficult every day, but which is still open: that of trying, if not to stop, at least to slow down global warming. With ForestaMi, Milan takes up this challenge and is a candidate to become one of its most active protagonists."

Stefano Boeri,
Technical University of Milan
Scientific Director of ForestaMI Project



STOCKHOLM “EUROPEAN GREEN CAPITAL”

The assessment of the European Commission was based on a number of criteria, including climate impact, local transports, green areas and air quality. Stockholm won for its outstanding, long historical track record of integrated urban management also confirmed by its ongoing credible green credentials. Stockholm is a fast-growing city, 40,000 new homes are planned until 2030. This entails many challenges to meet the goal of being a long-term sustainably growing city. The city plan from 2010, “The Walkable city”, states that urban sprawl should be prevented. New houses should be energy-efficient and built close to public transports. Particular importance is given to strengthen the many green areas and their values and to improve eco-system services, useful for mitigating the effects of climate change and improving the quality of life in the city. Many projects were undertaken during these years to compensate for green areas that has to be used for housing or other projects in the growing city. (“Stockholm – the first European Green Capital”, June 2015).

in Europe...

LONDON ENVIRONMENT STRATEGY

London is a growing city. By 2050, it is expected that up to 3 million more people will live there. A well-planned and managed green infrastructure network will be fundamental as the population becomes larger to help city adaptation to climate changes. London Urban Plan includes policies that protect green spaces and natural areas. However, the increasing need to exploit soil for building facilities means there will be few opportunities to create more traditional parks and nature reserves as the city grows. London must therefore become greener whilst also becoming denser. Green roofs, walls covered in plants, street trees and small pocket parks in between buildings and other urban greening act as part of London's green infrastructure network to meet this challenge and to reduce pollution, flooding risk and heat

islands. The London Environment Strategy aims to ensure that more than half of London will be green by 2050 and the city's tree canopy cover increases by 10 per cent. A new Urban Greening Factor was introduced to guide boroughs on the amount of greening that ought to be included in major developments and the concept of Healthy Streets, whose core element is the urban greening, was promoted. In parallel, the London Sustainable Drainage Action Plan helps the city to deal with the likely increase in heavy rainfall and consequent urban flooding through the implementation of Sustainable drainage systems, such as rain-gardens, street trees and other Nature Based Solutions. In addition, Green roofs and walls are an essential component of a greener, denser city especially in those areas that have historically had a deficiency in parks and green spaces. They can help store stormwater, provide additional wildlife habitat, or, increasingly, create greener public realm or roof gardens above our busy streets.





in the World...

CHICAGO SUSTAINABLE ACTIONS

The city of Chicago has an extensive mass transportation network with around 150 rail stations with its 8-rail line and over 200 bus routes. However, it is also very green with 12,429 total acres of parkland. Chicago benefited from green urban planning with the aim of transforming the city into one of the world's brightest examples of a sustainable metropolis. A path to this goal is found in the seven themes of "The Sustainable Chicago Action Agenda" which include Chicago's Climate Action Plan, Energy Efficiency & Clean Energy, Waste & Recycling, Waste & Wastewater, Transportation Options, Economic Development & Job Creation, and Parks & Open Space. Sitting next to Lake Michigan and atop a swampy marshy land, water management is crucial for Chicago to becoming a more sustainable and resilient city. Retrofitting strategies and new planning interventions involving green infrastructure are being used to mitigate stormwater discharge in the sewers.

Diane Cook and Len Jenshel
National Geographic
CHICAGO CITY HALL, CHICAGO
(USA)

NEW YORK GREEN INFRASTRUCTURES

The Green Infrastructure Plan will achieve better water quality and sustainability benefits by: Reducing CSO volume by an additional 3.8 billion gallons per year (bg), or approximately 2 bg more than the all-Grey Strategy; capturing rainfall from 10% of impervious surfaces in CSO areas through green infrastructure and other source controls; and providing substantial, quantifiable sustainability benefits that the current all Grey Strategy does not provide (cooling the city, reducing energy use, increasing property values, and cleaning the air). The Green Infrastructure Plan has five key components: the implementation of cost-effective grey infrastructures; the optimization of the existing wastewater system; the control of runoff from 10% of impervious surfaces through green infrastructures; the deployment of adaptive management; the engagement of stakeholders.

Diane Cook and Len Jenshel
National Geographic
EMPIRE STATE BUILDING, NEW
YORK (USA)

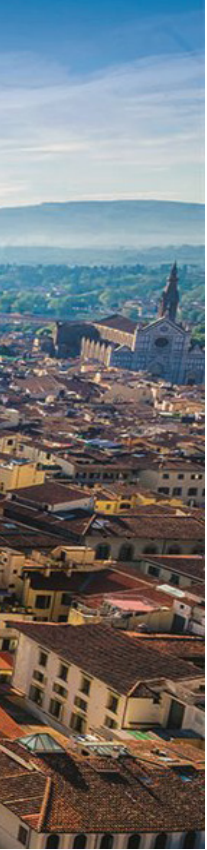




Susanne Kremer - National Geographic
FLORENCE (IT)

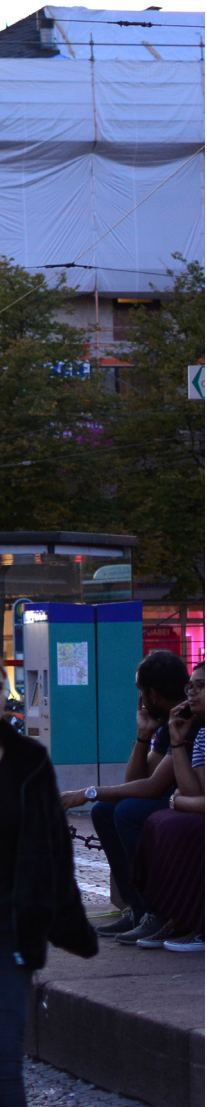


Alessandro D'Ambrosio - DARMSTADT (DE)



Research objectives and Partnerships

This research aimed at investigating sustainable strategies able to mitigate flooding risk in urban areas. In particular, the research activities featured an experimental part, held at the University of Salerno and focused on the technology of Green Roofs (GRs), and modeling studies, aimed at assessing SuDS benefits in the stormwater management at the catchment scale and carried out in collaboration with IRIDRA S.r.l. and the Technische Universität Darmstadt. The study of the hydrological behaviour of GRs under Mediterranean climate allowed understanding how design and climate variables could affect the role of these infrastructures in the mitigation of urban flooding. Specifically, this stage of the research focused on the analysis of the variation of retention performances of two extensive green roofs test beds, different in the drainage layer and located in the Campus of University of Salerno, according to the rainfall characteristics and design parameters. Both, in fact, proved to be crucial for the definition of soil moisture content, a key parameter in the performance of such infrastructures. Several studies were carried out to evaluate also the effect of Grs ageing on the overall performance of these systems. Moreover, to test their performance under controlled rainfall conditions and to understand how their size and design could affect their behaviour, an indoor experimental site was set up with Plexiglas cases customizable for reproducing different kind of GRs. To understand the role of different typologies of SuDS in the mitigation of urban flooding in urban contexts, modelling approaches were developed to assess the performance of these infrastructures in Sesto Ulteriano (Northern Italy), a catchment that experienced a fast soil sealing and is actually affected by several hydraulic and hydrological criticalities. EPA SWMM₅ simulations and comparison of a hard-technology scenario, representing the actual configuration of the drainage network, with design and model-based SuDS retrofitting scenarios, helped to assess how climate condition, SuDS spatial distribution, retrofitting potential, feasibility and land use could somehow affect the behaviour of these systems in urban catchments. In addition, to investigate how climate change may challenge these systems, an analysis of historical rainfall (1858-2019) enabled the identification of trends in precipitation extremes for the design of potential climate scenario within a 30-year future time window. Again, simulations were performed to test SuDS modeling scenarios under continuous and event-scale potential future rainfalls. As for the GRs analyses, results show an overall tendency of reduction of stormwater retention for large events (long duration, high cumulate depth and rainfall intensity) and mainly see the rainfall cumulate depth as the best predictor for retention coefficients. Drainage layer building practices and initial Soil Moisture Contents also seem to play a key role on the GRs retention properties. Urban-scale studies highlighted the importance of the awareness of the actual retrofitting potential of catchments in the prediction of the effectiveness of SuDS projects for flooding risk mitigation. Strategical solutions based on fixed and unaware project retrofitting percentages, would inevitably result in unsuccessful interventions, unable to pursue city resilience. Overall, findings achieved so far suggest that these infrastructures are actually able to mitigate the effects deriving from



urbanization and soil sealing. Although few are the retrofittable surfaces in developed urban context, such infrastructures are nevertheless a valid aid for traditional drainage systems in the management of stormwater, providing besides numerous additional benefits for human beings and nature. For sure, in planning such interventions, it must also be taken into account that the effect of climate changes seem to counteract their efficiency. Under future potential climate scenarios, in fact, slightly worse performances were registered, showing, at the same time, how SuDS can be valuable used to adapt to climate change conditions but that the resilience they provide in terms of stormwater management issue would be much more sensitive to climate input in the next future.

The research project has been funded by the National Research and Innovation Operational Program 2014-2020, European Social Fund, Action I.1 “Innovative Doctorates with Industrial Characterization”(Code: DOT1328490-2) and provided for a partnership with an Italian company, Iridra S.r.l. in Florence, and with a foreign university, the Technische Universität Darmstadt in Germany. Professor Antonia Longobardi oversaw the research carried out at the University of Salerno and supervised all the tasks. Professor Britta Schmalz, head of the Department of Engineering Hydrology and Water Management of the Technische Universität Darmstadt, was responsible for co-ordinating the work during the stage abroad from June 2019 to November 2019 (6 months) and had been involved in other subsequent activities. Anacleto Rizzo, Ph.D. and hydraulic engineer, and Nicola Martinuzzi, mechanical engineer and chief executive officer of Iridra S.r.l., handled the activities during the stage (6 months) in the company and provided the case study.



Those who are crazy enough
to think they can change
the world usually do!

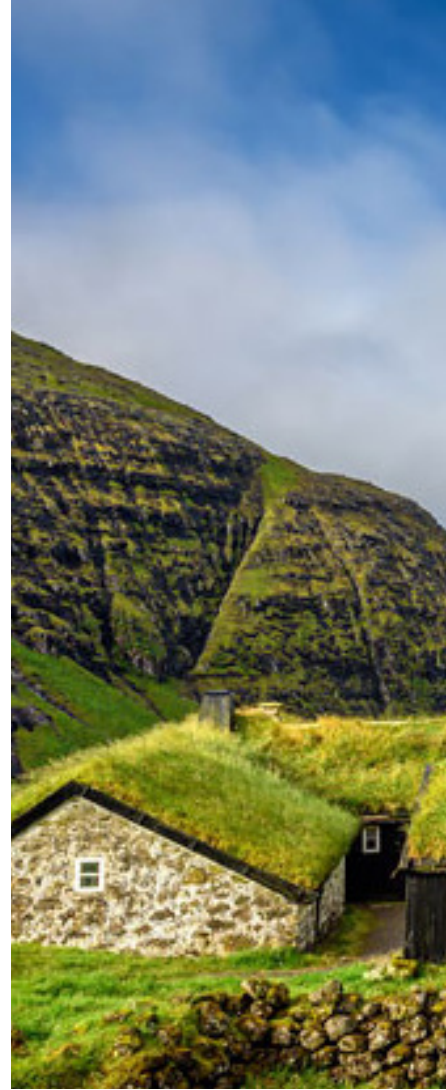
Steve Jobs

Chapter 2

Green Roofs : trials and insights

Details concerning Green Roofs

Green roofs are a particular type of SuDS installed on the top of the building for a number of reasons including reduction of surface water runoff, enhanced building performance, increase of the ecological, aesthetical value and improved physical and mental well-being. Green roofs can be divided into two main categories: Extensive roofs and Intensive roofs, also referred to as “roof gardens”. Low substrate depths, (20-150 mm) and subsequently low loadings on the building structure usually characterize extensive roofs. Even if they are preferred for their simple planting and low maintenance requirements, they are not accessible. On the other hand, intensive roofs, usually fully accessible, are characterized by deeper substrates (>150 mm) that can be suitable for a wide variety of planting. Green roofs with substrate depths of 100-200 mm are usually defined “semi-intensive roofs” and can include characteristics of both extensive and intensive roofs. If these infrastructures also include reservoir storage, they are called “blue roofs”. Additional adequate structural loading capacity and waterproofing considerations are needed in this specific situation. Although they are more expensive than conventional roofs, they can provide several long-term benefits. They are able, in fact, to protect underlying roof waterproofing materials from mechanical damages, ultraviolet radiation and temperature extremes. In addition, they are able to improve thermal insulation of buildings, reducing also energy costs, and if conceived among a larger roof retrofitting plan they are able to mitigate urban heat islands while improving air quality. Several expertise are needed for the successful design, implementation and maintenance of Green Roofs. Hydraulic and structural engineers, architects, landscapers and ecologist have to cooperate are all required. Green roofs can be installed on a variety of roofs, different for construction, size and slope. However, it is clear that their effectiveness can be challenged by these characteristics (i.e. steeper pitches imply less storage capacity!). The potential loads on the building and the environmental parameters such as height, orientation, exposure to winds, climate condition, ecological consideration and visual aspect should be taken into account in planning such interventions. In addition, the developer should pay specific attention to enhancing the Green Roof potential in pollutant treatment, amenity and biodiversity design and hydraulic and hydrological configuration.



Nick Fox - FAROE ISLANDS, NORWAY



Lindsay Snow - FAROE ISLANDS, NORWAY

“When it comes to
green roofs,
SCANDINAVIANS
have it all
figured out”

Kala Barba-Court
Plain Magazine (July, 14), 2016

Experimental Study: Predicting Stormwater Retention Capacity of Green Roofs

This research merged in a paper entitled “Predicting Stormwater Retention Capacity of Green Roofs: An Experimental Study of the Roles of Climate, Substrate Soil Moisture, and Drainage Layer Properties” published by the Journal “Sustainability” in 2019 (Longobardi, D’Ambrosio & Mobilia, 2019) and in several conference papers.

With reference to the stormwater management, the GRs appear able to make a significant contribution to the traditional stormwater management technologies during rainfall events by reducing stormwater volume and peak discharge. The retention performance of green roofs appears affected by multiple variables that can basically be divided into two categories: Climate variables (Simmons et al, 2008; Wang et al., 2017) and design variables (Akter et al., 2018; Schultz et al., 2018). A typically higher percentage of retention is indeed observed in thicker roofs and climate situations characterized by sporadic rains of moderate cumulative volume (Berndtsson, 2010; Chenot et al., 2017; Ferrans et al., 2018; Baryla et al., 2018). Climate conditions featuring relatively frequent severe events and changes between prolonged dry and wet seasons, as is typical for the Mediterranean climate type, appear rather critical for management of GRs (Brandao et al., 2017). However, the number of scientific contributions indicates an extremely variable level of rainwater reduction. GRs appear to reduce total yearly runoff volume by 40% to 90%, with an important seasonal fluctuation, while the peak flow rate can be even more attenuated, i.e., by 20% to 90% (Hiltner et al., 2008; Mobilia et al., 2017; Chai et al., 2017; Sartor et al., 2018). Identifying relationships between the GR retention capacities and the characteristics of meteorological and design variables is not generally a simple and successful task. Several authors actually reported on these difficulties (Nawaz et al., 2015; Soulis et al., 2017; Todorov et al., 2018) as well as highlighted the fact that regression analysis is unlikely to always provide an accurate model to predict GR retention for individual precipitation events (Simmons et al., 2008). The role played by the antecedent substrate moisture conditions—or alternatively, the length of the antecedent dry period—is also uncertain, as for some studies, they are of primary importance (Akter et al., 2018; Schultz et al., 2018; Sims et al., 2016), while in some others, only a weak correlation with retention properties has been highlighted (Nawaz et al., 2015; Soulis et al., 2017; Todorov et al., 2018; Stovin et al., 2012).





Roberta D'Ambrosio - GREEN ROOF EXPERIMENTAL SITE, FISCIANO, SA (IT)

This part of the research starts from the findings of an experimental installation including two extensive test beds located in the Campus of the University of Salerno, in a typical Mediterranean environment. An event scale analysis based on data from thirty-five rainfall–runoff events over two years was performed to identify the roles of climate, substrate moisture conditions, and building practices on GRs retention properties. Based on the empirical findings, it seems feasible to provide recommendations for a preliminary classification of rainfall–runoff events in order to better explain the GR hydrological behavior and to consequently improve the retention capacity (RC) prediction.

The experimental site and the monitoring system

In January 2017, two extensive green roof test beds (2.5 m²) were installed at the Maritime and Environmental Hydraulic Laboratory of the University of Salerno (Mobilia & Longobardi, 2017; Mobilia et al., 2020). The two experimental roofs have a total thickness of about 15 cm. They are made up of three layers: vegetation layer, substrate layer and drainage layer. A filter mat of non-woven fabric is interposed between the substrate and the drainage layer in order to prevent the soil from obstructing the voids between the particles that make up the drainage layer. The vegetation layer consists of a species of succulent plant called *Mesembryanthemum*, which is typical of the Mediterranean areas and is considered particularly suitable for facing the specific climatic features. The substrate layer, with 10 cm thickness, was made by TRIPLO soil and consisted of a mix of blond peat, Baltic brown peat, zeolites, and simple non-composted vegetable primer (coconut fibres), and was completed with

the addition of mineral fertilizer made of organic nitrogen fertilizer (bio-stimulant algae). Finally, the drainage layer, with 5 cm depth, was designed differently for the two roofs. In fact, one of them (GR₁) is made up of expanded clay aggregate (diameter from 8 to 20 mm), while the other (GR₂) is made up of a commercial plastic tray (MODI) of 60x6x5 cm; each was characterized by 13 cone-shaped concavities, extruded from their bases and filled with expanded clay aggregate. Laboratory experiments were conducted to characterize the substrate and drainage layer properties. For the substrate layer, a dry unit weight of about 3.63 kN/m³, a porosity n of about 63%, and a water holding capacity of about 37% were found. For the drainage layer, a dry unit weight of about 5.84 kN/m³ for the expanded clay aggregate, a porosity n of about 77%, and a water holding capacity of about 34% were found, which generated a 6.7 L/m² retention capacity in the case of the GR₁ site (5 cm expanded clay aggregate depth). In the case of the GR₂ site (5 cm height commercial plastic trays filled with expanded clay aggregate), a 7.9 L/m² retention capacity was found. Given the similarity in the substrate layer for the two sites, it can be assumed that the GR₂ system is characterized by a moderately larger retention capacity (about 18%) compared to GR₁. The experimental site was monitored (5 min time step) by a weather station, Watchdog 2000 Series (Model 2550), which includes: Tipping bucket rain gauge, hygrometer for air humidity measurement, pyranometer with silicon sensor (spectral field 300–1100 nm, range 1–1250 W/m²) for solar radiation measurements, and an anemometer for wind speed and direction measurements. Runoff from the experimental sites was collected in circular-shaped tanks located above digital calibrated scales in order to measure (5 min time steps) the stormwater volume. Volumetric water content within the

substrate layer was monitored with the use of the commercial moisture sensor SM 100. It is shaped as a thin plate with a sharp tip at the bottom. The sensor has a thickness of 3 mm, a height of 60 mm, and a width of 20 mm, and was installed vertically. The sensor is made up of two electrodes that act as a capacitor, with the surrounding soil serving as the dielectric. An 80 MHz oscillator drives the capacitor and a signal proportional to the soil's dielectric permittivity is converted to the output signal. In order to achieve a greater accuracy, soil-specific calibration was performed

in the laboratory, relating the capacitance sensor's electronic readings to the actual volumetric water content, according to the product manual specification. Volumetric moisture content during calibration ranged between 4% and 60%. The actual volumetric water content at each calibration condition was measured by the gravimetric method with oven drying. The method involves weighing a moist sample, oven drying it at 105 °C for 24–48 h, reweighing, and calculating the mass of water lost as a percentage of the mass of the dried soil.

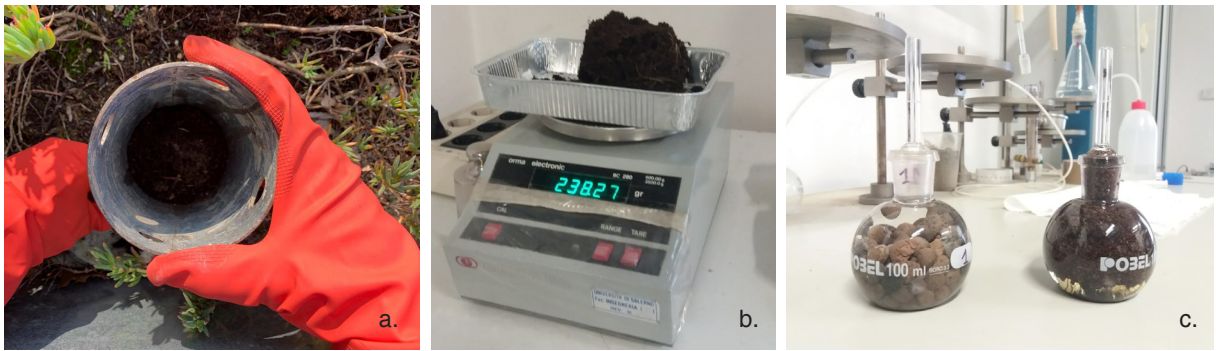


Fig. 2.1 Laboratory experiments conducted to characterize the substrate and drainage layer properties: a. soil sampling; b. weighing; c. pycnometers for expanded clay specific weights determination.

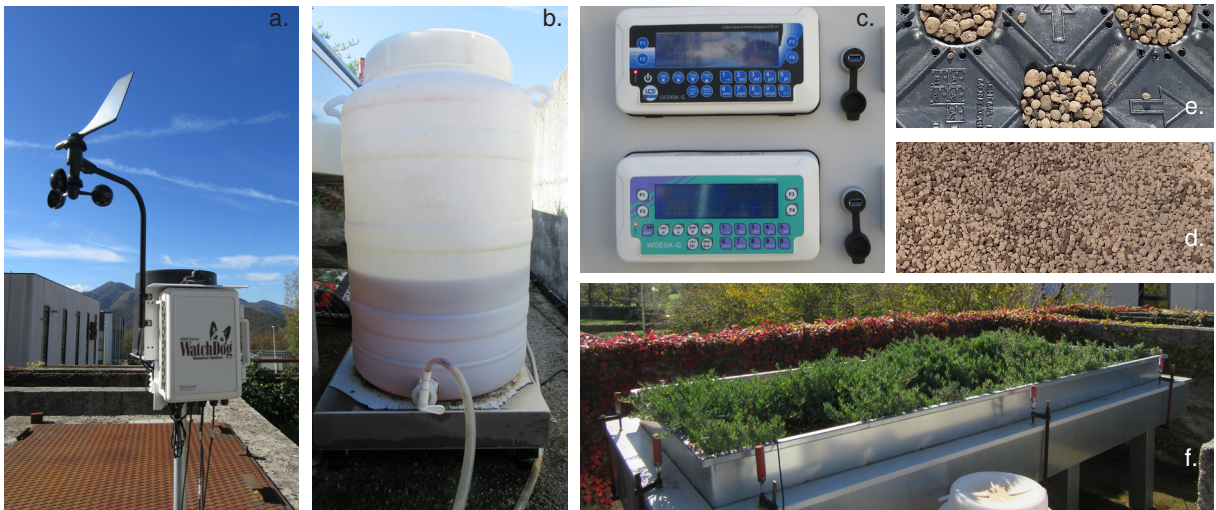


Fig. 2.2 Experimental site instrumentation: a. meteorological station; b. water storage tank; c. scales control boards; d. storage layer GR1; e. storage layer GR2; f. green roof model.

Evaluation of GRs evolution impact on substrate soil water content by FDR sensors calibration

GRs retention capacity depends on numerous variables such as climatic conditions, design parameters and substrate ageing (Wang et al., 2017; Akther et al., 2018; Schultz et al., 2018; Bouzouidja et al., 2018). In particular, the evolution of physical and chemical properties of the substrate and vegetation layers of a green roofs may lead to substantial changes in their hydraulic parameters and in the overall hydrological behaviour. The growth of the roots in the substrate layer, above all, seems to affect the interpretation of the soil moisture content (Kizito et al., 2008; Kang et al., 2019). The latter, especially in Mediterranean regions, characterized by long periods of drought and heavy rainfall, is considered one of the key parameters in the definition of GRs retention performance (Chenot et al., 2017; Longobardi et al., 2019) . Generally, FDR (Frequency Domain Reflectometry) sensors are widely used in the assessment of the volumetric water content (VW) of the soil for their durability and reliability but a calibration procedure of these tools is essential to get accurate assessments.

This study investigated changes in FDR sensors calibration caused by the presence of root system in an experimental GR. In order to assess how the presence of root system affect FDR sensor calibration and therefore also soil moisture content observations, two substrate soil samples were collected from one of the experimental GR (GR₁) located within the campus of the University of Salerno and presented in previous paragraph. The samples differ in the presence of root system since the first one was collected during the construction phase in 2017 while a second one was collected two years later. FDR measurements from the two samples were plotted against actual volumetric water content to obtain calibration curves.

GR substrate soil sampling

A first substrate soil sample (S₂₀₁₇) was collected in 2017, at the moment of the GR installation. It consists of a mix of blond peat, Baltic brown peat, zeolites and simple non-composted vegetable primer (coconut fibres), completed with the addition of a mineral fertilizer (bio-stimulant algae). More information about physical and hydraulic properties are reported in (Longobardi et al. 2019). A second sample (S₂₀₁₉) was then collected two years later, in 2019 (Figure 2.3), and in this case a well developed root system was detected within the previously mentioned soil mix . The sample was taken making sure to preserve vegetation and GR functionality.

On the left Fig. 2.3 GR soil sampling in 2019 and picture of the sample with the roots





FDR calibration curves

The FDR calibration curve was obtained by plotting each value of the soil moisture content provided by the FDR sensor against the corresponding volumetric water content (VW) of the sample. In total, 18 FDR measurements were collected for S2017 and 20 for S2019. For each reading the VW has been derived as:

$$\text{VW \%} = \text{GW (\%)} \cdot \text{BD}$$

Where BD is the the bulk density of the soil (g cm^{-3}) calculated as the ratio between Dry Weight and Volume of the sample, and GW is the gravimetric water content given by:

$$\text{GW (\%)} = (\text{Wet Weight} - \text{Dry Weight}) / (\text{Dry Weight}) \cdot 100$$

In the previous equation, “Dry Weight” is the weight of the dried sample while “Wet Weight” is the actual weight of the sample during the single measurement. The calibration of FDR sensors was made within the range of 0-40% VW, above the substrate soil water holding capacity of about 30%. Figure 2.4 shows calibration curves obtained by soil moisture content measurements of sample S2017, green dots, and sample S2019, green dots. From the observation of Figure 2.4, it results that the same reading provided by the FDR sensor could return, for the sample with root system, a VW at most 90% larger than for the sample without the root system. The closer the VW is to the water holding capacity of the soil, the lower is the difference between actual VW of S2017 and S2019. On the other side, the same value of actual VW returns a lower FDR reading for the sample with root system. This finding would suggest that, likely, a part of the water inside S2019 is adsorbed by the root system but FDR sensor is not able to measure this amount of water. Overall the study highlighted that from the analysis of



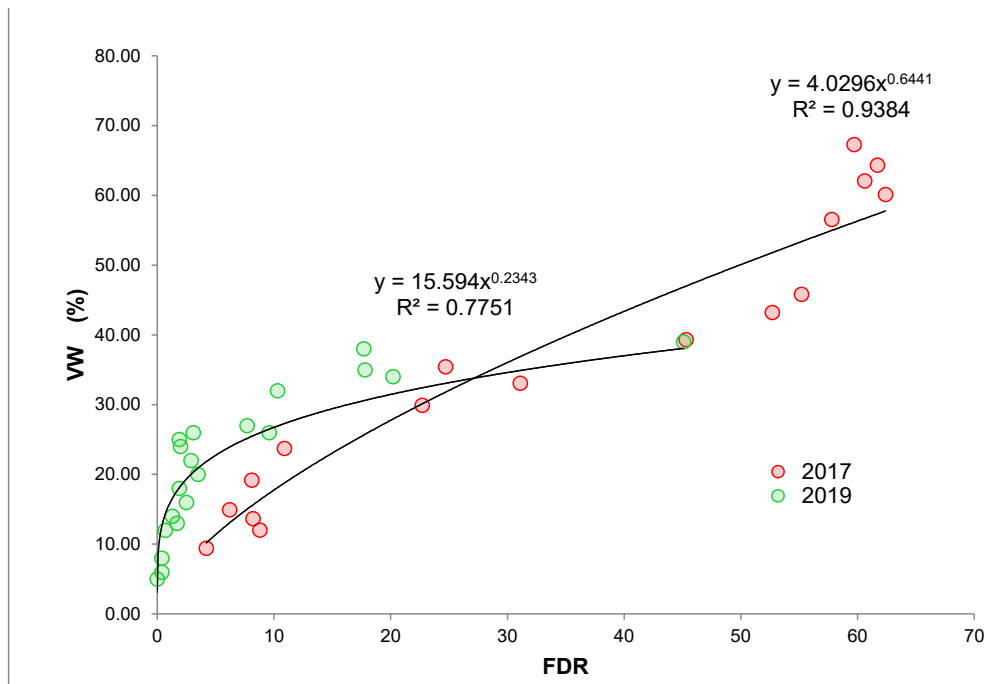


the two samples (with and without root system), the GR hydraulic and physical characteristics could change in a small time period (within 2 years); the use of a unique relationship between FDR measurements and actual VW, calibrated during the GR installation phase would have led to an underestimation in time of the observed values of VW with associated consequences; the monitoring of the VW should be carried out by considering the GR ageing effects.

Below Fig. 2.4 FDR calibration curves

On the left from the top Fig. 2.5 FDR measurement of soil sample Water Content;

Fig. 2.6 FDR sensors WaterScout, Spectrum Technologies;



Long term and event scale climate characterization

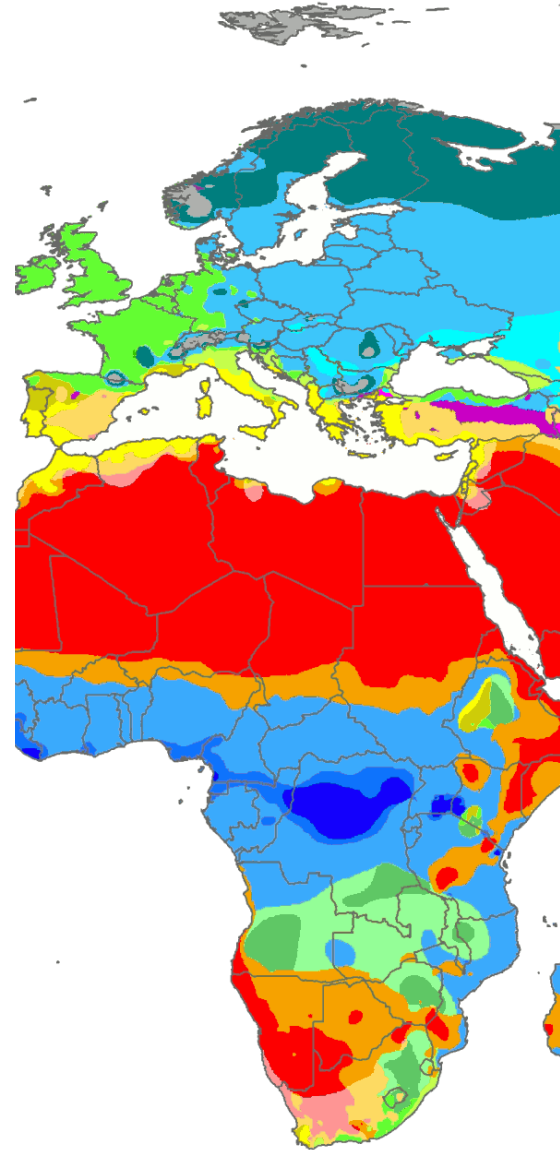
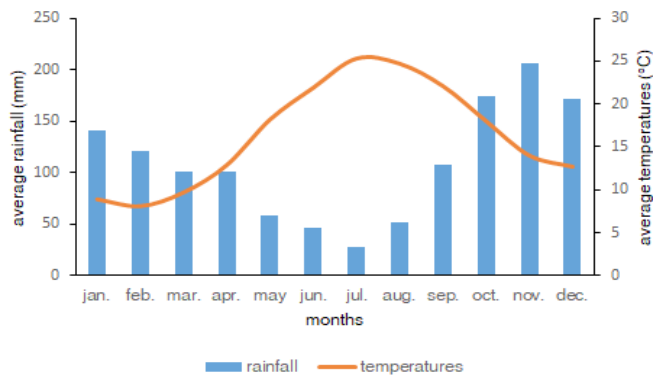
The experimental roofs are located in an outdoor area close to the Maritime and Environmental Hydraulics Laboratory of the University of Salerno (40.770535, 14.789522, 245.50 m a.s.l.). The average annual temperature is 16.4° C while the average annual rainfall is 1307.09 mm. In August, the hottest month of the year, the average temperature is 24.7° C while in February, the coldest month there is an average temperature of 8.1° C. Rainfall and air temperature are clearly characterized by out of phase patterns. The largest fraction of annual rainfall occurs indeed in the period of lowest temperature and lowest evapotranspiration losses, when likely the green roof is characterized by the lower retention capacity. For an event scale characterization, rainfall depth-duration relationships have been estimated according to a regional procedure, where the cumulate precipitation quantile estimation, with non-exceedance probability F , $h(F)$, is obtained by combining the quantile function of the fitted distribution, $g(F)$, commonly referred to as regional growth curve, with the index value, h_m , by using the following expression:

$$h(F) = h_m \cdot g(F)$$

and provided the relation between the return period T and the non-exceedance probability F :

$$T = 1/(1-F)$$

an approximate relation between the growth coefficient for a given value of T , $g(T)$, and value of T itself has been calibrated for extreme rainfall for the homogeneous region the experimental site belongs (Mobilia et al., 2015). Rainfall depth-duration relationships for $T = 2, 5, 10$ and 20 years have been estimated for the purpose of further comparison with the rainfall events occurred at the experimental site.



On the left Fig. 2.7, monthly average rainfall (mm) and temperature (°C) at the experimental site;

Above Fig. 2.8, partial representation of Koppen-Geiger climatic classification from Global Historical Climatology Network (GHCN). The case study climate area is hot-summer Mediterranean climate (Csa)

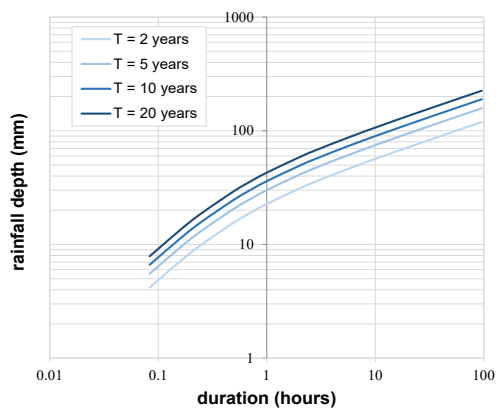
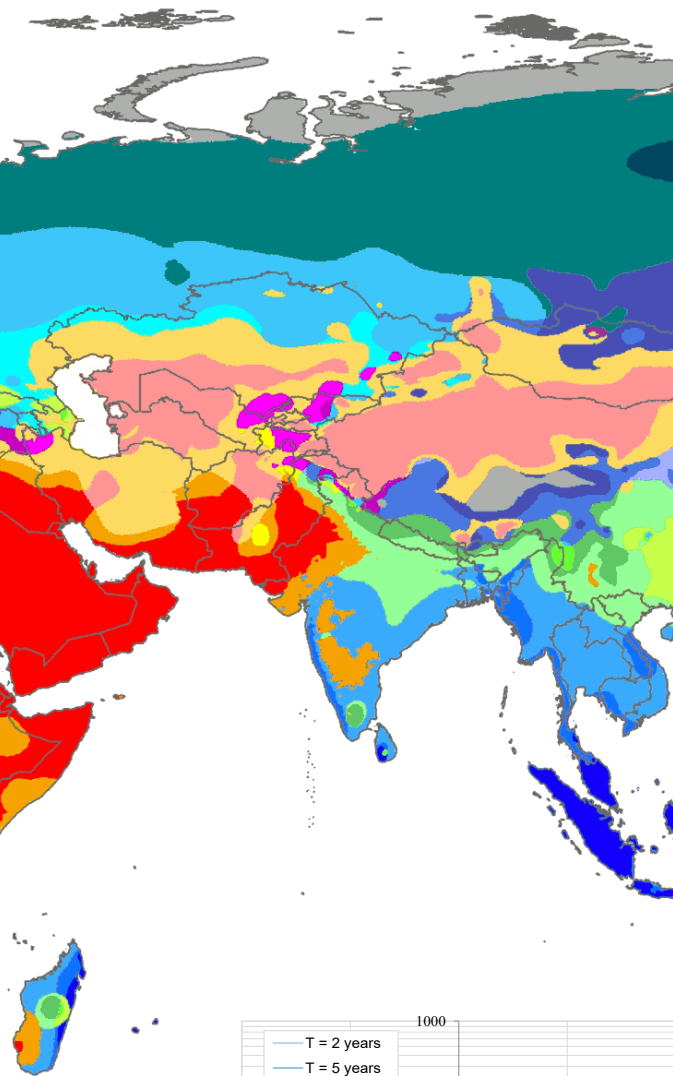


Fig. 2.9 rainfall depth-duration intensity relationships at the experimental site for 2,5,10 and 20 years return period T

Methodology

The event scale analysis concerned 35 rainfall-runoff events that occurred in a period between July 2017 and April 2019. Measurements collected during the first six months of the monitoring period, from January 2017 to July 2017, were not taken into account because the system was considered to be at an early stages and not fully or properly working. The period of observation, although too short to observe and collect severe rainfall, is in line with similar research observation times (Stovin et al., 2012; Nawaz et al., 2015). To avoid mutual dependence of consecutive rainfall-runoff events, an antecedent dry water period of at least 7 hours between two consecutive rainfall events was set as a threshold to select independent events, according to the relevant literature (Nawaz et al., 2015; Soulis et al., 2017; Sims et al., 2016; Stovin et al., 2012). Starting from the raw data, the cumulative rainfall for each selected event, the duration, the maximum 5-minute peak intensity and the return period have been evaluated. The runoff generated by each of the considered rainfall events has been analyzed in order to study the hydrological performance, summarized by the retention capacity (RC):

$$RC=1-(V \text{ runoff})/(V \text{ rainfall})$$

where V is the total volume produced during each event. Volumetric soil water content (VW %) within the substrate layer, collected at a 5 minute step through the capacitance soil moisture probes and converted to actual values through the calibration relationship as previously mentioned, were used to characterize the hydrological initial conditions for each specific event. In order to assess the relative role of climate features, substrate soil moisture content and drainage layer properties on the prediction of green roofs stormwater retention capacity, the correlation between the mentioned variables has been investigated within a multi-step regression approach for both GR₁ and GR₂. Estimates from the optimal regression approach and observation are compared to measure the ability of the regression tools to predict the GRs retention coefficient. Results are reported in the following.

Results

The quantitative characterization of the analyzed rainfall events is reported in Table 2.1. The duration of the rain events ranges from a minimum of 35 minutes to a maximum of about 3 days. As for the cumulative rainfall, it goes from a minimum

value of 0.50 mm to a maximum value of 122.17 mm while, as regards to the peak five minutes' intensity (intended as the maximum rainfall value in a range of 5 minutes), it goes from 0.25 mm/5 min to a maximum of 6.604 mm/5 min.

Event	Duration min	Cumulative rainfall mm	Peak 5-min Intensity mm/5 min
25/07/2017	50	1.78	2.54
26/07/2017	345	22.09	4.31
07/09/2017	545	6.60	1.52
22/10/2017	2235	48.51	6.60
21/01/2018	625	26.16	1.77
01/02/2018	1140	7.11	0.76
12/02/2018	923	4.83	0.50
13/02/2018	40	0.76	0.25
14/02/2018	195	4.82	0.25
18/02/2018	1735	11.17	0.25
20/02/2018	1020	11.43	0.50
02/03/2018	160	3.30	1.01
03/03/2018	635	11.43	0.50
04/03/2018	4565	59.69	3.30
09/04/2018	275	6.35	0.76
12/04/2018	450	0.50	0.25
17/04/2018	290	5.84	2.03
04/05/2018	465	1.52	0.25
09/05/2018	35	1.01	0.25
15/05/2018	630	28.44	5.08
17/05/2018	50	0.51	0.25
22/05/2018	1730	122.17	5.08
05/10/2018	135	2.79	0.25
14/10/2018	335	3.04	0.25
22/10/2018	850	44.7	3.04
27/10/2018	175	4.82	1.77
28/10/2018	165	7.11	0.76
30/10/2018	55	1.01	0.50
22/11/2018	330	1.52	0.50
03/12/2018	1560	13.46	1.01
08/12/2018	20	2.79	1.52
11/03/2019	385	32.00	1.77
12/04/2019	100	5.33	0.50
22/04/2019	85	3.55	0.25
22/04/2019	85	3.55	0.50

Tab. 2.1 Rainfall properties at the event scale

As well as rainfall properties, also runoff and retention capacity values vary widely among the analyzed events as it can be observed from the table below (Table 2.2). Retention capacity ranges

between 4 and 100% in the case of GR₁ (expanded clay aggregate drainage) with an average value of 69%. It ranges between 11 and 100% in the case of GR₂ with an average value of 67%.

Event	VW ₁ %	VW ₂ %	RC ₁ %	RC ₂ %
25/07/2017	5.93	7.12	83	88
26/07/2017	8.43	9.44	71	69
07/09/2017	5.78	3.21	78	78
22/10/2017	7.93	10.75	49	57
21/01/2018	29.90	32.65	31	18
01/02/2018	14.85	18.25	84	80
12/02/2018	23.88	27.62	83	80
13/02/2018	26.23	29.12	91	80
14/02/2018	26.28	29.30	81	77
18/02/2018	24.64	27.37	82	78
20/02/2018	29.89	31.06	20	29
02/03/2018	32.16	32.24	38	40
03/03/2018	32.05	34.09	18	39
04/03/2018	32.04	34.06	4	11
09/04/2018	19.36	22.77	81	81
12/04/2018	18.56	21.31	100	100
17/04/2018	8.85	9.36	85	81
04/05/2018	5.63	4.00	97	79
09/05/2018	21.74	17.00	95	86
15/05/2018	7.89	8.35	76	72
17/05/2018	25.81	25.69	100	85
22/05/2018	7.76	8.60	58	53
05/10/2018	9.42	6.13	86	76
14/10/2018	8.79	7.83	90	80
22/10/2018	7.42	8.05	64	66
27/10/2018	6.44	7.29	84	79
28/10/2018	7.77	7.83	84	74
30/10/2018	20.05	15.01	89	83
22/11/2018	25.24	18.06	75	75
03/12/2018	22.00	27.13	49	51
08/12/2018	18.77	22.16	86	80
11/03/2019	1.78	3.66	63	66
12/04/2019	32.53	28.60	26	38
22/04/2019	5.67	8.09	91	87

Tab. 2.2 Initial substrate soil water content VW (VW₁ and VW₂ refer respectively to the GR₁ and GR₂) and retention coefficient RC (RC₁ and RC₂ refer respectively to the GR₁ and GR₂) at the event scale

As it is well known how the soil water content or relevant proxies can strongly impact the hydrological response of a particular system to a rainfall event, it was considered appropriate to first investigate the experimental relationship between retention capacity (RC) and soil moisture content within the substrate layer prior to the rainfall event occurrence (VW %) (Figure 2.10 a). Contrary to what is conceptually expected, but as it is quite common in the literature because of the nature of experimental data, RC has shown a broad variability, for both GR₁ and GR₂, which unfortunately, both at a first visual inspection and by regression models, has not been justified by the

soil moisture VW values. A polynomial regression between VW and RC only explains about 60% of the RC variance indeed for both GR₁ and GR₂. While in fact a reduction of the retention capacity values (lower than 40%) is detectable for the higher soil water contents (larger than 35%), there is a large range of VW, between 5 and 30%, where the values of RC assume apparently random values between 40 and 100%. As well as for the initial substrate soil water content, according to the correlation coefficient of the regression models (Figure 2.10 b, c and d) also rainfall properties do not appear to adequately explain the RC variance, as confirmed by similar literature studies.

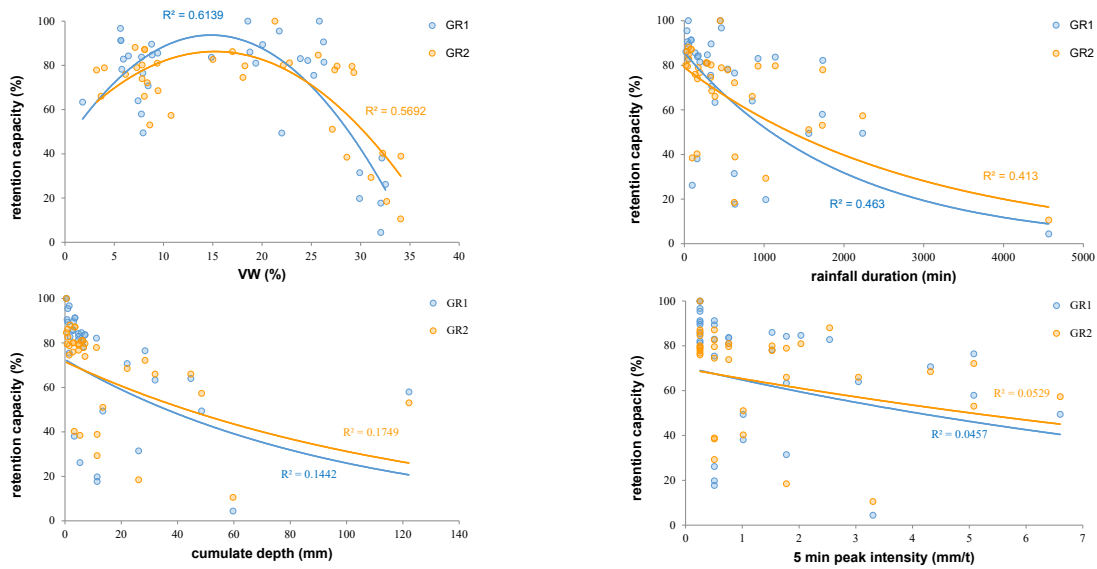


Fig. 2.10 Retention Capacity dependence on initial soil water content VW (a), rainfall duration (b), cumulative depth (c) and rainfall intensity (d)

Multiple regression approaches have also been calibrated for both GR₁ and GR₂, where all of the considered variables are accounted for:

$$RC = -1.12 \cdot DUR - 1.82 \cdot DEPTH - 0.27 \cdot PEAK + 0.01 \cdot VW + 97.24 \quad GR_1$$

$$RC = -1.53 \cdot DUR - 4.32 \cdot DEPTH - 0.21 \cdot PEAK + 0.01 \cdot VW + 109.62 \quad GR_2$$

with DUR rainfall duration, DEPTH cumulative rainfall, PEAK 5 min peak intensity, VW volumetric water content. The explained variance associated to each of them is still relatively poor, amounting to about 56% and 57% respectively for GR₁ and GR₂.

A more detailed investigation of the scatter plot between RC and VW illustrated in Figure 2.10 reveals how runoff events show a tendency to distribute themselves into three distinct groups according to VW thresholds (Figure 2.11). A first group, group A, is characterized by events with intermediate initial soil water content, between 15 and 35%, and a considerable retention capacity, above 75%, and on average about 86%. A second group, group B, is characterized by events with low initial soil water content, between 5 and 15%, and a highly variable retention capacity between 50% and 100%. A third group, group C, is characterized by high soil water content, larger than 30% and retention capacity that never exceeded 50%.

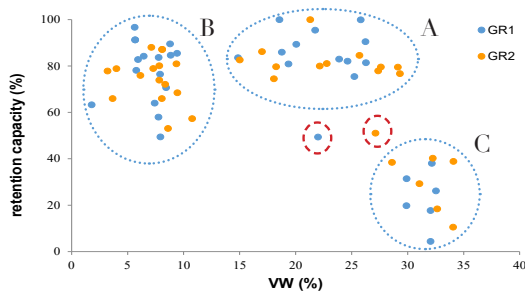


Fig. 2.11 Runoff events groups delineation on the base of initial VW thresholds value. Red shaded circles represent the single event which represents an exception to the general grouping rules

These findings of the empirical analysis lead to the idea that the relationships between the retention capacity and the initial soil water content, and in general, the hydrological response at the investigated experimental site appears governed by VW thresholds. As later shown, points that belong to each of the outlined groups appear in fact to share particular relationships that link the hydrological response RC to certain characteristics of precipitation and which are different for each group and also for each building practice. Further analyzing the relationships

between the initial substrate soil water content and the retention capacity, it was understood that all the rainfall-runoff events belonging to the first group, group A, resulted being characterized by a cumulative rainfall value of less than 11.2 mm and peak 5 minutes intensity lower than 0.762 mm/5 min. These events, about 40% of total analyzed events, even if do not generate large rainwater volume and are therefore irrelevant as regards the quantitative management issues, are instead of considerable importance for what concerns the stormwater quality management. In many cities around the world in fact small stormwater events are drained straight into urban streams causing major ecological issues and the large retention observed in this experimental study could provide indication on how to lower the frequency of such flows. In the case of group A the hydrological behavior of the green roof seems not to be influenced by the initial state of the water content, further returning a very moderate variability of the retention coefficient. For this particular group, GR₁ appears to have a moderately better hydrological performance, with average RC values of about 86% compared to GR₂ characterized by average RC values of about 80%. No significant relationship was additionally found for this group between the retention coefficient and the remaining parameters describing the characteristics of the rainfall. An exception to this grouping is represented by a single event, occurred on 12/03/2018 (Figure 2.11, red dashed circles) which, according to the initial VW values, should belong to group A, but which shows significantly lower retentions, compared to this group, most likely due to a cumulative rainfall and a rainfall peak intensity that exceed the thresholds identified for group A (13.46 mm and 1.01 mm / 5 min respectively). As regards, instead, to the second group of events, group B, as they

are characterized by low initial water content of the substrate soil layer (between 5 and 15%), they are potentially prone to a significant reduction in stormwater volumes. They represent the most frequent type of events at the experimental site, as they amount to 45% of the total analyzed events. A high variability is highlighted for the values of the retention coefficient, which does not appear strongly dependent on initial substrate soil moisture content but can be actually explained according to the characteristics of the rainfall events, as illustrated in Figure 2.12 left panel (a, b, c). As a general trend, the GR retention capacities related to this type of events (group B) decrease as the duration (Figure 2.12_l a), the cumulative depth (Figure 2.12_l b) and the precipitation intensity increase (Figure 2.12_l c). A regression analysis found a negative exponential relationship between the retention properties and the rainfall duration and cumulative volume. This circumstance would indicate significant changes in the GR retention capacities in the case of short and moderate rainfall events. A linear relation was instead found between retention properties and peak 5 minutes intensity. The Pearson correlation coefficients of the regression models illustrated in Figure 2.12_l b, showed that the cumulative rainfall volume appeared to be the best predictor for GR retention properties within this specific group B (explained variance of about 80% for both GR₁ and GR₂). According to the quantitative estimation and the regression analysis, the difference between GR₁ and GR₂ retention coefficients is negligible in the case of group B, amounting on average to about 7 % (minimum difference 0.3% maximum difference 11.7%). It is also evident that the major differences between GR₁ and GR₂ are observed for minor events. As the severity of the rainfall event increases, the retention coefficients for GR₁ and GR₂ approach similar values. The

third group of events, group C (Figure 2.11), represents the set of runoff events characterized by the lower retention performances associated to the larger substrate soil water content prior to the triggering rainfall event. They represent the least frequent type of events at the experimental site, as they amount only to 15% of the total analyzed events. A larger number of events would certainly have given greater significance to the empirical analysis but, probably due to the very fast vertical drainage process within the substrate layer, GR systems are very unlikely to persist in the state of large substrate soil water content. As in the case of group B, a high variability is highlighted for the values of the retention coefficient, never larger than 50%, which does not appear strongly dependent on initial substrate soil moisture content but can be actually explained according to the characteristics of the rainfall events, as illustrated in Figure 2.12 right panel (a, b, c). Also in this case, the GR retention capacities related to this type of events (group C) decrease as the duration (Figure 2.12_r a), the cumulative depth (Figure 2.12_r b) and the precipitation intensity increase (Figure 2.12_r c). A regression analysis found a negative exponential relationship between the retention coefficients and all of the considered rainfall properties, included the 5 min peak intensity. Again, this circumstance would indicate significant changes in the GR retention capacities in the case of short and moderate rainfall events, also in the case of large prior VW. According to the Pearson correlation coefficients of the regression models illustrated in Fig 2.12_r a and b, both the rainfall duration and the cumulative rainfall volume (explained variance of about 59% and 86% respectively for GR₁ and GR₂) appeared to be the best predictor for GR retention properties within group C. Contrarily to what occurs in the case of group B, a non-negligible difference between GR₁

and GR2 retention coefficients can be detected from the regression analysis, amounting on average to about 26 %, with GR2 showing the better hydrological performances. As previously discussed and based on the results of laboratory experiments, provided the same substrate layer building practices for each of the test beds, the differences in the GRs retention properties could be ascribed to the differences in the drainage layer building practices. It is likely that in the case of large initial VW, contrarily to what occurs in the case of low initial VW, the faster drainage from the substrate to the drainage layer sees the drainage layer largely involved in the retention

process. Congruently, the GR2, which has a larger retention capacity than the GR1, exhibits the best performance. The differences between the retention capacities of the two test beds, measured in the laboratory, amount to around 18% but they can probably be larger in consideration of a “storage” effect that the MODI tray panel generates because of its shape (the difference could increase up to 34% in the case the MODI plastic tray is not filled with the expanded clay). Differences between GR1 and GR2 hydrological performances are almost the same regardless for the rainfall event characteristics, with a negligible larger difference in the case of larger events.

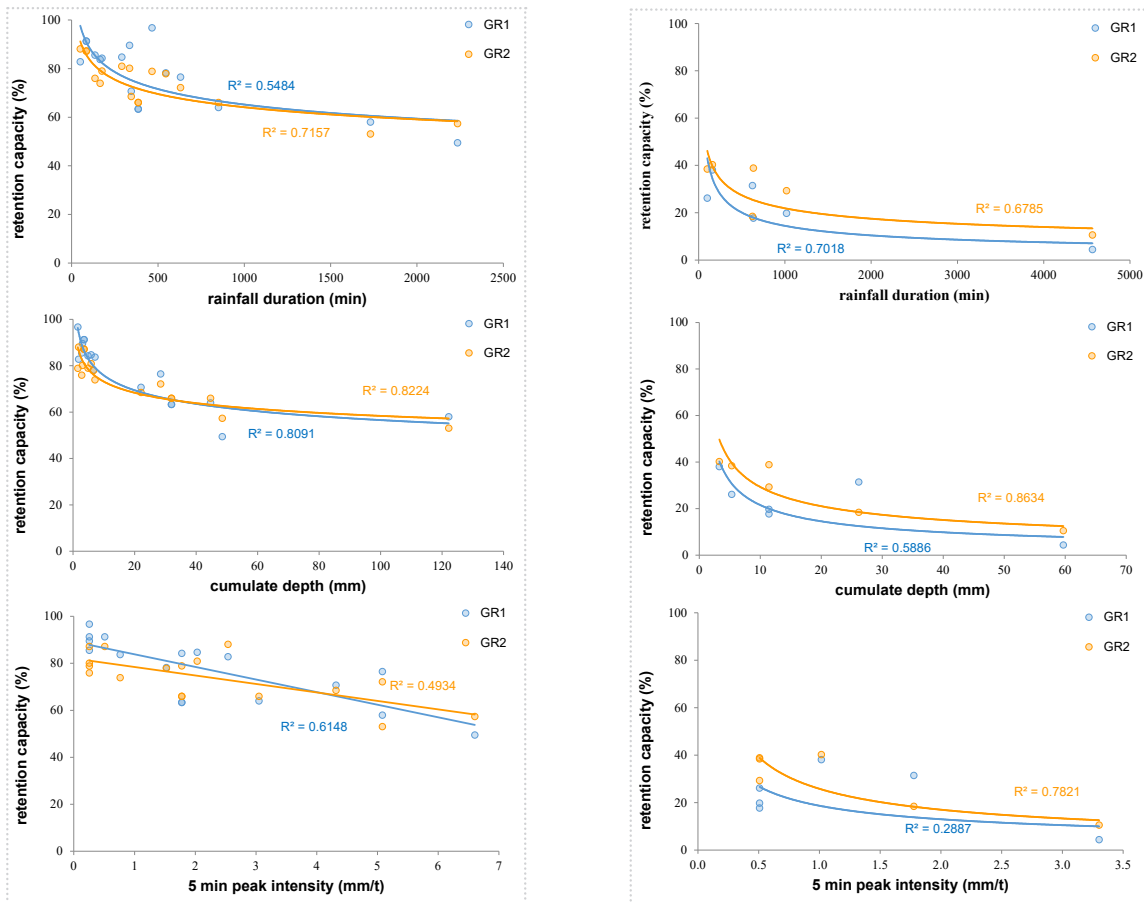
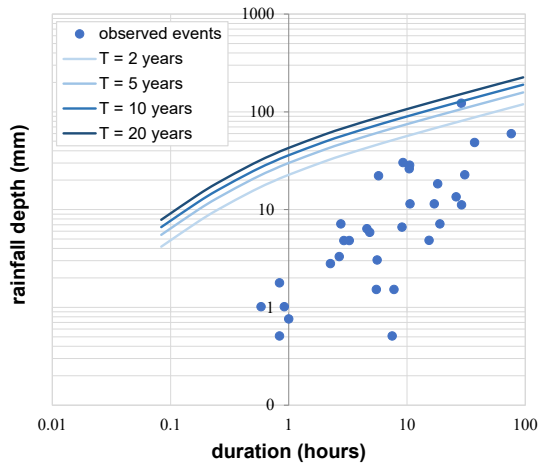


Fig. 2.12 Relationships between Retention Capacity and rainfall duration, cumulative depth, peak 5-min intensity. Left panel (2.12_l): group B (soil moisture content between 5-15%). Right panel (2.12_r): group C (soil moisture content > 30%)

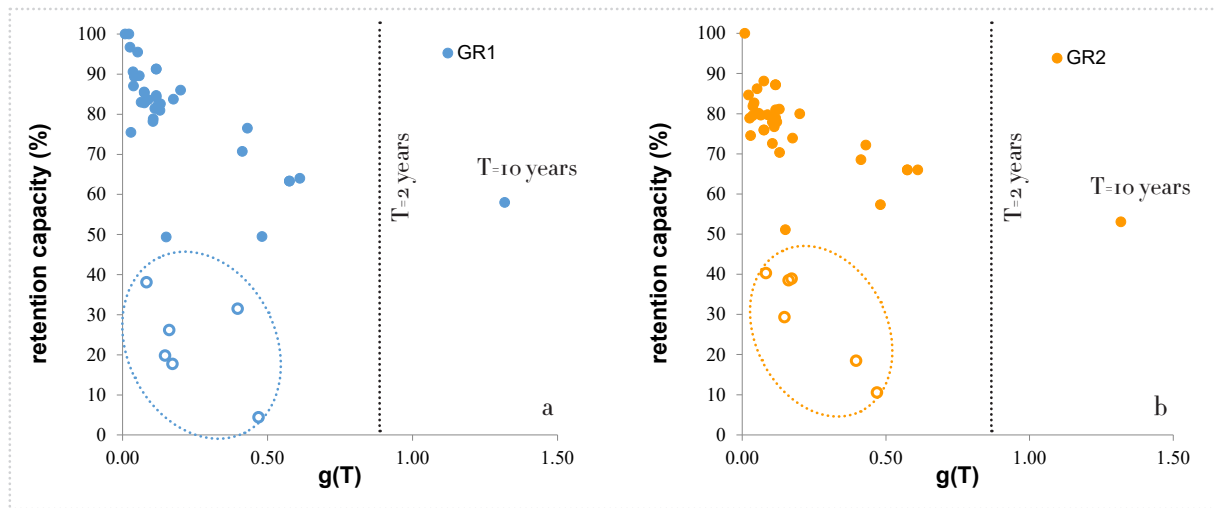
The combination of rainfall depth and duration for the analyzed events are reported in Figure 2.13, along with the rainfall depth-duration-intensity regional curves, plotted for different return periods. Occurred events do not appear particularly severe. They are indeed clearly bounded by a two years return period rainfall depth-duration curve, with an exception for the 22 May 2018 event, for which the maximum cumulative rainfall of about 122 mm is characterized by a return period of about 10 years. Rainfall severity, measured through the rainfall return period, also appears to play a role in the variability of the retention coefficient. For each of the analyzed events, the growth coefficient

for each event has been assessed and plotted against the corresponding retention coefficient for both GR₁ and GR₂, as represented in Figure 2.14 a and b. If the groups of the events with initial soil moisture larger than 30% is excluded from the analysis (group C), for both GR₁ and GR₂ the retention coefficients appear to decrease for increasing value of $g(T)$ that is for increasing T . Even though a single severe event ($T = 10$ years) was recorded during the monitoring period, 22 May 2018, the retention coefficients for the investigated experimental sites appear significant also in this specific case.



On the left Fig. 2.13, rainfall depth-duration intensity relationships at the experimental site for 2,5,10 and 20 years return period T . Shaded circles represents the analyzed rainfall events;

Below figure 2.14, Retention Coefficient at GR₁ (a) and GR₂ (b) as a function of the rainfall growth coefficient $g(T)$



To measure the reliability of the idea that the identification of homogeneous rainfall-runoff event groups can help improve the prediction of RC in a regressive approach, the empirical relationships which link the RC values to the climatic variables as represented in Figure 2.12 were used to predict the value of RC. The results are shown in Figure 2.15. The comparison between the predicted and observed data, together with the

large explained variance ($R^2 = 0.93$ for GR₁ and $R^2 = 0.92$ for GR₂) and the prediction intervals represent a model verification of the proposed approach, also as regards to the prediction in the case of events characterized by a high return period, evidencing the effectiveness of RC prediction from rainfall data with a prior identification of groups of similar hydrological behavior.

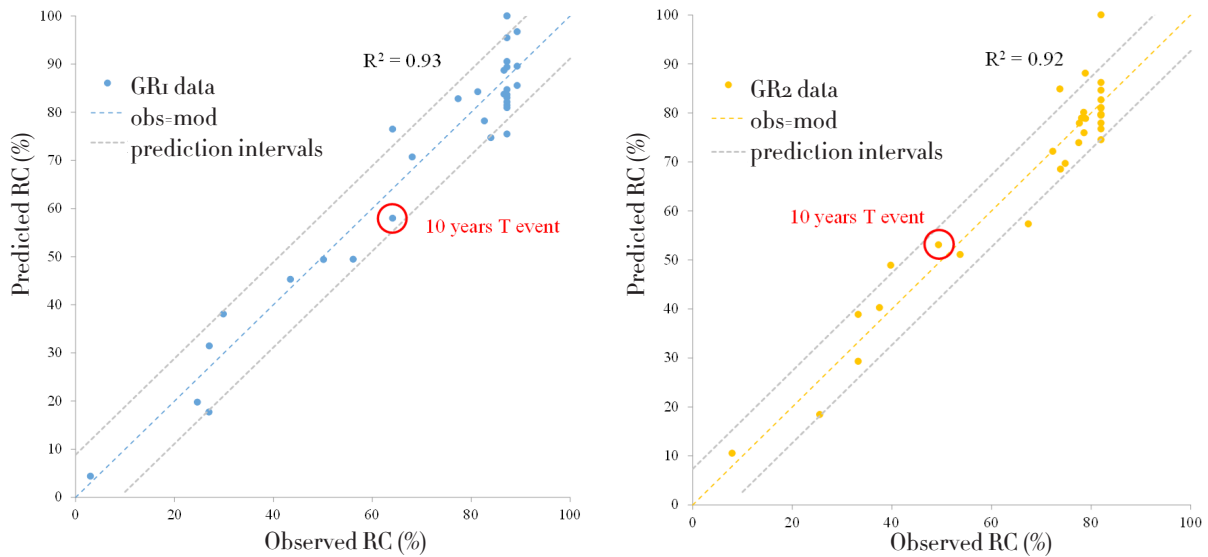


Fig. 2.15 comparison between observed and predicted retention coefficients at both GR₁ (left panel) and GR₂ (right panel). Prediction intervals at 5% confidence level are plotted



Assessing Green Roofs performance under controlled conditions: Set up of indoor GRs test site

This research is not yet completed but it is considered important to report here the key assumptions, the experimental set up and the objectives.

This research activity arises from the need to investigate how physical constraints of the outdoor experimental site could somehow affect the behaviour of these systems. In fact, the dimensions of the models and the impossibility to test GRs performance under severe rainfalls, due to limits in the runoff assessment, led to the set-up of indoor experiments under controlled conditions. In addition, reproducing the same design of outdoor GRs, a comparison between the two experimental sites can be interesting for analysing the effect of ageing (i.e. increase soil layer compaction and the presence of a developed root system) on the performance of these infrastructures. In order to have a greater flexibility in planning such experiments, two plexiglass cases of various sizes have been designed and ordered. The idea was to fill them based on occurrence, according to GRs layouts different for design and technological parameters (i.e. layer depths and materials). Design schemes are reported in Figure 2.16 and 2.17.



On the right Fig. 2.18 Experimental set-up, earlier tests

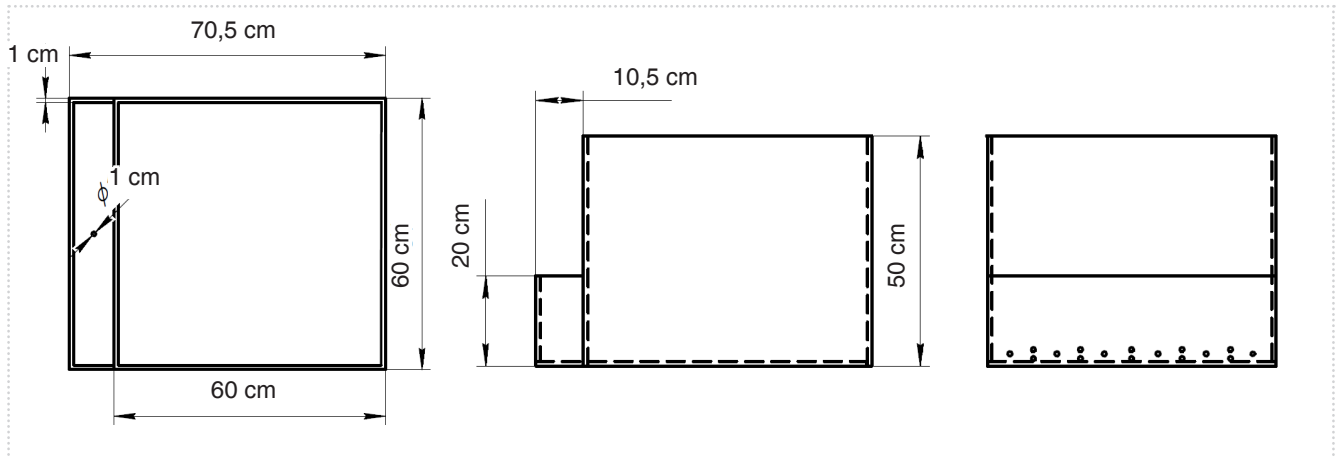


Fig. 2.16 Design schemes of “Small” GR plexiglass case

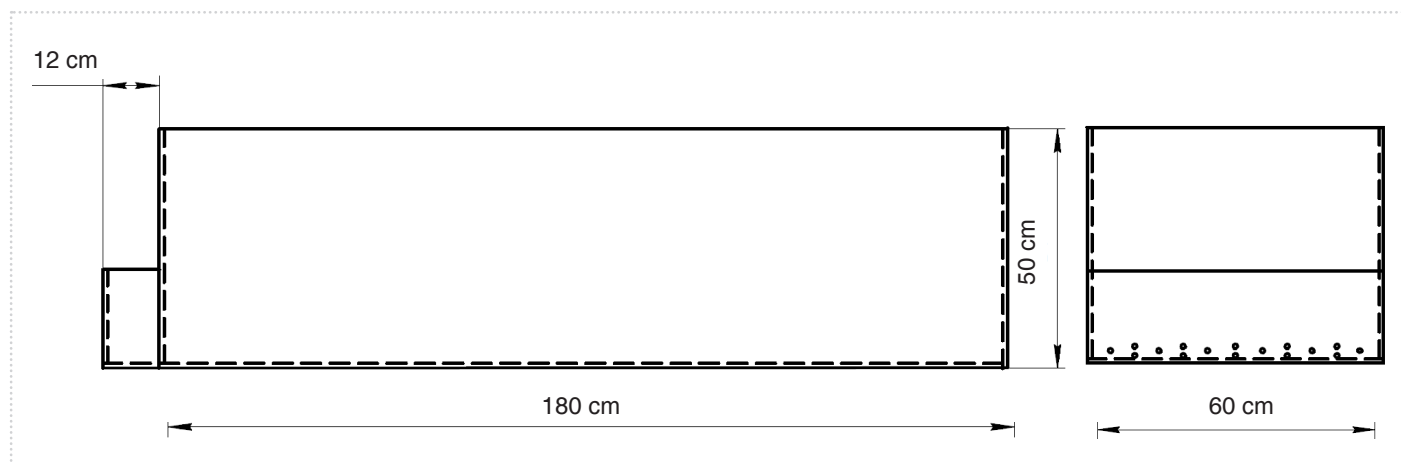


Fig. 2.17 Design schemes of "Large" GR plexiglass case

Such experimental activity involves different steps: definition of objectives, programming of experiments, soil moisture probe calibration, set-up of indoor experimental green roofs, tests, data collection and analysis of results. Early experiments (Figure 2.19) provide the reproduction of GR_i design in both the plexiglass cases (using the same materials and layers depths) to test their performance, in terms of

runoff retention and detention (delay time), under growing intensity precipitation inputs and to understand how the dimensions can affect GRs behaviour. Runoff, collected into tanks, is monitored and measured through scales; soil moisture content, considered a key element, is measured in specific point of the test roofs (5 for the “small” and 8 for the “large”) using TDR probes “Hydrosense II” by Campbell Scientific.



Fig. 2.19 Experimental set-up latest tests, materials and instruments



Fig. 2.20 Soil sample preparation for calibration of TDR Hydrosense II probes

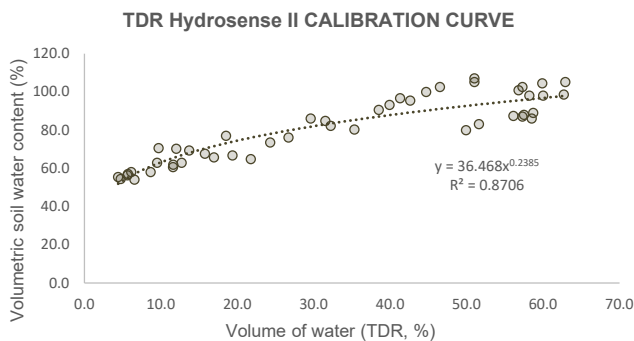
In a borosilicate glass of 1500 litres (430 g) 310 g of soil constituting the substrate layer of GRs have been inserted. The soil is made of a mix of blond peat, baltic brown peat, zeolites and simple non-composted vegetable primer (coconut fibers), completed with the addition of a mineral fertilizer (biostimulant algae). In order to obtain the wettest condition, 1640 g of water have been inserted into the glass and, after the first soil moisture measurement by TDR, the drying process began. The TDR calibration curve was obtained by plotting each value of the soil moisture content provided by the TDR sensor against the corresponding volumetric water content (VW) of the sample. In total, 47 TDR measurements were collected. For each reading the VW has been derived as:

$$VW \% = GW (\%) \cdot BD$$

Where BD is the the bulk density of the soil (0.20 g cm^{-3}) and GW is the gravimetric water content given by:

$$GW (\%) = (\text{Wet Weight} - \text{Dry Weight}) / (\text{Dry Weight}) \cdot 100$$

In the previous equation, “Dry Weight” is the weight of the dried sample while “Wet Weight” is the actual weight of the sample during the single measurement.



On the left Fig. 2.21 TDR Hydrosense II calibration curve

Assessment of GRs retrofitting surface to counteract land use changes effects: the case study of Mercato San Severino (SA)

This research merged into the paper “Sustainable strategies for flood risk management in urban areas. Enhancing city resilience with Green Roofs” for the journal UPLanD (D’Ambrosio, Longobardi, Mobilia & Sassone, 2021).

This study focused on the identification of land use changes and hydraulic vulnerability increase in a catchment in the Municipality of Mercato San Severino (Sa, Campania Region, IT) for the identification of the Green Roofs retrofitting surface able to restore drainage patterns typical of the period prior to the urban development. Mercato San Severino’s climate is classified as warm and temperate. According to Köppen and Geiger, this climate is classified as Csa. The average temperature is 15.4 °C. The average rainfall is around 868 mm per year. The least amount of rainfall occurs in July (24 mm on average). Most of the precipitation falls in November, averaging 128 mm while the highest temperatures occur in August (on average 23.4 °C). January is the coldest month, with temperatures averaging 8.2 °C. The variation in the precipitation between the driest and wettest months is 104 mm while throughout the year, temperatures vary by 15.2 °C. The study area, included in the Sarno catchment, experienced over the years a substantial anthropization, which altered its natural conformation increasing flooding risk. Therefore, several floods affected the area during the years (1995-2016) with a substantial increase (+350 %) of this phenomena in the last decades (2005-2016), characterized by invasive urbanization dynamics and soil sealing (Longobardi et al., 2016). In addition, for a correct evaluation of the Hydraulic Risk in the study area, from the Hydrogeological Plan (P.S.A.I.) of the Campania Region Basin Authority, maps with specific reference to the hydraulic risk were downloaded and analysed. The cartography shows that the territory in which the case study is located, is mainly characterized by a moderate and medium risk with numerous areas potentially prone to high risk. In Figure 2.23 the identification of the watershed and its subdivision in 5 areas (A1, A2, A3, A4, A5) is represented.

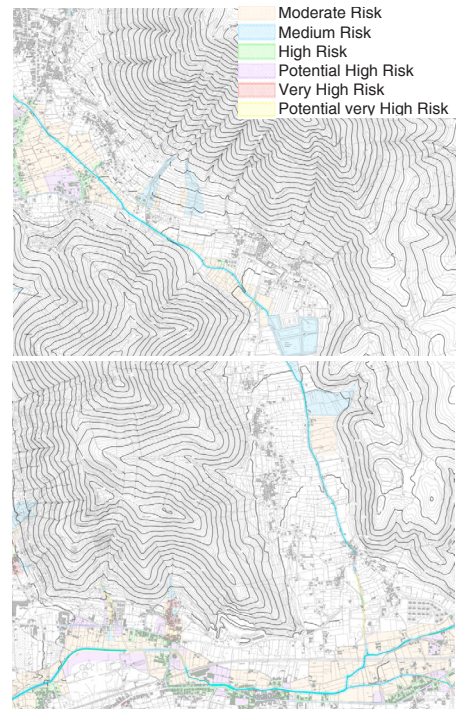
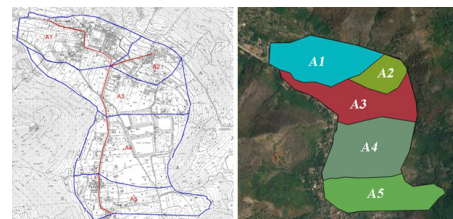


Fig. 2.22 Sarno Catchment Authority, Hydraulic Risk Map (n. 449132, n. 467011);

Below Fig. 2.23 Identification of the watershed and its subdivision in 5 areas



SAR images elaboration for the detection of variation in build-up area

The land use change in the study area between 1995 and 2016 was investigated by means of elaboration of SAR images (Mobilia et al., 2018). The processing chain included three major blocks: data download, pre-processing phase and the feature extraction. The first step consisted in the acquisition of SAR images relating to the years 1995 and 2016 and respectively provided by ERS and Cosmo-SkyMed missions (Figure 2.24). The pre-processing chain aimed at the data coregistration and at the coherence estimation. The coregistration is a key procedure to be carried out before starting the analysis; it involves the matching of two SAR images at up to one or two-pixel accuracy. The coherence (γ) of the images, instead, is extracted and represents the spatial correlation of the interferometric phases of two SAR images (v_1 and v_2) given as:

$$\gamma = \frac{E[v_1 v_2^*]}{\sqrt{E[v_1]^2 E[v_2]^2}}$$

where $E[.]$ means the expected value and the $*$ the complex conjugate. It moves from 0 to 1 where 0 refers to the natural land cover and 1 to the built-up area. The feature extraction block included: the execution of the temporal average of the multitemporal SAR images in order to reduce the speckle; the coherence threshold assessment using Otsu's algorithm for the conversion of grey level image to monochrome (or binary) image where the white pixels represent the impervious surfaces while the black one the pervious ones; and the threshold application which allows to subsequently quantify the paved and non/paved surfaces using the QGIS software. For each sub-catchment of the municipality, the white and black pixels were identified in the threshold images and the corresponding area was calculated according to the following equations:

$$A_{\text{imp}} = (N_{\text{whitepixels}} * A_{\text{tot}}) / N_{\text{totalpixels}}$$

$$A_{\text{perv}} = (N_{\text{blackpixels}} * A_{\text{tot}}) / N_{\text{totalpixels}}$$

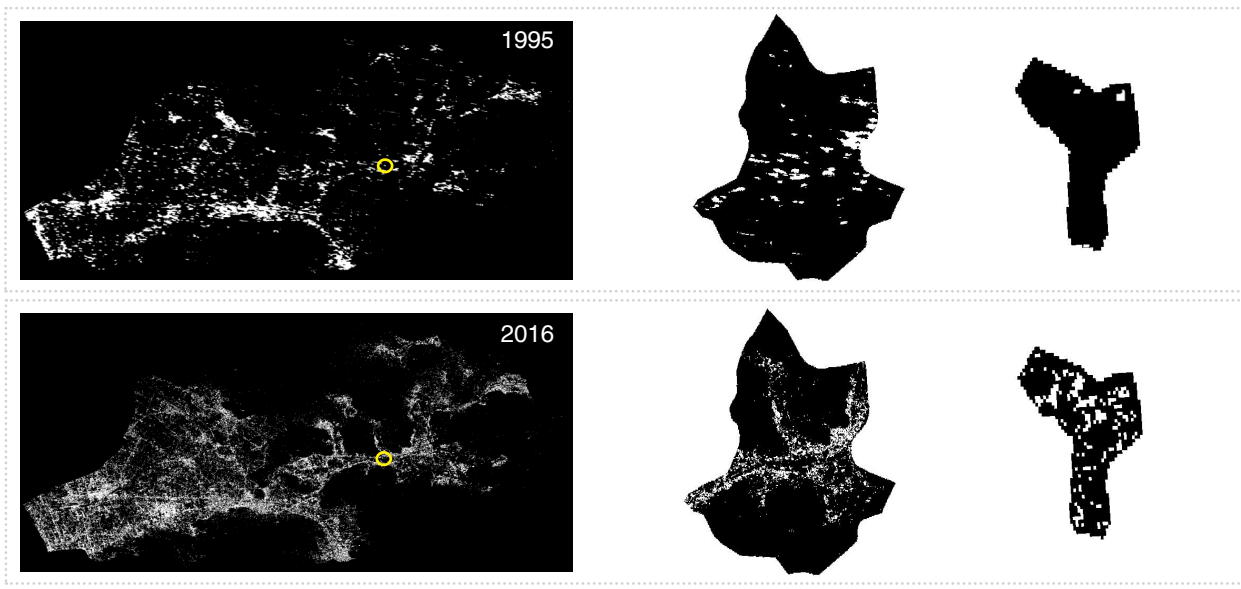


Fig. 2.24 Sarno Catchment, Mercato San Severino and case study area raster images in 1995 and 2016

Where:

$N_{\text{pixel white}}$ = number of white pixels

$N_{\text{pixel black}}$ = number of black pixels

$N_{\text{pixel tot}}$ = number of total pixels

A_{perv} = pervious area

A_{imp} = impervious area

A_{tot} = total area

Estimation of hydraulic and hydrological variations of the catchment between 1995 and 2016

In order to investigate the effect of land use change between 1995 and 2016 on stormwater generation, a series of fundamental parameters have been calculated and compared for each year and for each sub-basin. The selected parameter are: critical duration (d) runoff coefficient (C^*), average rainfall intensity for critical duration ($i_m(d)$), average flow rate (Q_m) and peak flow rate (Q_T).

$$d = 1.40 \cdot L^{0.24} \cdot P_i^{-0.24} \cdot P_m^{-0.16}$$

$$C^* = 0.8 \cdot \frac{A_{\text{imp}}}{A_{\text{tot}}} + 0.1 \cdot \frac{A_{\text{per}}}{A_{\text{tot}}}$$

$$i_m(d) = \frac{i_0}{[1 + d/d_c]^{C-DZ}}$$

$$Q_m = C^* \cdot A_{\text{tot}} \cdot i_m(d)$$

$$Q_T = K_T \cdot Q_m$$

Where L is the is length of pipe, P_i is the ratio between the imperviousness area of the basin (A_{imp}) and the total area (A_{tot}), P_m is the slope of the pipe, A_{per} is the pervious area of the basin, i_0 , d_c , C , D are constant values given by the regional law in four parameters of VAPI Campania report (Rossi & Villani, 1994) and tabulated according to

homogeneous areas, z is the altitude of the basins, K_T is the probabilistic factor of growth expressed as:

$$K_T = -0.0373 + 0.517 \cdot \ln(T)$$

Where T is the return period set at 10 years.

Green roof retrofitting scenario

In order to return to the pre-development condition, a widespread implementation of green roofs was hypothesized within the studied catchment. The quantitative estimation of potential area for green retrofit (A_{GR}) was made by equalling the runoff coefficient relating to the year 1995 (C_{1995}^*) which corresponds to the pre-development scenario, to the runoff coefficient which refers to a GR conversion scenario (C_{GR}^*):

$$C_{1995}^* = 0.8 \cdot \frac{A_{\text{imp}}}{A_{\text{tot}}} + 0.1 \cdot \frac{A_{\text{per}}}{A_{\text{tot}}}$$

$$C_{\text{GR}}^* = 0.8 \cdot \frac{A_{\text{imp}}}{A_{\text{tot}}} + 0.1 \cdot \frac{A_{\text{per}}}{A_{\text{tot}}} + c_{\text{GR}} \frac{A_{\text{GR}}}{A_{\text{tot}}}$$

Where c_{GR} , expressed as “i-RC”, can be deduced from the relation between retention capacity (RC) and 5-minute peak intensity of Figure 2.12 (left panel, group B) found in the previously mentioned experimental analysis (Figure 2.25), once known the rainfall intensity of each sub-basin.

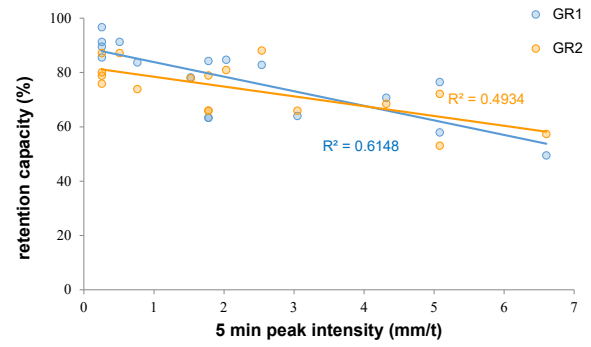


Fig. 2.25 Relation between retention capacity (RC) and 5-minute peak intensity from the experimental analysis on Green Roofs conducted at Unisa

Results

Table 1 summarizes the assessment of permeable and impermeable surfaces (expressed in m²) referred to the year 1995 and 2016. The results of this first analysis made it possible to understand

that the impervious surface of 1.17% of the year 1995 changed into 19.17% in the year 2016. From the difference between the percentages of impervious areas recorded in the two years, a variation of the impervious fraction of 18% was obtained

Surface	Type	Proportion pixel-area (1995)			Proportion pixel-area (2016)		
		Number pixels	Total Area (m ²)	Area (m ²)	Number pixels	Total Area (m ²)	Area (m ²)
A1	pervious	448	246288,23	244108,69	389	246288,23	211960,45
	impervious	4		2179,54	63		34327,78
A2	pervious	149	101065,52	96530,53	123	101065,52	79686,28
	impervious	7		4534,99	33		21379,24
A3	pervious	1029	608945,02	602504,26	896	608945,02	524629,56
	impervious	11		6440,76	144		84315,46
A4	pervious	1562	944519,04	937914,01	1403	944519,04	842441,33
	impervious	11		6605,03	170		102077,71
A5	pervious	1974	1140431,12	1128992,49	1796	1140431,12	1027188,71
	impervious	20		11438,63	198		113242,41

Tab. 2.3 From pixels to impervious and pervious area in each subcatchment for the year 1995 and 2016

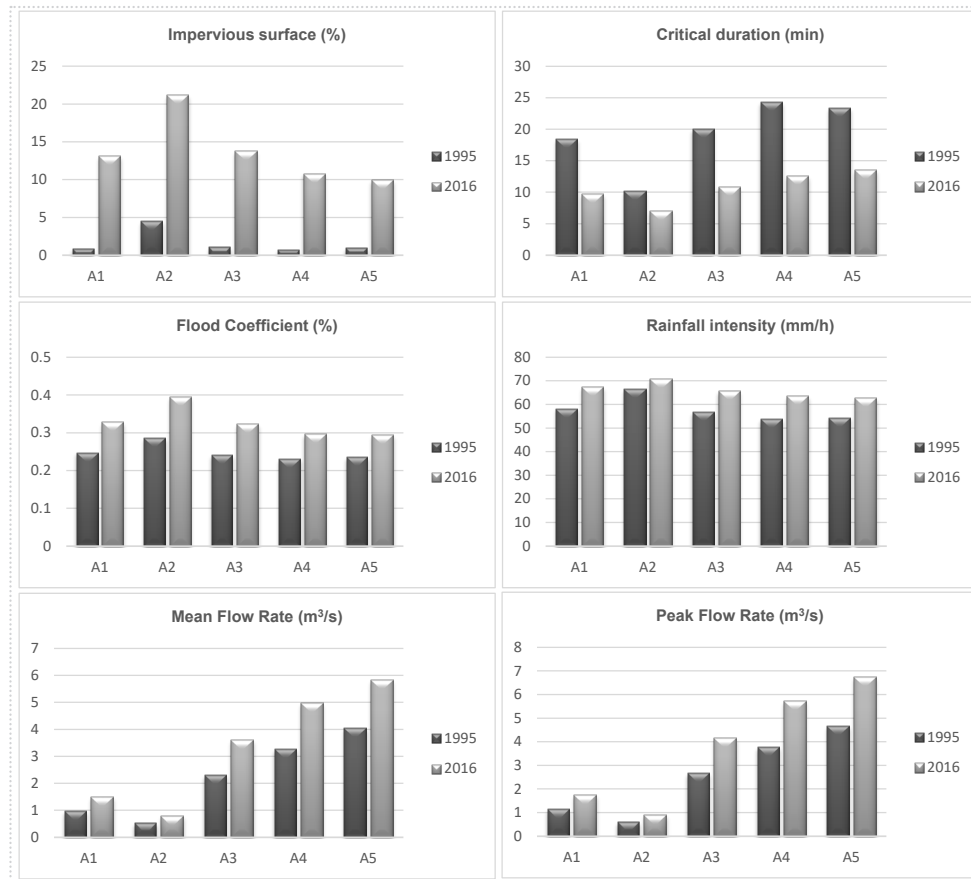


Fig. 2.26 Hydrological parameters comparison between year 1995 and 2016 in each subcatchment

for the case study area. From the observation of the plots shown in Figure 2.26, we notice that over time, together with a clear and predictable increase in the impermeable surface, the values of the parameters listed above also increased. The critical duration is an exception as an increase in impervious areas is usually associated to an enhancement of flash flood phenomena and a lowering of this variable. The parameters which appeared to be affected at a larger extent by the land use changes are the critical duration and the runoff coefficient. These variables, both dependant on the imperviousness of the soil, recorded an average percentage of variation of 32% and 42% respectively, which than translated into a flow rate increase of about 50%. Overall, land use changes led to an overload of the drainage network, actually affected by several criticalities in many sections of the drainage network, and to

an increase of urban flooding phenomena. The previously analysed parameters are inextricably linked to the percentage of imperviousness of the basin. Therefore, the only chance to restore the initial conditions of the territory is to implement retrofitting actions of the urbanized areas through typical urban greening strategies that directly affect the flood coefficient C and, indirectly, the flow rate Q that the drainage network must handle. However, as we can see from Table 2.4, in order to make the implementation of these sustainable infrastructures more effective in the management of urban flooding, a too large portion of the current impermeable surface should be retrofitted, almost 70%. The preferable strategy, so, is that of using green roofs only as mitigation techniques, aiming not at the total restoration of the conditions prior to construction but at a partial reduction of the load introduced into the sewer.

Catchment Section	Area	Retrofitting percentage (%)
C	A1	83
C	A2	45
D	A3	66
E	A4	80
F	A5	76

Tab. 2.4 Identification of the percentage of Roof Greening to avoid hydraulic criticalities



Modern representation of Babilonia roof-gardens
<https://cultura.biografieonline.it/giardini-pensili-babilonia/>

Final discussions

Starting from two years of data collected at two experimental extensive green roof test beds, located in Southern Italy, the hydrological performance of such infrastructure was studied. Moreover, considering GRs performance strongly dependent on substrate soil moisture content, prior experiments helped to understand that the GR ageing, and in particular the growth of the root system, impacted the FDR sensors measurement of the water in the substrate. A careful calibration procedure was then needed to return accurate measurements of VW and to avoid an incorrect assessment of the GR performances. Through the joint analysis of rainfall events characteristics, substrate soil water content prior to the triggering rainfall event and building practices, an empirical rainfall-runoff analysis of 35 selected events was performed, highlighting the role that each of the mentioned variables has, for the case under analysis, on the GRs retention properties. Uncertainty in the application of simple or multiple regression approaches and in the role played by the VW on RC prediction has been confirmed by the present study. The dependence of RC from VW does not appear strongly functional but important to the a-priori identification of groups of rainfall-runoff runoff events which leads to an improvement in regressive approaches for RC prediction. In particular, based on VW thresholds, two groups were identified for the case study, group B with low initial moisture content (between 5 and 15%) and group C with a high initial moisture content (> 30%), within which the prediction of RC values can be performed referring to the specific characteristics of the rain events. A third group A is also outlined for which the relation of RC with VW totally disappears. It can be identified referring to a rainfall depth

threshold of 11.2 mm and a peak 5 minute intensity threshold of 0.762 mm/5 min and is characterized by an almost constant RC value. The functional relationships that relate the RC coefficients to the rainfall properties have a different calibration for each group but all describe a tendency in a reduction of retention properties for large events and mainly see the rainfall cumulate depth as the best predictor for RC estimation, with an explained variance of about 80%. The functional relationships that relate the RC coefficients to the rainfall properties furthermore appear different, within the same group, for GR₁ and GR₂, highlighting the role played by the drainage layer building practices on the GRs retention properties. In fact, since the two test beds are characterized by the same vegetation, substrate depth and hydraulic properties, the differences in the RC quantitative assessment can only be ascribed to the drainage layer properties. It was found that the difference in the GRs hydrological performance in the case of low initial VW (group B) are almost negligible (7%). This circumstance would probably entails that for this particular type of events the main role in the retention process is played by the vegetation and substrate layers. Differences in the hydrological behavior increase up to 26% in the case of high initial VW (group C). In the case of large initial VW the faster drainage from the substrate to the drainage layer sees the drainage layer largely involved in the retention process. The GR₂, which has a larger retention capacity than the GR₁, exhibits the best performance indeed. The severity of the rainfall events, as described by the return period, was only accidentally studied for the case study as only one of the thirty-five selected rainfall events is featured by an high return period, of 10 years. The retention coefficients for this particular



COPHILL, COPENAGHEN (DK)
<https://www.cph.dk/en/cph-business/aviation/copenhagen-connections/copenhill>

event appeared significant, amounting to 58% and 53% respectively for GR₁ and GR₂. This particular event occurred for low initial VW conditions indeed, which could have been the reason for a significant retention nevertheless the rainfall severity. As mentioned, the characteristics of the rainfall events selected depend for sure on the site climate conditions but also on the length of the monitoring period (about 3 years), too short to observe numerous severe precipitations although in line with similar research observation times. Longer monitoring period and indoor experiments under controlled conditions would probably increase the probability to face larger return period rainfall events in order to detect the relevant GRs hydrological performance and to understand if the results discussed so far could also apply in occasion of severe rainfall ($T > 5$). Thereafter, the effectiveness of green roofs retrofitting strategies was assessed for a case study area, included in the Sarno catchment, that experienced between 1995 and 2016 an increase of the impervious fraction of 18% and consequently flooding risk. However, in order to make green roof retrofitting effective in the reduction of stormwater volumes and in the restoration of the natural pattern prior to the massive urbanization, a too large portion of the current impermeable surface should be retrofitted. Green Roofs undoubtedly represent a useful tool to make cities more resilient against hydraulic risk due to their stormwater retention and detention capacity. Nevertheless, findings suggest that the preferable strategy is that of implementing a combined approach in which Green Roofs and other Sustainable Drainage Systems located within the urban context (drainage trenches, bioretention cells, pervious parking lots, rain gardens) support the traditional drainage systems in the management and reduction of urban flooding.

If building sprang up suddenly out of the ground like mushrooms, their rooftops would be covered with a layer of soil and plants.

VERLYN KLINKENBORG,
“Up on the roof”, National Geographic, May 2009



Picture by a "Traveller" on Pinterest - FAROE ISLANDS, NORWAY

Chapter 3

Re-think urban drainage with SuDS

SuDS implementation in urban catchments: the case study of Sesto Ulteriano (MI)

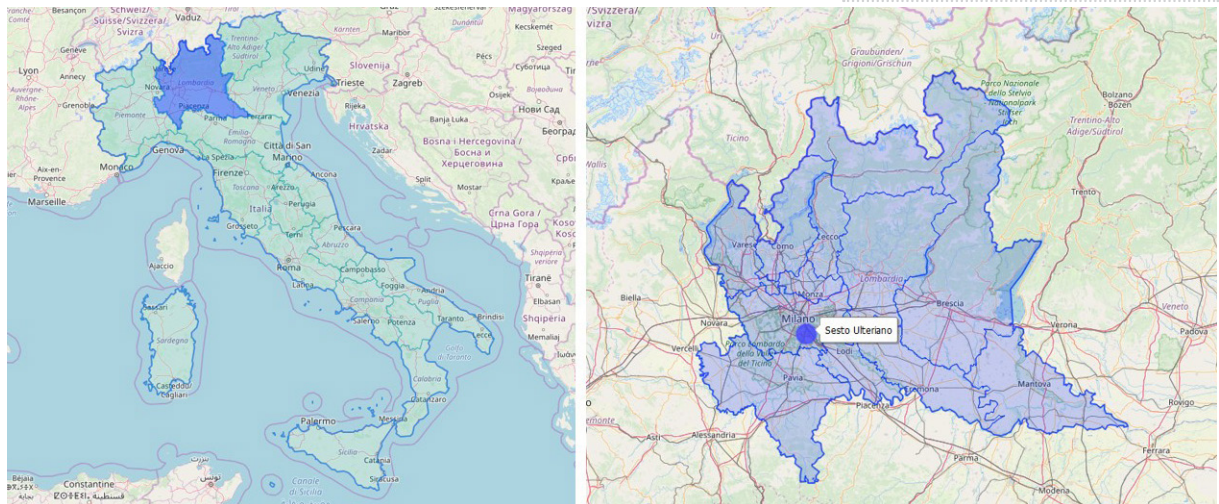
This research merged in a paper entitled “Re-think urban drainage following a SuDS retrofitting approach against urban flooding: a modelling investigation for an Italian case study” submitted in 2021

During the last decades many countries began to implement Sustainable Drainage Systems able to manage stormwater in a more sustainable manner and making the cities more resilient towards climate change and hydrological risks (La Loggia et al., 2012; Larsen et al., 2016; Kabisch et al., 2017; Versini et al., 2018; Lashford et al., 2019; Bertilsson et al., 2019). The growing need of the urban water agencies to enhance the city resilience through retrofitting projects along with the difficulties usually encountered in the overall performance assessment of SuDS (Golden & Hoghooghi, 2018; Zhang & Chui, 2019) led researchers to start experiencing trials and models able to simulate the hydrological behaviour of sustainable stormwater management infrastructures. Although valuable for the assessment of the hydrological performance of SuDS, field and experimental studies (Stovin et al., 2012; Longobardi et al., 2019;) mostly rely on single structure and do not give a complete overview of the potential of such systems in the management of stormwater in a complex urban context, characterized by hydraulic and hydrological criticalities. However, the few studies aimed at verifying the performance of already implemented SuDS at the catchment scale, can be valuable for results comparison, even if experienced under different design or climatic conditions (Avellaneda et al., 2017; Jiang et al., 2020). Therefore, research studies involving modelling attempts and performance-based scenario analyses can be considered a valid solution to test SuDS performance at the city scale both in terms of stormwater quantity and quality (Quin et al., 2013; Sparkman et al., 2017; Radinja et al., 2019; Li et al., 2019; Hua et al., 2020; Samouei et Ozger, 2020). In some particular region, such as the Mediterranean basin, where research mainly focused on the impact of climate feature, additional evidence on the potential of SuDS in complex urban contexts is needed (Gimenez-Maranges et al., 2020). Nevertheless, modeling sustainable drainage infrastructure in large urban areas often requires simplifying assumption that could somehow affect the analysis and enhance relevant results uncertainties (Palla & Gnecco, 2015; Hernes et al. 2020; Palermo et al., 2020). These include, for example, the need to use algorithms for the identification of the potential retrofitting percentage and SuDS localization. Studies conducted so far showed that runoff volume and peak flow reduction varies according to both these features (Qin et al., 2013; Ercolani et al., 2018; Bai et al., 2019; Li et al., 2015) beyond climate and building practices, but additional evidence is needed to quantify their practical impact at the catchment scale. Nevertheless, especially those with whom this study share some common points, can be used as a reference in the result discussion. This study starts from an analysis of the critical issues related to the stormwater quantitative management arising in the Sesto Ulteriano urban catchment, in the suburbs of Milan (Northern Italy), emblematic example of a problem shared by the most part of contemporary cities. SuDS implementation was proposed for a sustainable stormwater management and several Italian firms founded by PoliS-Lombardia, a regional institute for policy purpose, developed a detailed design of SuDS choice and localization, for an

extensive and comprehensive retrofit design involving the whole Sesto Ulteriano urban catchment. Thanks to the peculiarities of the case study, this research activity strives for answering key research questions: what is the real importance of having a SuDS project implementation aware of the real retrofitting capabilities of the urban context affected by hydrologic and hydraulic criticalities? How a potential SuDS model-based scenario compares to the real feasibility of the project? Does localization affect SuDS performance? To the purpose, a number of event scale and long-term scale simulation of the Sesto Ulteriano urban catchment were performed by the SWMM model (EPA Storm Water Management Model). The simulations aimed at a comparison of a number of different SuDS retrofitting scenarios characterized by different spatial distributions and areal extension implementation. Both hard-technology scenario (by PoliS Lombardia agency) and modelling scenarios (designed for the purpose of comparison) were compared in terms of maximum flow, total volume and drainage network pipes filling degree reduction coefficients with an hard-technology scenario, describing actual catchment configuration, where no SuDS were implemented.



Below Fig. 3.1 Localization of the case study area; On the right Fig. 3.2 Sesto Ulteriano urban development

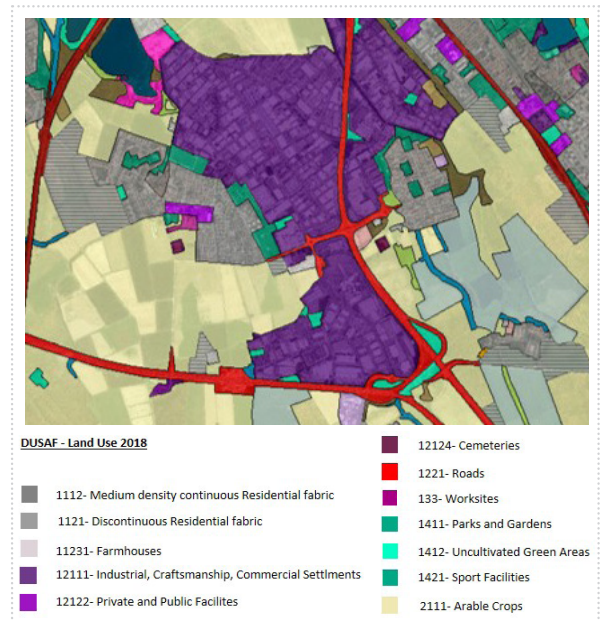


The case study

Sesto Ulteriano (45°23'45"N 9°15'13") is a small village of about 1100 ha and 3500 inhabitants in the municipality of San Giuliano Milanese, belonging to the Metropolitan Borough of Milan, Lombardy Region (Italy) (Figure 3.1). Lambro River, located on the eastern border of San Giuliano Milanese, represents the main hydrographic element. Besides, a dense network of artificial irrigation channels crosses the area. Among them, "Roggia Vettabbia" of Roman origin crosses the industrial area of Sesto Ulteriano. According to Geo-hydrological Hazard and Risk Plan of the Lombardia Region, the major flood-prone areas marginally concern the study area and are mainly related to the mentioned Roggia in the hamlet of Civesio. Hazard and Risk Maps point out that a Medium Hazard Level characterizes the flood-prone areas with an occurrence of flood with a return period of 100-200 years. Concerning the Risk assessment, the mentioned area is mainly characterized by a Medium Risk Level, except for one spot, mainly residential and for this reason characterized by a greater vulnerability. Between 1954 and 2015, it was possible to observe, in the Lombardy region, a remarkable urban development that led to an increase of the impervious surface of about 200% (Munafò, 2017). This factor had significant effects on the increase in the vulnerability of the territory: reduction of stormwater delay times with intensification of floods, reduction of groundwater recharge rate, increase in runoff with relative soil erosion and water pollution, reduction of ecosystem and landscape services deriving from the presence of natural pervious areas (Graziano et al., 2019). Figure 3.2 refers to Milan' Southeast area and represent the increase of the urbanized areas during the last decades. Such phenomenon led to an alteration of hydrological cycles and to the

arise of the mentioned criticalities. The village of Sesto Ulteriano is part of this urban context and can be considered an emblematic example of the unconscious development process of the last decades responsible, at least partially, for the ongoing problems related to the stormwater management. The urbanization process led to an increase of the impervious surfaces of 1000% between 1954 and 2000 and 15% between 2000 and 2015. Sesto Ulteriano, surrounded by large cultivated areas, exploited for productive purposes but also useful for regulation of environmental and hydrological functions, enclose dense impervious surfaces mainly intended for commercial or industrial use (Figure 3.3). The sewerage drainage network of Sesto Ulteriano is mainly combined, delivering both stormwater and wastewater. It proceeds roughly from north to south until the final delivery of the diluted black wastewater in the sewage treatment plant located immediately downstream. The excess stormwater is discharged into the mentioned irrigation ditches, through

Below Fig. 3,3 Sesto Ulteriano Land Use Maps



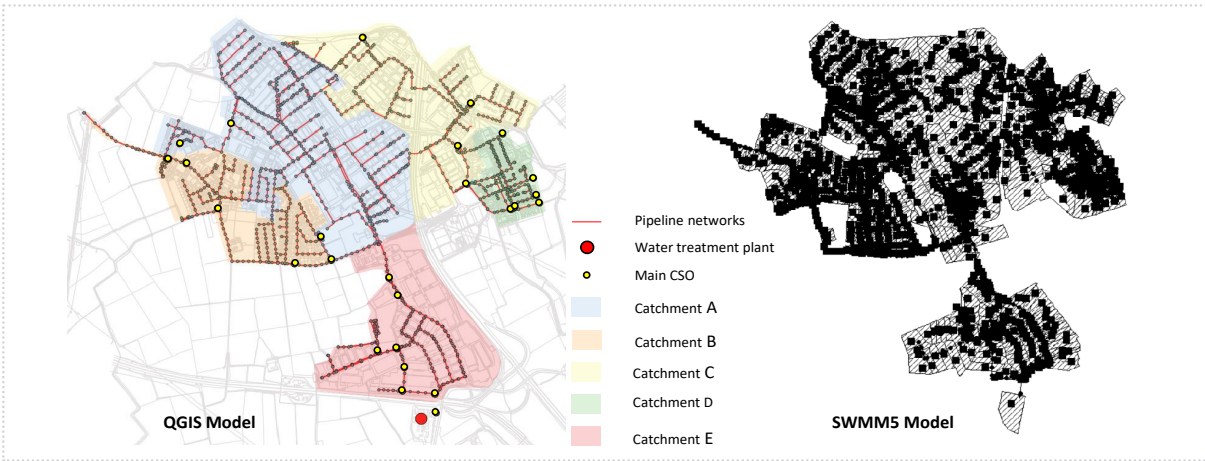


Fig. 3.4 QGIS map of Sesto Ulteriano drainage network with its subdivision into five macro-catchments and SWMM₅ study area model

several combined sewer overflows (CSOs) placed along the network (Figure 3.4). Two main ridges of the net can be identified, one coming from the north that collects the central part of the built-up area, the other from the west that collects the western part. The point of confluence between the two main collectors, located in the centre of the productive-commercial area of Sesto Ulteriano, represents an important hydraulic node of the network. Due to the impervious surface increase and the limited capacity of irrigation channels in which excess water are discharged, Sesto Ulteriano is partially affected by criticalities related to urban flooding phenomena. In addition, the existence of a strong interconnection between hydrographic network and sewer system is the cause of water quality issues. In order to focus on the urbanized context and its major criticalities, the study area does not occupy the entire territory of Sesto Ulteriano but only a part of it, about 290.33 ha, characterized mainly by both industrial (73%) and residential settlements (27%), and expressed by the basin visible in Figure 3.4.

SuDS Scenarios and hydrological-hydraulic modelling

As mentioned in the introduction, the study involved hydrological-hydraulic simulations based on a number of SuDS and climate scenarios. In particular design-based, model-based and hard-technology scenarios were accounted for to investigate the importance of a feasible versus a potential SuDS design and to assess furthermore the importance of location and spatial extent of green infrastructures implementation. The scenarios properties and characteristics will be described in the following. A summary table is also provided (Table 3.1).

Design-based scenarios (GREEN)

In order to mitigate the effect of urban flooding and making sure to optimize the retrofitting capability of the study area, the design-based scenario, namely “GREEN 100%”, provided for a very detailed identification of impervious areas suitable for retrofitting with SuDS and the implementation of these green infrastructures fully connected with the infrastructural pre-existences. It was designed in the framework of the PoliS-Lombardia study and saw a retrofitting of 24.2 ha over about 290 ha, for a percentage of retrofitting of about 8.3%. This represents

a great challenge, considering that completed projects hardly ever exceed 1% of retrofitting surface without involving Green Roofs (Perales-Momparler et al., 2017). In Figure 3.4, the subdivision into five macro-catchment of the study area is made explicit. Specifically, in the industrial areas (73% of study area, included in catchment A, D and E) it was considered appropriate to intervene on a series of public green areas with multi-size rain gardens. Where possible, one or two draining trenches (vegetated or not) or permeable parking lots were inserted at the edges of the roadway. In the residential areas (27% of total catchment, catchment B and D), draining trenches were located at the edges of some roadways and, just in a few surfaces, pervious parking lots and rain gardens were planned (Figure 3.5). Each SuDS typological was designed and located by evaluating the real transformation potential of the impervious areas; design details were created for a subsequent modeling reproduction of each system. Of the 24 ha of designed retrofitting areas, about 17.60 ha of impervious surface were converted into drainage trenches and rain gardens (6% of the total area), both modelled in SWMM5 using the “Bio retention Cell” module, and 6.40 ha into permeable parking lots (2.3%), modelled as “Pervious Pavements”. Overall, the design-

based scenario provided for about 9.2 ha (3.2 % of the study area) of SuDS retrofitting surface for catchment A, 0.3 ha (0.1 %) for catchment B, 7.6 ha (2.6 %) for catchment C, 0.3 ha (0.1 %) for catchment D and 6.8 ha (2.4 %) for catchment E. To analyse the impact of SuDS implementation areal extension in the Sesto Ulteriano urban context, along with the design-based scenario “GREEN 100%”, additional configurations were taken into account. Therefore, other two SWMM5 models were created in which only the 50% and the 10% of the design-based SuDS implementation were accounted for: “GREEN 50%”, with a percentage of retrofitting of about 4.2%, and “GREEN 10%”, with a percentage of 0.8% (Table 3.1).

Model scenarios (UNI)

Looking at the spatial distribution of SuDS within the catchments as another significant driver of the performance of the overall design, a different model scenario, namely “UNI” (3.6 c), was set up, in which SuDS were evenly distributed in the subcatchments of the study area. Specifically, for a given SuDS type, in the UNI configuration, the same areal extension is considered in each of the subcatchments (A, B, C, D and E) which corresponds to the total areal extension considered in the GREEN configuration for the whole catchment,

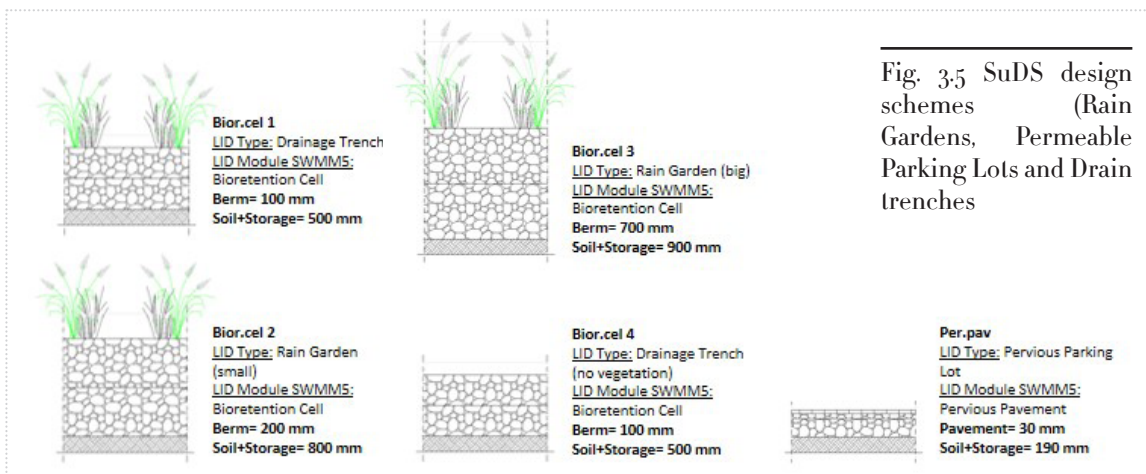


Fig. 3.5 SuDS design schemes (Rain Gardens, Permeable Parking Lots and Drain trenches)

ignoring the feasibility of the retrofitting project and only accounting for potentiality. As an example, if permeable pavements cover the 2.3 % of the overall catchment area in the GREEN scenarios (3.6 b), they would cover the 2.3% of each subcatchment in the UNI scenario. Even for the UNI configuration, the same three different degree of areal extension implementation of the design-based scenario were considered, that are “UNI 100%”, “UNI 50%” and “UNI 10%”. The results of the comparison between the “GREEN” and the “UNI” scenarios would represents an assessment of the impact of a feasible (design-based) versus a potential (model-based) retrofitting scenario and additionally an assessment of the importance of SuDS localization within the catchment.

Modeling comparison

The 3 SuDS design-based scenarios and 3 SuDS model scenarios were compared with the hard-technology scenario, representing the actual configuration of the drainage network. Being SuDS currently not implemented, comparison between model and hard-technology scenarios would help quantify the performance of SuDS in the mitigation of urban flooding risk in

Sesto Ulteriano urban catchment. Water utility CAP Holding provided the information for the development of the hard-technology scenario, involving 1148 nodes, 1141 conduits, 27 combined sewer overflow, for a total of 36 km network (Figure 3.5). The network pipelines, circular or box-like, are mainly made of concrete with sections in PVC and stoneware. The slopes are generally modest, around 0.1. Among the various hydrological models developed for urban runoff management purposes, EPA SWMM₅ had shown the greatest acceptance and the highest suitability. According to literature, good performances in the assessment of punctual flood depth values had been registered especially in the case of multiple land cover variation and SuDS implementations (Samouei et Ozger, 2020). For these reasons, in this study SWMM₅ was chosen for modeling both hard-technology and design-based scenarios. Each one of SuDS macro-categories showed more than one configuration due to their different geometric features and design. Specifically, a deeper analysis made it possible to identify 5 homogenous category of SuDS (Table 3.2), different for geometric features such as length or depth, modelled in SWMM₅ using two

SuDS Scenarios		SuDS Area	A_Industrial	B_Residential	C_Industrial	D_Residential	E_Industrial	Total
GREEN 100%	Feasible	ha	9.2	0.3	7.6	0.3	6.8	24.2
		%	3.2	0.1	2.6	0.1	2.4	8.3
GREEN 50%	Feasible	ha	4.6	0.1	3.8	0.1	3.4	12.1
		%	1.6	0	1.3	0	1.2	4.2
GREEN 10%	Feasible	ha	0.9	0	0.8	0	0.7	2.4
		%	0.3	0	0.3	0	0.2	0.8
UNI 100%	Potential	ha	8.7	3.5	5.3	1.8	4.9	24.2
		%	3	1.2	1.8	0.6	1.7	8.3
UNI 50%	Potential	ha	4.4	1.7	2.7	0.9	2.5	12.1
		%	1.5	0.6	0.9	0.3	0.8	4.2
UNI 10%	Potential	ha	0.9	0.3	0.5	0.2	0.5	2.4
		%	0.3	0.1	0.2	0.1	0.2	0.8

* The percentage here expressed was calculated as the ratio between SuDS Area and the whole study area

Tab. 3.1 Project scenarios with identification of SuDS retrofitting percentage and its distribution into the five macro-catchments of the study area intended for both industrial and residential use

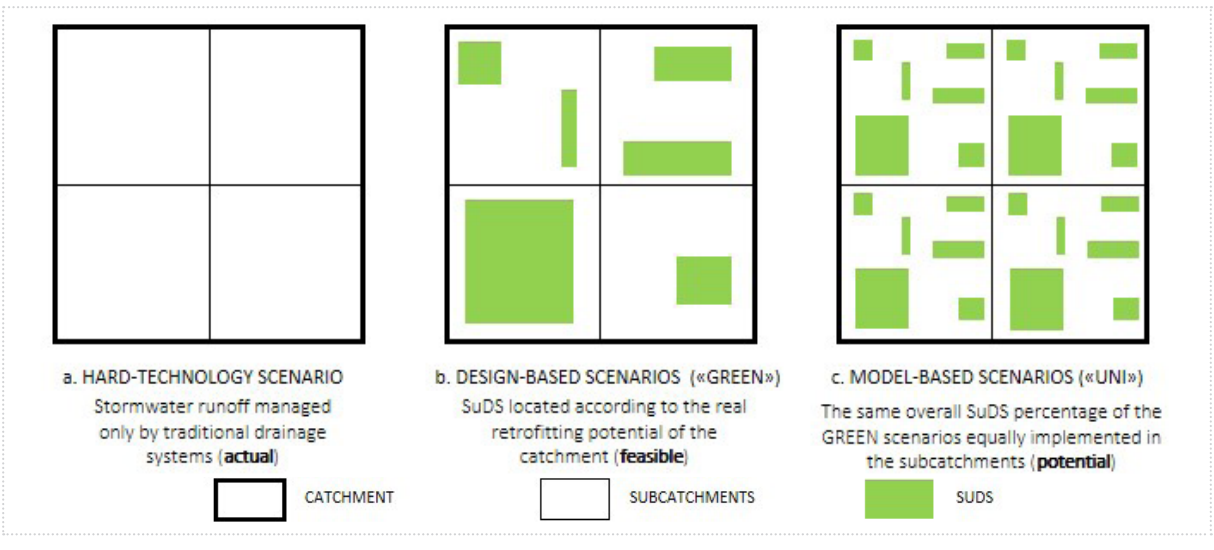


Fig. 3.6 Conceptual representation of the drainage scenarios modelled in SWMM₅

main objects (Bio-retention Cell and Permeable Pavements) and varying parameters related to surface, soil and drainage layers, and drain. Parameters of each infrastructure were chosen according to the project, literature review (Palla & Gnecco, 2015), Ballard’s SuDS Manual suggestions and EPA SWMM₅ User’s manual ranges (Table 3.2a, 3.2b). The Curve Number, assigned to each subcatchment according to the land use, run infiltration dynamics and Thornthwaite monthly potential evapotranspiration was calculated and inserted as climatic variable in each model.

Rainfall dataset analysis

An event scale analysis and a continuous long-term analysis were performed. Precipitation data from 10 weather station close to Sesto Ulteriano were collected for the definition of rainfall input necessary for SWMM₅ simulations. Weather stations were characterized by different time span and some period of missing data. Therefore, it was deemed appropriate to apply Inverse Distance Weighting interpolation of punctual rainfall observation in order to obtain continuous

rainfall observations typical of Sesto Ulteriano. Historical dataset derived from interpolation was used for the identification of annual rainfall while intensity-duration-frequency curves typical of the case study area, acquired from the Regional Agency for the Environmental Protection “ARPA” of the Lombardy Region, were used for the identification of different rainfall events. As regards event scale analysis, the critical duration of the catchment was assessed and three rainfall events with a duration equal to the critical one (9 hours) and return period of 2, 5 and 10 years were reconstructed. Respectively they featured a cumulative rainfall of 44.7 mm, 61.9 mm and 74.8 mm. Instead, as regards long period analysis, it was decided to simulate the hydrological-hydraulic behaviour of the catchment in the year 2014, characterized by the maximum cumulative value over the 5-year period 2014-2018 of data availability (1481.7 mm).

a. Bio-Retention cell

Surface	ranges	Bior.cell 1	Bior.cell 2	Bior.cell 3	Bior.cell 4
Berm Height (in or mm)	152.4-304.8	100.00	200.00	700.00	100.00
Vegetation Volume Fraction	-	0.20	0.20	0.20	0.00
Soil					
Thickness (in or mm)	609.6-1219.2	250.00	400.00	450.00	250.00
Porosity (volume fraction)	0.45-0.6	0.35	0.35	0.35	0.35
Field Capacity (volume fraction)	0.15-0.25	0.11	0.11	0.11	0.11
Wilting Point (volume fraction)	0.05-0.15	0.10	0.10	0.10	0.10
Conductivity (in/hr or mm/hr)	50.8-139.7	108.00	108.00	108.00	108.00
Conductivity Slope	30-60	-	-	-	-
Suction Head (in or mm)	50.8-101.6	50.00	50.00	50.00	50.00
Storage					
Thickness (in or mm)	152.4-914	250.00	400.00	450.00	250.00
Void Ratio (voids/solids)	0.2-0.4	0.35	0.35	0.35	0.35
Seepage Rate (in/hr or mm/hr)	-	32.00	32.00	32.00	32.00

*All other SWMM parameters are set with default values

b. Permeable Pavement

Surface	ranges	Perv.pav
Berm Height (in or mm)		0-2.54
Surface Roughness (Manning's n)		-
Surface Slope (%)		-
Pavement		
Thickness (in or mm)		76.2-152.4
Void Ratio (voids/solids)	0.15-0.25 (Contin.)/0.1-0.4 (Block)	0.25
Permeability (in/hr or mm/hr)	711.2-44450 (Contin.)/127-3810 (Block)	1968.50
Soil/ Sand filter layer		
Thickness (in or mm)		203.2-304.8
Porosity (volume fraction)		0.25-0.35
Field Capacity (volume fraction)		0.15-0.25
Wilting Point (volume fraction)		0.05-0.10
Conductivity (in/hr or mm/hr)		127-762
Suction Head (in or mm)		50.8-101.6
Storage		
Thickness (in or mm)		152.4-914.4
Void Ratio (voids/solids)		0.2-0.4
Seepage Rate (in/hr or mm/hr)		-

*All other SWMM parameters are set with default values

Tab 3.2.a and b SuDS parameterization in SWMM₅ according to SWMM Manual ranges and supported by literature review Drainage trenches and rain gardens are modelled in SWMM₅ using the “Bio retention Cell” modules (Table 3.2.a, 4 configurations according to the different geometric features); permeable parking lots are modelled using the “Permeable Pavement” module.

Output analysis and definition of key parameters

The assessment of SuDS behaviour in the studied catchment aimed at identifying their impact on frequency reduction or mitigation of critical events. In order to do this both “hydrological” and “hydraulic” analysis were carried out. The “hydrological” analyses was provided for the evaluation of each CSO Maximum Flow (Q_{max}) and Total Volume (V_{tot}) variations, comparing the results obtained from the different SuDS scenarios under the mentioned rainfall inputs. The hard-technology scenario was selected as the reference scenario and the reduction in terms of total volume (D_v) and maximum flow (D_Q) was evaluated as in the following:

$$D_{V(OUTX)} (\%) = [(V_{TOT(X)_HT} - V_{TOT(X)_MOD}) / (V_{TOT(X)_HT})] * 100$$

$$D_{Q(OUTX)} (\%) = [(Q_{MAX(X)_HT} - Q_{MAX(X)_MOD}) / (Q_{MAX(X)_HT})] * 100$$

Where:

X= Specific CSO

$V_{TOT(X)_HT}$ = Total Volume in the CSO X reached in the hard technology scenario

$V_{TOT(X)_MOD}$ = Total Volume in the CSO X reached in the specific model scenario

$Q_{MAX(X)_HT}$ = Peak Flow in the CSO X reached in the hard technology scenario

$Q_{MAX(X)_MOD}$ = Peak Flow in the CSO X reached in the specific model scenario

The spatial distribution of the maximum flow and total volume reduction coefficients was furthermore studied over the identified sub-catchments, to measure the effectiveness of the particular implemented SuDS and their specific location. In order to detect if land use can play a major role in the performances of SuDS infrastructures, “mean($D_{Q(X),adj}$)” and “mean($D_{V(X),adj}$)” coefficient for each macro-catchment were calculated as follows:

$$\text{mean}(D_{Q(X),adj}) = [\text{mean}(D_{Q(X)}) / \text{SuDSX}\%]$$

$$\text{mean}(D_{V(X),adj}) = [\text{mean}(D_{V(X)}) / \text{SuDSX}\%]$$

where:

mean($D_{Q(X)}$)= mean values of D_Q for each scenario

mean($D_{V(X)}$)= mean values of D_v for each scenario

SuDSX% = percentage of SuDS retrofitting areal extension in each macro-catchment

The “hydraulic” analysis aimed at the evaluation of the effects of the SuDS implementation on the nodes of the network with the main objective of enhancing the reduction of the number of flooded nodes and critical events in the occasion of extreme rainfall. The temporal variability, at the event scale, of the drainage network pipes filling degree was evaluated at each node of the network with an automatic procedure that required the extraction from the output of the maximum water depth data of each node over time and the calculation of the ratio between the latter and the node depth. For each scenario, the number of nodes exceeding a 0.7 threshold of filling degree was calculated and plotted over time and scenarios with the same climate condition were compared to enhance the reduction of the flooded nodes. For the scenarios tested under the most severe rainfall, the maximum percentage of flooded nodes and its time of occurrence were evaluated and plotted using a coloured map for comparison.

Hydrological and Hydraulic analysis results

As mentioned, the analysis of the simulations outputs, aimed at identifying the main differences between the hard-technology scenario and those characterized by the presence of the SuDS, were carried out accounting for both hydrological and hydraulic aspects. For each of the aforementioned assessment, therefore, key parameters were identified that could provide details about SuDS performance.

Hydrological analysis results

Hydrological analysis results can be at first evaluated through an assessment of Table 3.3 and 3.4. This preliminary overall analysis provided for mean values of D_v and D_Q , that is the average value over the whole CSOs localized within the urban catchment. On average, the design-based scenario provided about 50% D_v with some differences for the rainfall severity and, more evidently, for what concerns the degree of areal implementation. If, at the sub-catchment scale, the same areal extent was retrofitted with a more uniform SuDS distribution (model scenario UNI), it resulted in an improved average hydrological performance, with D_v reaching up to 70%. Evidently, as in Table 3.1, a UNI scenario provided for an implementation of SuDS practices even in areas where a GREEN scenario would not foresee such retrofitting. Very similar results hold in the case of D_Q (Table 3.4).

Mean D_v following SuDS implementation (%)

scenario		2014	T=2	T=5	T=10
GREEN 100%	feasible	54	53	49	45
GREEN 50%	feasible	52	49	42	39
GREEN 10%	feasible	31	31	20	17
UNI 100%	potential	79	78	75	74
UNI 50%	potential	72	76	67	61
UNI 10%	potential	40	40	23	21

On the left Tab 3.3 Mean maximum flow reduction following SuDS implementation in each of the investigated scenarios

Mean D_Q following SuDS implementation (%)

scenario		2014	T=2	T=5	T=10
GREEN 100%	feasible	44	55	45	44
GREEN 50%	feasible	39	51	38	39
GREEN 10%	feasible	15	35	18	14
UNI 100%	potential	65	81	68	71
UNI 50%	potential	36	79	60	60
UNI 10%	potential	16	45	19	21

On the left Tab 3.4 Mean total volume reduction following SuDS implementation in each of the investigated scenarios

It should be noted, here and for the future results, that, for the specific case study, a uniform distribution of green infrastructure did not entail for the same percentage of application of SuDS in each of the sub-catchments the urban catchment is divided into. A uniform distribution foresaw the implementation of all SuDS typologies in each subcatchment proportionally to their retrofitting potential in the whole study area and also the extent of the specific subcatchment. Figure 3.7 and 3.8, including respectively mean values of D_Q and D_V for each scenario, illustrate results according to the subdivision into five macro-catchments, with indication for mainly residential or industrial land use. In this way, among the performance assessment, also land use can be taken into account. Analysing Figure 3.7, it is possible to observe on one hand that, for the specific case study, regardless for the climate scenario (continuous or event scale), there was no significant variability in maximum flow reduction moving from 100% to 50% SuDS implementation scenarios, especially for the event scale analysis. Instead, noticeable differences could be detected when comparison were made for the 10% implementation model scenario. On the other hand, provided a given percentage of retrofitting areal extension, it appeared for the current case study that the presence of SuDS affected approximately at the same extent both continuous simulations and event scale simulations, and that, at the event scale, the rainfall return period seemed not to significantly affect the maximum flow reduction. More evident differences appeared for the low percentage of retrofitting implementation (10%). For what concerns a potential (model) versus a feasible retrofitting scenario (design-based) comparison, differences were not strongly evident, with an exception for

the sub-catchment B and D, both intended for residential use. The points mentioned above also applied to Figure 3.8, which illustrates the mean total volume reductions at the sub-catchment scale. Nevertheless, especially for the continuous simulations, it can be noted that SuDS effect on volume reductions seemed even stronger than in the case of maximum flow reduction. Results, collected in Table 3.5(a, b) and Table 3.6(a, b), showed that land use may affect the catchment hydrological performance. Sub-catchments B and D are characterized by discontinuous residential fabric, farmhouses, park, gardens and sport facilities. They are featured by the lowest percentage of impervious area and for this reason by the lowest percentage of SuDS retrofitting (Table 3.7). Nevertheless the low impact of green infrastructures in catchments B and D, the peak flow and volume reduction in these sub-catchments appeared the most effective (Table 3.5.a, 3.5.b, 3.6.a and 3.6.b). For seek of completeness, for each SuDS and climate scenario, the maximum flow and volume reduction at each CSOs were noted and boxplots were represented to investigate the relevant empirical distribution (Figure 3.9 and 3.10). Besides the previous quantitative results, Figure 3.9 and Figure 3.10 illustrate the actual difference between the GREEN and the UNI scenarios, which so far was not effectively identified. Regardless for the percentage of areal implementation, a SuDS retrofitting plan based on a relatively uniform spatial distribution generated a more uniform spatial distribution of CSOs loads that is a more uniform retention in terms of peak flow and runoff volume. This effect appeared particular evident in the case of the continuous simulation and for what concerns the runoff volume reduction (Figure 3.10).

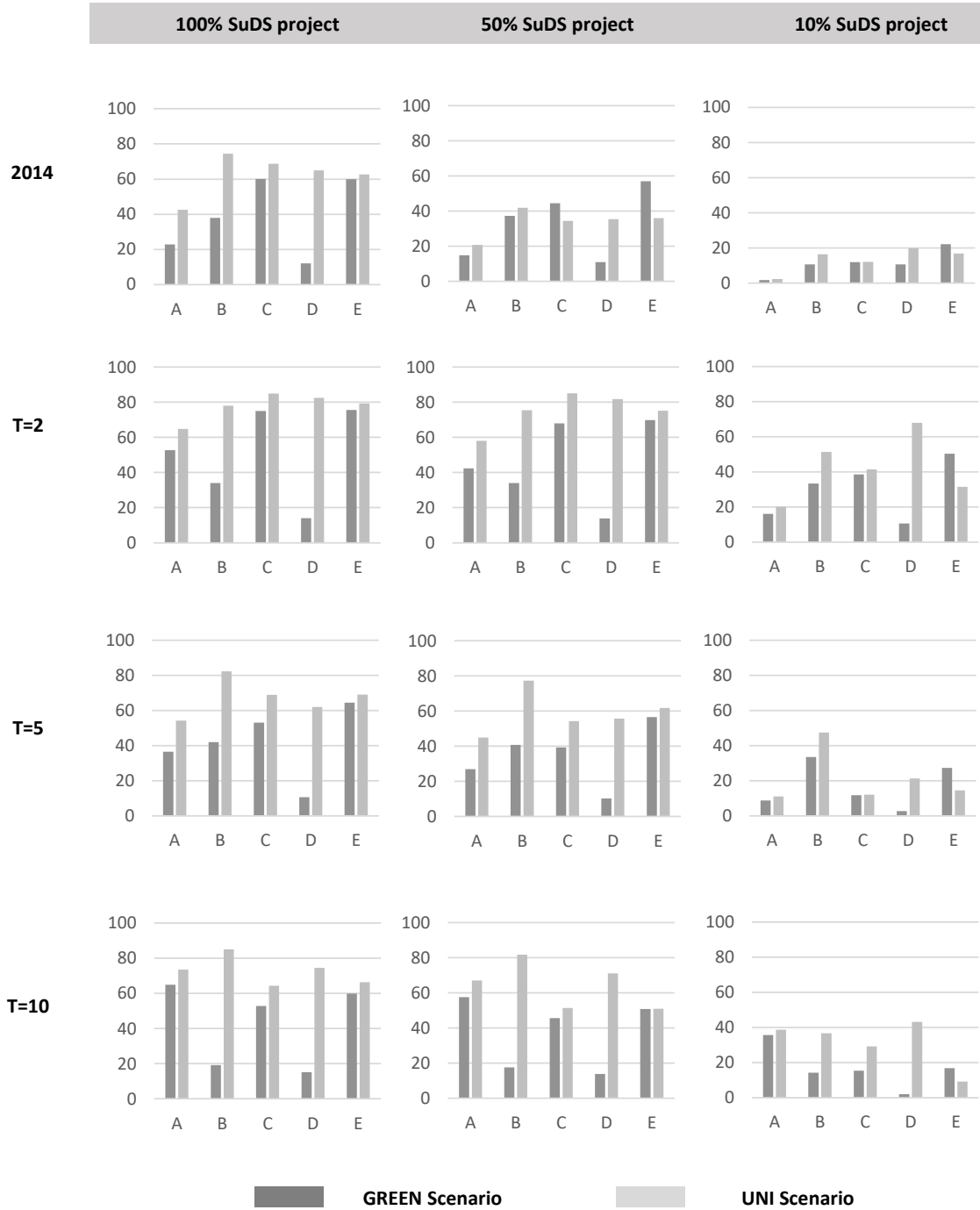


Fig. 3.7 Identification of Maximum Flow mean reduction following SuDS implementation in each of the five macro-catchments and for each of the investigated scenarios

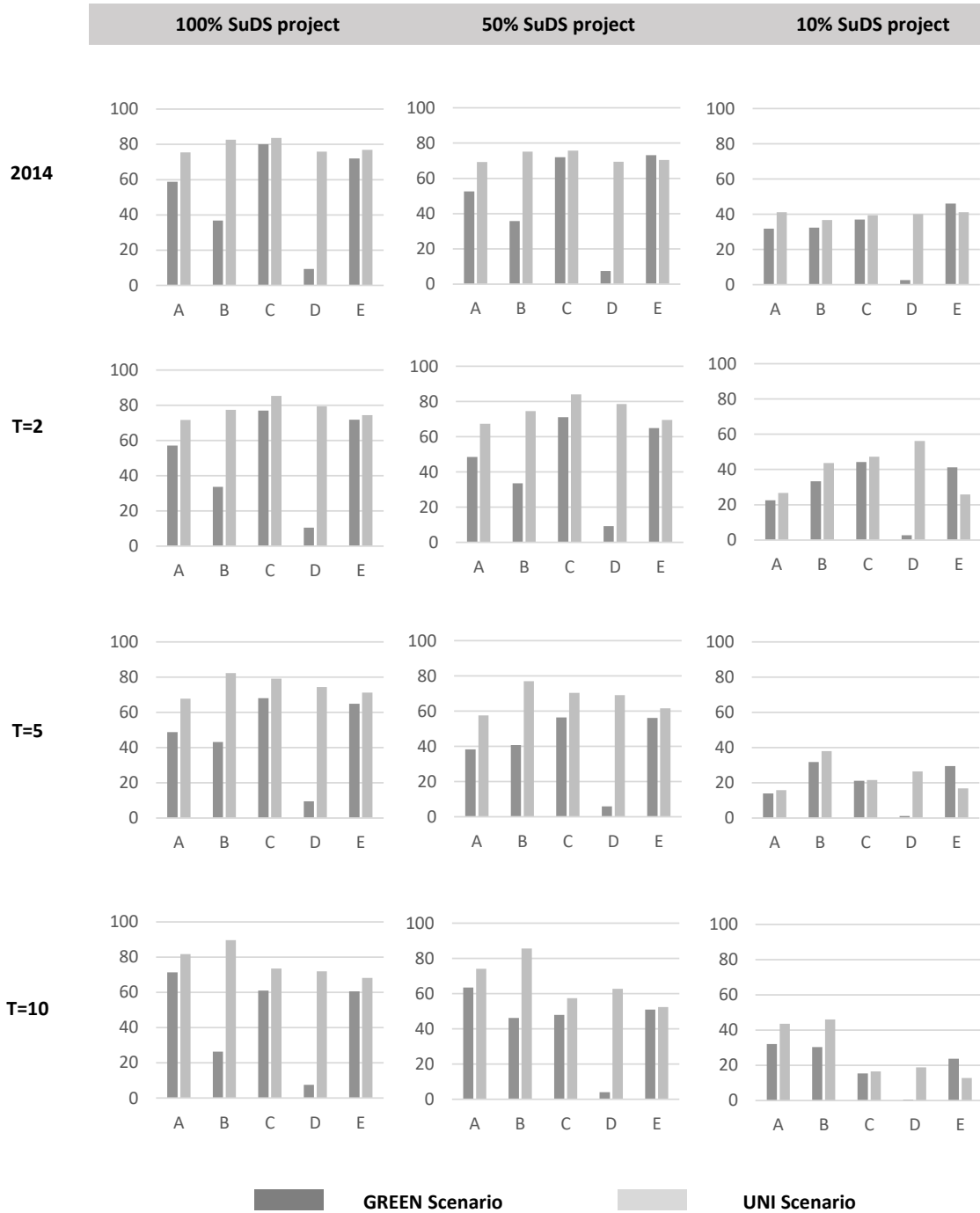


Fig. 3.8 Identification of Total Volume mean reduction following SuDS implementation in each of the five macro-catchments and for each of the investigated scenarios

a.

GREEN mean $D_{Q(x),adj}$

%	SuDS	2014			T=2			T=5			T=10		
		100%	50%	10%	100%	50%	10%	100%	50%	10%	100%	50%	10%
A	38	0.6	0.4	0.0	1.4	1.1	0.4	1.0	0.7	0.2	1.7	1.5	0.9
B	1	31.9	31.4	9.0	28.7	28.7	28.1	35.4	34.3	28.2	16.2	14.8	12.0
C	31	1.9	1.4	0.4	2.4	2.2	1.2	1.7	1.3	0.4	1.7	1.5	0.5
D	1	10.9	10.0	9.6	12.7	12.6	9.7	9.7	9.3	2.4	13.8	12.5	1.8
E	28	2.1	2.0	0.8	2.7	2.5	1.8	2.3	2.0	1.0	2.1	1.8	0.6

b.

UNI mean $D_{Q(x),adj}$

%	SuDS	2014			T=2			T=5			T=10		
		100%	50%	10%	100%	50%	10%	100%	50%	10%	100%	50%	10%
A	36	1.2	0.6	0.1	1.8	1.6	0.6	1.5	1.2	0.3	2.0	1.9	1.1
B	14	5.2	2.9	1.2	5.5	5.3	3.6	5.8	5.4	3.3	6.0	5.7	2.6
C	22	3.1	1.6	0.6	3.9	3.9	1.9	3.1	2.5	0.6	2.9	2.3	1.3
D	7	8.7	4.8	2.7	11.1	11.0	9.1	8.3	7.5	2.9	10.0	9.5	5.8
E	20	3.1	1.8	0.8	3.9	3.7	1.6	3.4	3.0	0.7	3.3	2.5	0.5

Tab. 3.5 (a, b) Land use effect on SuDS peak flow mitigation for design-based (a) and model-based (b) scenarios. The design-based scenarios, also called “GREEN”, are characterized a punctual SuDS choice and localization while model-based scenarios feature a uniform distribution of such infrastructures

a.

GREEN mean $D_{V(x),adj}$

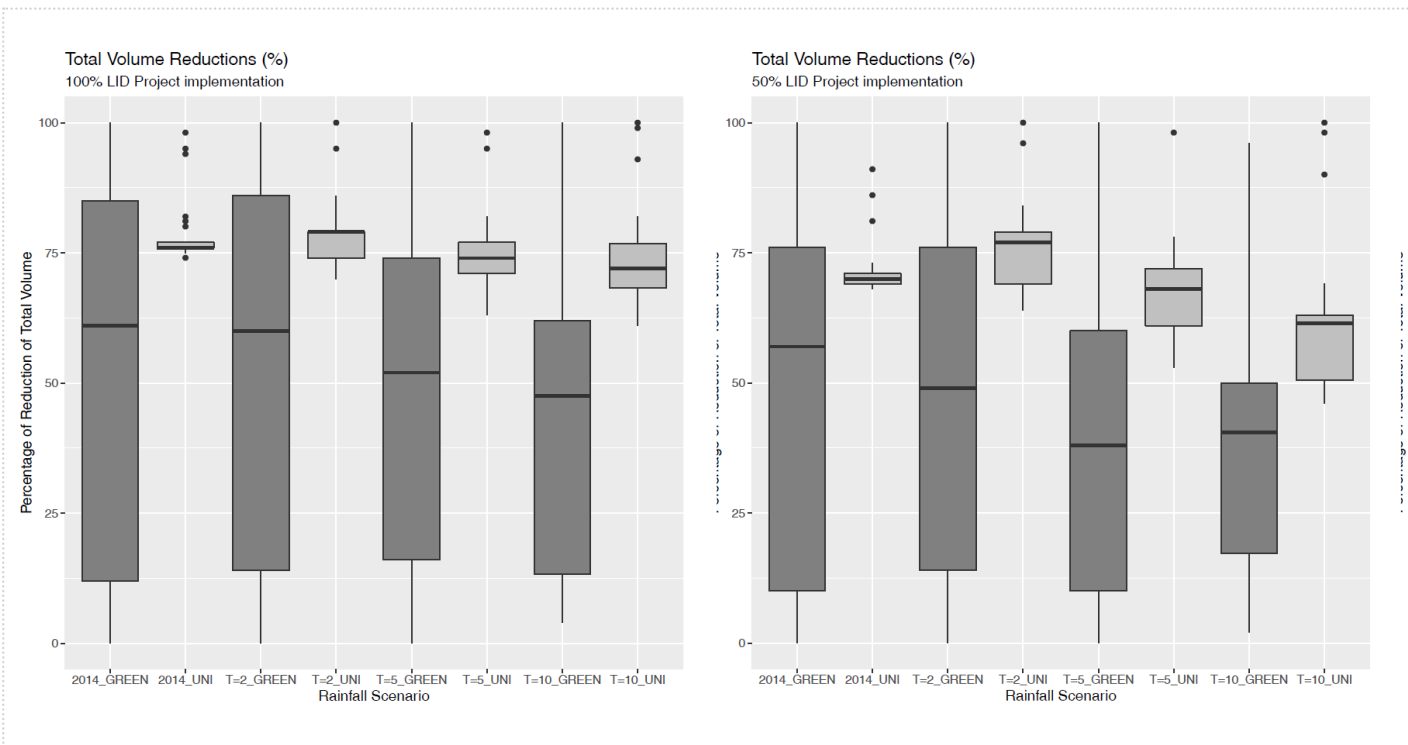
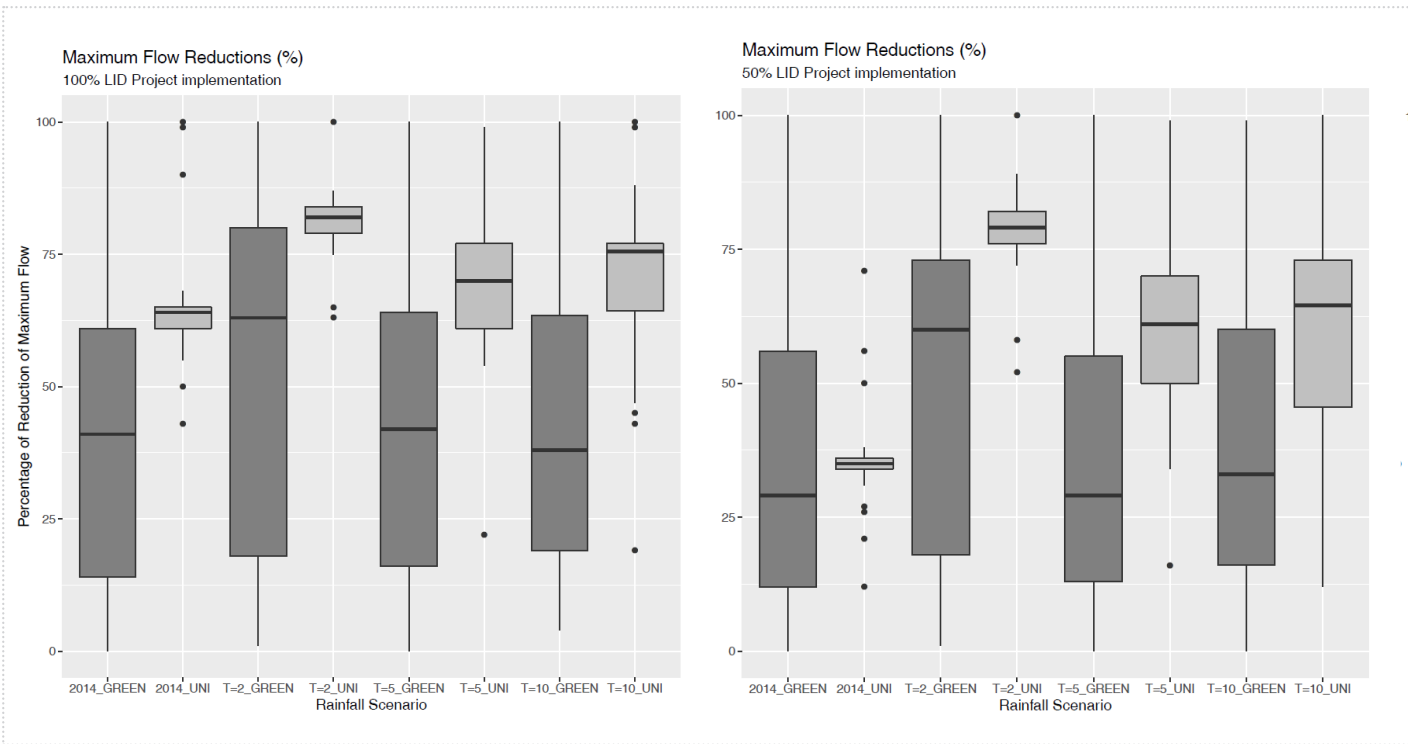
%	SuDS	2014			T=2			T=5			T=10		
		100%	50%	10%	100%	50%	10%	100%	50%	10%	100%	50%	10%
A	38	1.5	1.4	0.8	1.5	1.3	0.6	1.3	1.0	0.4	1.9	1.7	0.8
B	1	31.0	30.2	27.3	28.3	28.3	28.1	36.3	34.3	26.8	22.1	38.9	25.5
C	31	2.6	2.3	1.2	2.5	2.3	1.4	2.2	1.8	0.7	1.9	1.5	0.5
D	1	8.5	6.8	2.4	9.5	8.3	2.4	8.6	5.4	1.0	6.7	3.7	0.6
E	28	2.6	2.6	1.6	2.5	2.3	1.5	2.3	2.0	1.0	2.1	1.8	0.8

b.

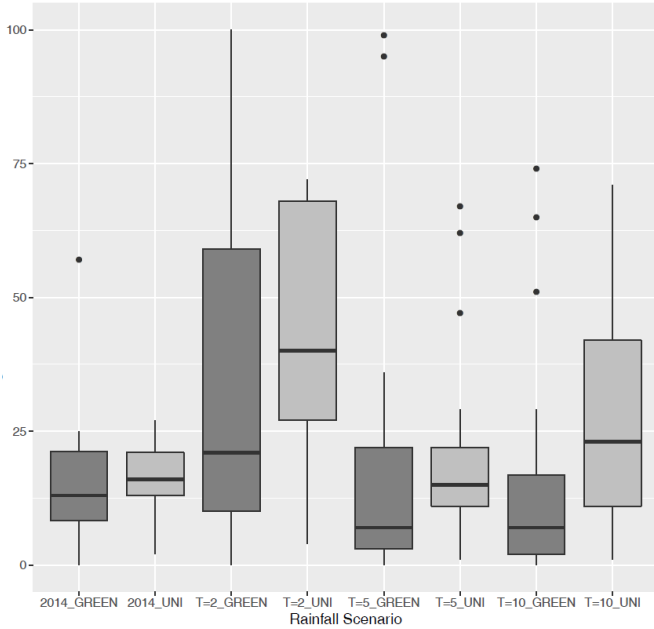
UNI mean $D_{V(x),adj}$

%	SuDS	2014			T=2			T=5			T=10		
		100%	50%	10%	100%	50%	10%	100%	50%	10%	100%	50%	10%
A	36	2.1	1.9	1.1	2.0	1.9	0.7	1.9	1.6	0.4	2.3	2.1	1.2
B	14	5.8	5.3	2.6	5.4	5.2	3.1	5.8	5.4	2.7	6.3	6.0	3.2
C	22	3.8	3.5	1.8	3.9	3.8	2.2	3.6	3.2	1.0	3.4	2.6	0.8
D	7	10.2	9.3	5.4	10.7	10.6	7.5	10.0	9.3	3.5	9.6	8.4	2.5
E	20	3.8	3.5	2.0	3.7	3.4	1.3	3.5	3.0	0.8	3.4	2.6	0.6

Tab. 3.6 (a, b) Land use effect on SuDS total volume mitigation for design-based (a) and model-based (b) scenarios. The design-based scenarios, also called “GREEN”, are characterized on a punctual SuDS choice and localization while model-based scenarios feature a uniform distribution of such infrastructures



Maximum Flow Reductions (%)
10% LID Project implementation



On the left from the top:

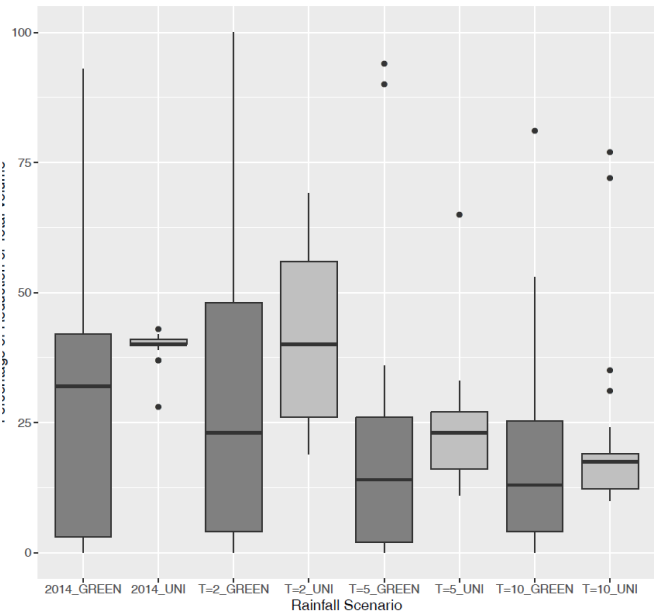
Fig. 3.9 Frequency Analysis of maximum flow reduction percentages in each CSO of the drainage network according to different SuDS configuration scenarios (feasible-GREEN and potential-UNI) and three different implementation degree of SuDS project (100%, 50% and 10%), tested under T=2, 5, 10 rainfall events;

Figure 3.10 Frequency Analysis of total volume reduction percentages in each CSO of the drainage network according to different SuDS configuration scenarios (feasible-GREEN and potential-UNI) and three different implementation degree of SuDS project (100%, 50% and 10%), tested under continuous rainfall and T=2, 5, 10 rainfall events.

Below:

Tab. 3.7 Percentage of impervious surfaces and SuDS in each macro-catchment

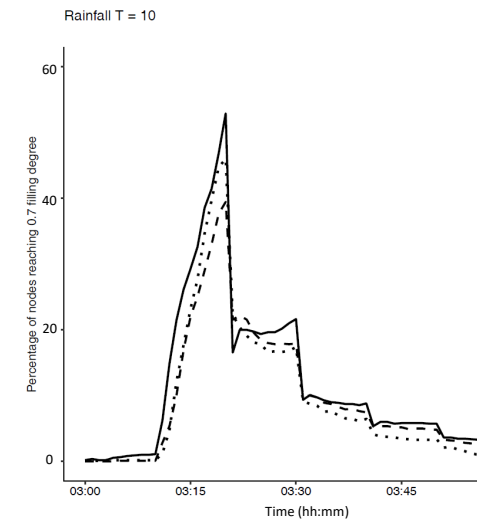
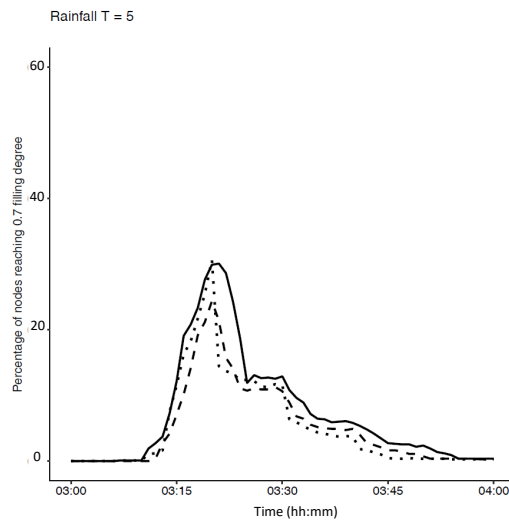
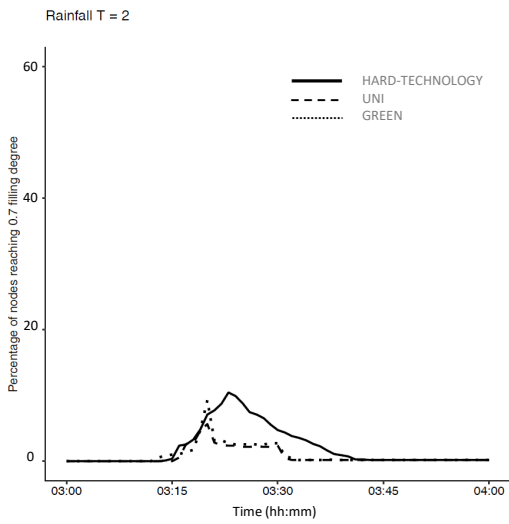
Total Volume Reductions (%)
10% LID Project implementation



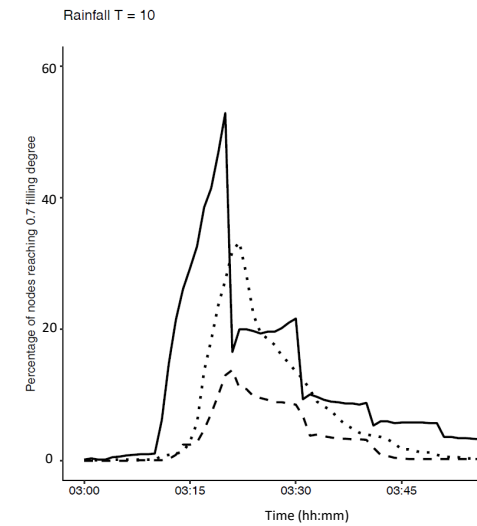
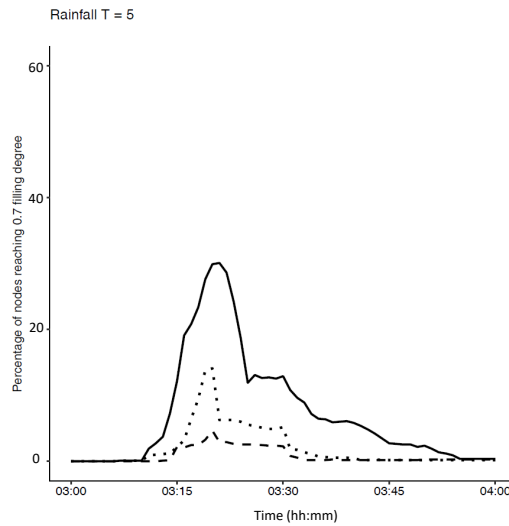
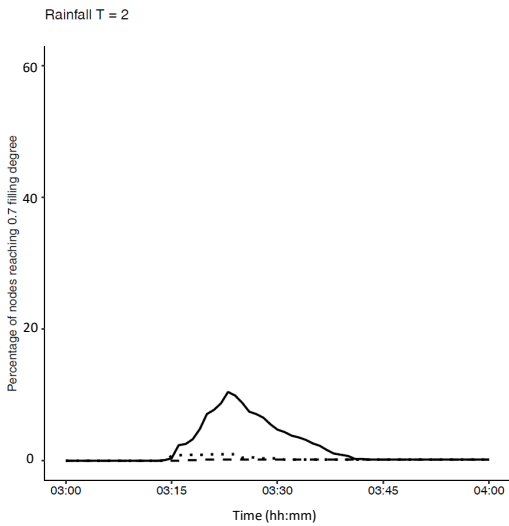
	Area (ha)	A _{imp} (ha)	%A _{imp}	SuDS Area (ha)	% SuDS
A	104	56	54	9.2	38
B	41	13	31	0.3	1
C	65	56	87	7.6	31
D	22	7	32	0.3	1
E	59	41	70	6.8	28
total	290	173	60	24.2	

*SuDS Area and % SuDS refer to GREEN 100% Scenario

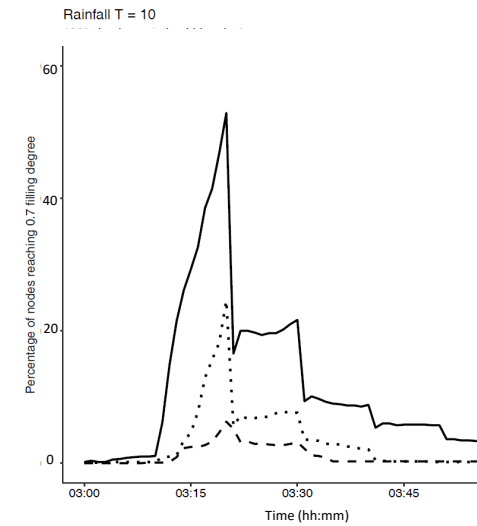
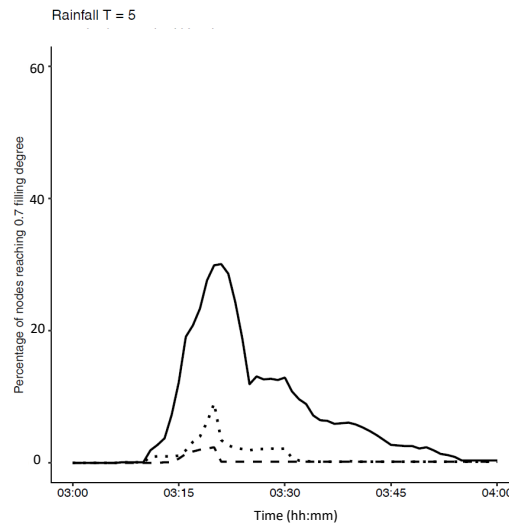
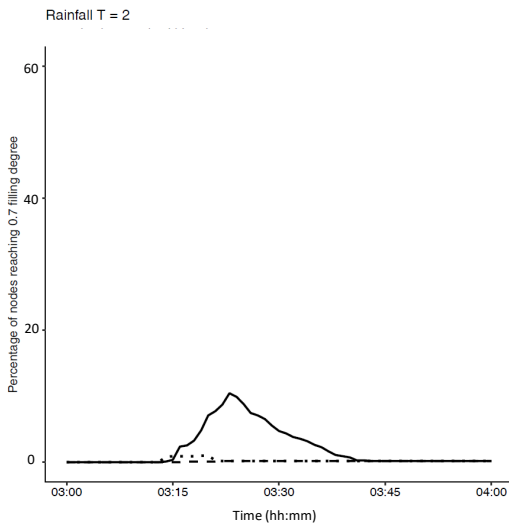
10% SuDS project implementation



50% SuDS project implementation



100% SuDS project implementation



On the left Fig. 3.11 Number of nodes over time reaching 70% node depth for different implementation scenarios and under event scale rainfall inputs (T=2, 5, 10)

Hydraulic analysis results

Results of the performance assessment of SuDS impact on the nodes of the network, in terms of reduction of the number of flooded nodes during severe rainfall events, are illustrated in Figure 3.11. The percentage of nodes reaching the 70% node depth was plotted over time (since rainfall start) and compared according to the distinction into drainage configuration scenarios (hard-technology, model-based and design-based). Each plot represents a different level of SuDS project implementation (100%, 50% and 10%) tested alternatively under 2-year, 5-year and 10-year return period events. The hard-technology scenario simulations highlighted an increase in the percentage of nodes filled up to 70% with the return period, with the 10%, 30% and 50% of nodes corresponding respectively to T = 2 years, T = 5 years and T = 10. In consideration of the common engineering practice that prescribes the use of T = 10 years design hyetograph for urban drainage network design, the large percentage of nodes (50%) filled up to 70% for this specific rainfall event, is an indication of the criticalities and peculiarities of the studied area. As expected, major differences between SuDS and hard-

technology scenarios occurred for the higher areal SuDS implementation such as 100% and 50% and for the lower intensity events. In this specific circumstance, SuDS, regardless for a GREEN or an UNI scenario, appeared able to led to an important reduction of the percentage of critical nodes. No SuDS impact was detected for the lower degree of areal implementation (10%) for this specific analysis. Focusing on SuDS scenarios, both GREEN and UNI scenario, especially for the higher degree of implementation, successfully reduced the number of flooded nodes over time even in the occurrence of severe rainfall. GREEN scenarios in particularly appeared associated to the largest impact of nodes filling during severe rainfall events. Figure 3.12 collects pictures of the drainage network representing over-threshold nodes (red) and under-threshold node (green) when the maximum percentage of flooded nodes was reached (70% filling degree). Coloured maps gave the possibility to visualize the distribution of critical nodes when the maximum percentage was reached and to understand the differences between the various SUDS configuration scenarios. To investigate the effect of the worst rainfall condition analysed, only scenarios tested under 10-years return period precipitation were chosen. In particular these pictures represent hard-technology, GREEN and UNI scenarios in the three areal degree of implementation of SUDS project. Results indicate, now more explicitly, that under the same SuDS retrofitting surface, UNI scenarios registered better performance than the GREEN one. Analysing the maps under the same SuDS scenario, major differences in the number of critical nodes could be observed between 10% and 50% SuDS project implementation. Not significant were the differences between 50% and 100%.

TRADITIONAL Scenario, T=10

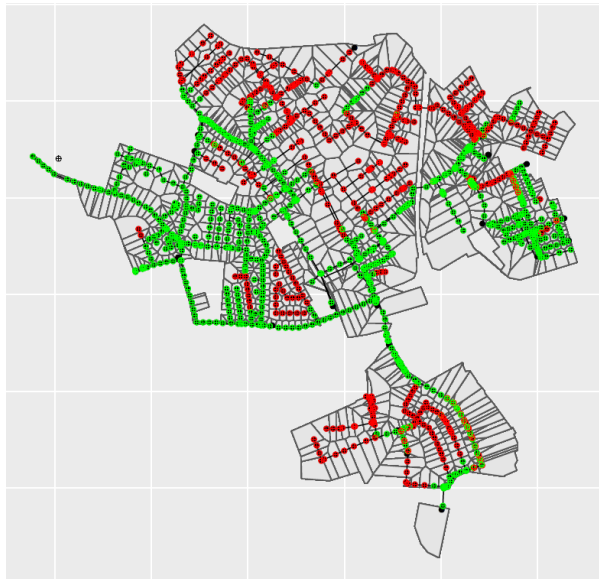


Fig. 3.12 Distribution and characteristics of nodes at the time when maximum percentage of flooded nodes has been reached, for different implementation scenarios and for T=10 rainfall event

GREEN Scenario, T=10

UNI Scenario, T=10

10% SuDS project implementation; T=10



50% SuDS project implementation; T=10



100% SuDS project implementation; T=10



Centralized and diffuse storage in urban areas: the case study of Sesto Ulteriano (MI)

Traditional structural measures such as the installation of additional drainage facilities, including pump stations and detention reservoirs, are usually adopted to prevent and mitigate urban stormwater runoff (Lee et al., 2016). However, even nowadays, there is no lack of examples of excess stormwater directly discharged into receiving water bodies, severely polluting the ecosystem (Borchardt and Sperling, 1997). In 90's reducing stormwater overflows became finally a concern and several international strategies on environmental pollution refer directly to urban stormwater discharges were established (European Water Framework Directive, 2000; U.S Clean Water Act, 2010). Throughout Europe and North America, stormwater detention tanks (SWDTs) are of particular importance in controlling the negative impact of stormwater discharges (e.g. Bertrand-Krajewski and Chebbo, 2002; Calabrò and Viviani, 2006). In Italy, for example, Lombardia Region (Lombardia Regional Law 12 December 2003, N.26 and Regional Regulations 24 March 2006, N. 3 and 4) requires SWDTs in various situations both in residential and industrial catchments to safeguard the quality of the receiving environment. In this context, several studies were conducted to understand the hydraulic and environmental behaviour of SWDTs. According to Todeschini et al., 2012, stormwater detention tanks represent a useful environmental tool against stormwater pollution. This facility is commonly used in all water distribution systems (Walski, 2000). However, design configurations and operating conditions significantly affect the extent of the ecological benefit, investment and maintenance costs, and functionality of the urban drainage system and the wastewater treatment plant. In particular, during the last years, major projects focused on constructing the right-sized tank in the right location. The location of storage, in fact, provides an opportunity to make the most of a given volume of storage. However, because of restrictions on availability, terrain, and aesthetics, good storage sites may be difficult to find (Walski, 2000). Several researches focused on the identification of SWDTs volumes distribution, mainly aiming at cost-effective solutions able to minimize flood, pollutant load and storage cost (Wang et al., 2017). According to Di Matteo et al., 2019, also private/residential/allotment SWDTs, directly connected with roofs, can potentially reduce runoff peaks to downstream stormwater drainage systems during rare, long duration storms.

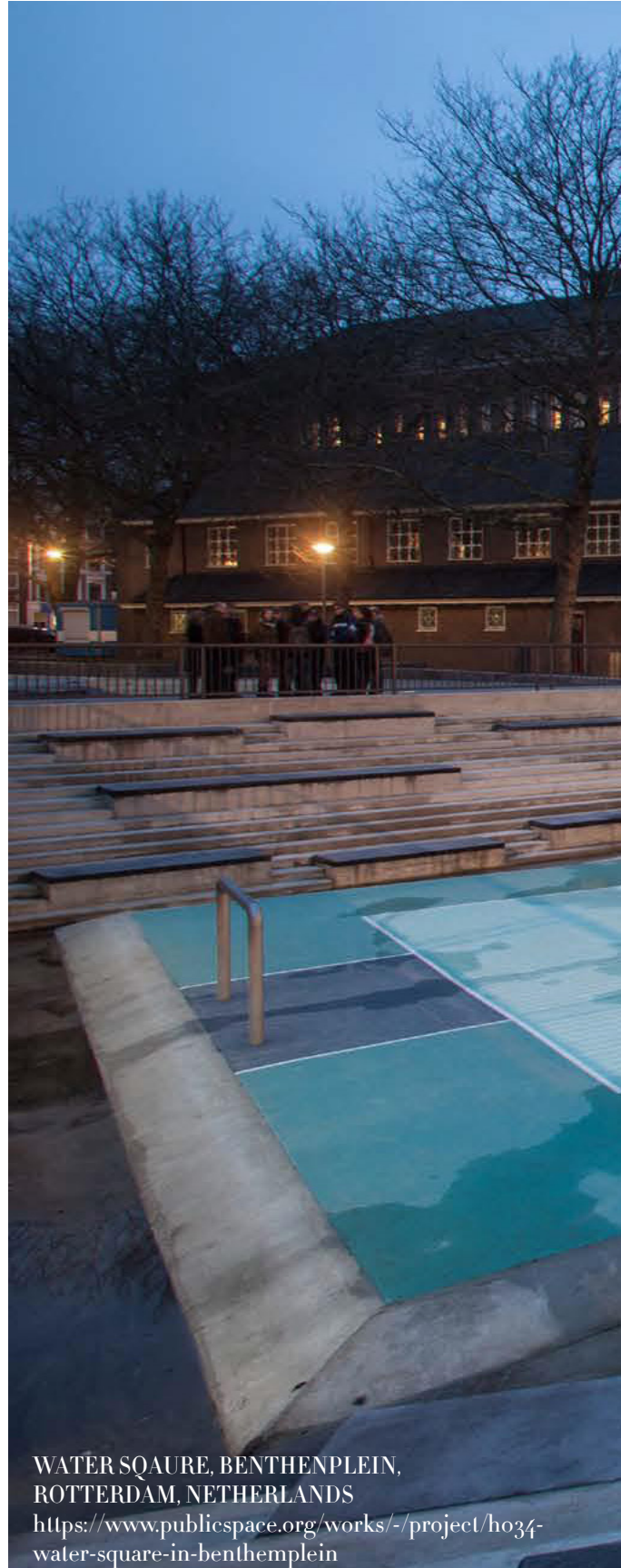
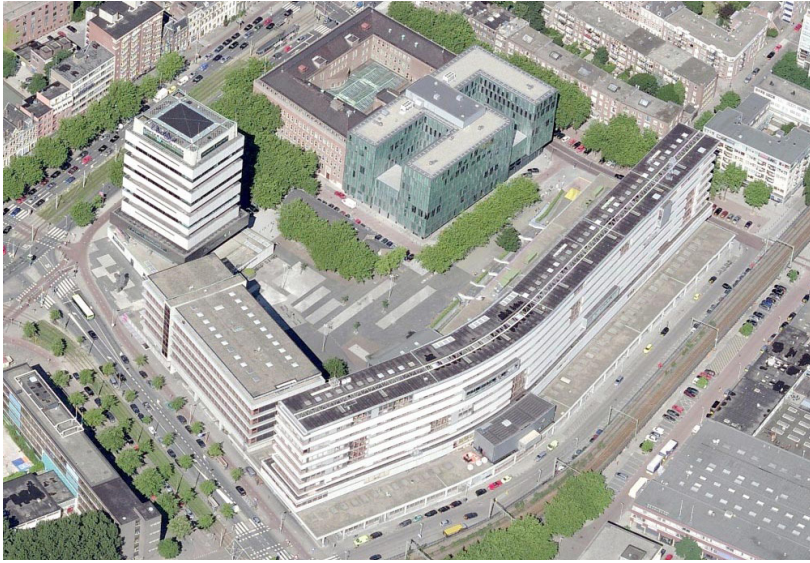
Moreover, as already mentioned, during the last decades many countries began to implement Nature Based Solutions able to support the pre-existing drainage network in retaining, delaying and filtering stormwater (Woods Ballard et al.,





VASCHE DEL LURA, SARONNO (MI), ITALY

<https://ilsaronno.it/2020/05/20/cento-mila-metri-cubi-dacqua-nelle-vasche-di-laminazione-e-evitano-la-piena-del-lura-a-saronno-e-caronno/>



WATER SQAURE, BENTHENPLEIN,
ROTTERDAM, NETHERLANDS
<https://www.publicspace.org/works/-/project/h034-water-square-in-benthemplein>



2015; Scholz, 2015; Perini & Sabbion, 2016; Everett et al., 2016; Andreucci, 2017; Eckart et al., 2017; Brears, 2018; Bell, 2018).

For these reasons, an integrated approach (SWDTs+SuDS) could be the best solution to manage urban flooding in large urban areas and to improve city resilience (Dong et al., 2017). Scientific literature agreed that both traditional (grey/hard-technology) and sustainable (green/SuDS) infrastructures could improve urban resilience but green ones are characterized by a higher adaptability to deal with uncertain future. In fact, climate change seems to have potentially effects on the design and performance of sewer storage tanks. Research conducted in 2007 on a case study in London (Butler et al., 2007) registered a 35% increase in the number of storm events that cause filling of the tank and a 57% increase in the average volume of storage required.

Recent studies focused on the identification of the most suitable blending of hard-technologies and sustainable drainage systems and authors (Kapetas & Fenner, 2020) studied infrastructure localization within the urbanized context and their adaptation to climate change.

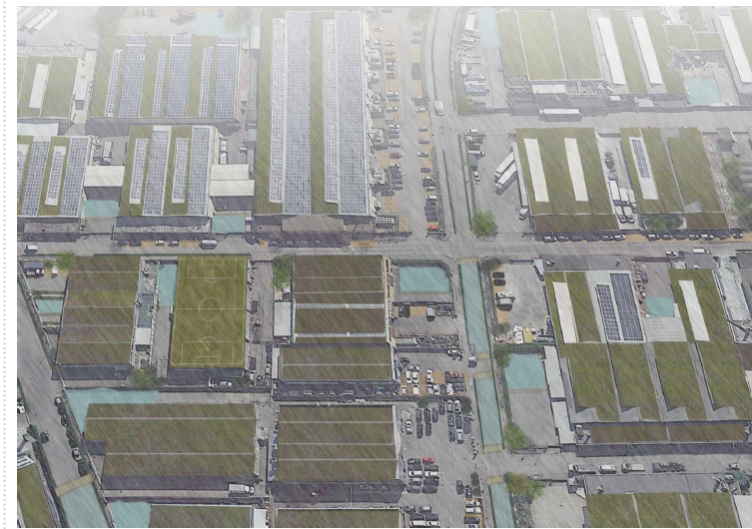
This work set out its basis on the concept of floodability, defined as the ability of a system to withstand floods that occur still maintaining a sufficient level of operation (La Loggia et al., 2020). After relevant flooding events, floodable systems may not recover their previous state as resilient systems do but may evolve to a new equilibrium that is more adapted to flooding (La Loggia et al., 2020). Floodable urban areas are able to avoid damages and disruptions, looking for a new balance and considering the flooding an event to live with, and for this reason are more than resilient. In particular, the research strove for understanding if Sustainable Drainage Systems reproducing floodable street and squares could represent an effective solution for managing excess stormwater in an urban catchment in Northern Italy, particularly prone to flooding risk. In addition, looking at the floodability as a “diffuse-storage” approach, through the comparison with “central-storage” typical of traditional SWDTs several differences between these two strategies were detected to give decision-makers significant elements for structuring planning choices.

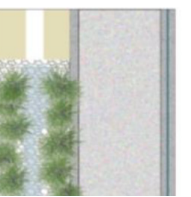
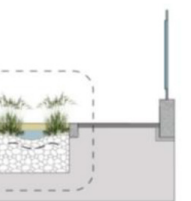
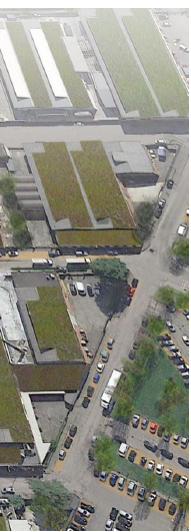
Floodability concept was here proposed for a sustainable stormwater management and a detailed design of diffuse-storage choice and localization (Figure 3.13) was developed using SuDS and involving both residential and industrial catchments of the case study basin: Sesto

Ulteriano (MI). Thanks to the peculiarities of the area, this part of the research research strives for comparing the mentioned diffuse-storage scenarios (SuDS +Hard-Technology storage) with the centralized-storage scenario in which only storage tanks downstream were provided and identifying whether centralized storage tanks volumes could be reduced pursuing the integrated approach typical of the diffuse-storage scenarios, previously mentioned.

To the purpose, following the identification of floodable streets (in residential catchments) and squares (in industrial catchments) for the diffuse-storage project design, SuDS modules available in SWMM₅ (rain barrel, pervious pavements and drainage trenches) were chosen. Besides, sensitivity analyses were carried out in order to understand under different rainfall conditions and design choice (technological parameters) the behaviour of these infrastructures. Simulation under different rainfall inputs were performed and diffuse-storage scenarios (“SuDS”+”Hard-Technology” storage) were compared with the centralized-storage scenario in which only storage tanks downstream were provided.

Results were assessed in terms of peak flow, total volume discharged and excess stormwater. Integrated approaches, involving the use of both SuDS and Hard-Technology in the solution of stormwater management issue, could be a great opportunity to lower the weaknesses typical of traditional storage tanks (realization and maintenance costs, limits in treatment of pollutant, poor adaptation to climate change effects), increasing also city resilience and resistance against urban flooding aspects.





Above Fig. 3.13 Identification of floodable streets and squares in the Sesto Ulteriano Urban catchment;

On the left Fig. 3.14 Simulation of the floodability concept in the area identified with the red circle in Fig. 3.13 and schetch of a floodable street produced within the Polis Project

The case study: central storage vs diffuse storage approach

Again in the urban context of Sesto Ulteriano (MI), this time the question addresses the importance of implementing diffuse storage strategies (SWDTs + SuDS) in the overall improvement of the performance of the drainage network, consequently reducing impacts, volumes and costs of traditional and punctual storage tanks (SWDTs). The “Central-Storage” scenario only provides the realization of a storage tank downstream each of the industrial catchments (A, C, E) as shown

in Figure 3.15. The “Diffuse-Storage” scenario envisages, apart from the SWDTs expected in the “Central-Storage” scenario, also floodable streets and squares (Figure 3.14). These infrastructures, located within the urban fabric of the same three industrial catchments, have the ambitious objective of partially detain stormwater runoff, reducing both peak flows and total volumes discharged from the CSOs of the network and hopefully positively affecting the stormwater volumes to be discharged into detention tanks.

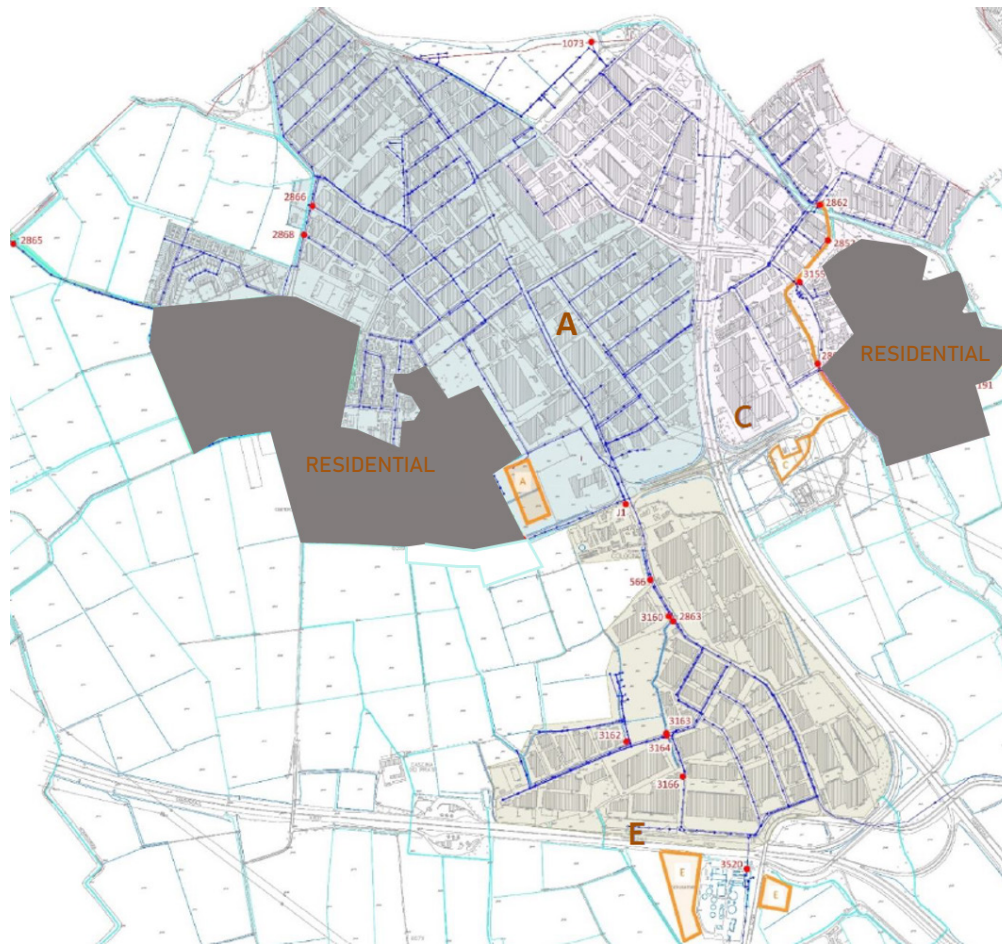


Fig. 3.15 Localization of stormwater detention tanks in the three industrial catchments of Sesto Ulteriano

The project of detention tanks in the “Central-Storage” scenario

Local legislative regulations were taken into account in order to calculate the volume of the detention tanks. In particular, Lombardia Region with the Regional Regulation n.7 of the 23 November 2017 (“Regulation containing criteria and methods for compliance with the principle of hydraulic and hydrological invariance according to regional law n.12 of 11 March 2005”) identified in 40 l/s per hectare of impervious surface the maximum flow rate to be discharged into the receiver. This threshold is of fundamental importance for the assessment of the stormwater volume to be discharged into the detention tank and consequently for the definition of the volume of the tank itself. The results of the event scale (T=2, 5, 10 year) SWMM₅ simulations carried out on the “Hard-Technology” scenario (discussed in the previous paragraph of this chapter) were used to identify for each CSO of the Sesto Ulteriano drainage network Maximum Flows (Q_{max}) and Total Volumes (V_{tot}). According to the maximum threshold of 40 l/s per hectare of impervious surface, the eligible flow by law was calculated (Q_{Law}) multiplying the mentioned value by the impervious surface treated (A_{imp}) by each CSO. Once identified the threshold, the maximum

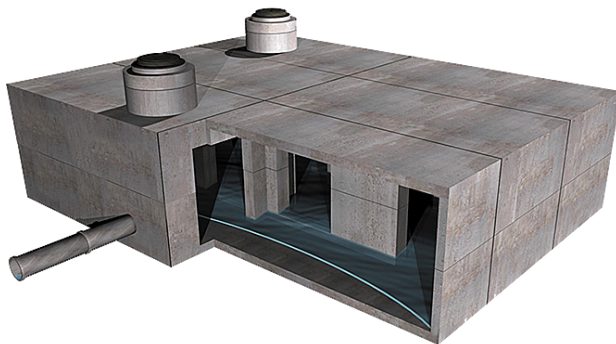


Fig. 3.16 Detention tank scheme, picture from the web

allowed runoff volume and consequently the volume to be treated by detention tanks (V_{Lam}) were identified for each CSO.

Sensitivity Analysis Low Impact Development modules: rain barrels, drainage trenches and pervious pavements

In order to test the overall behaviour and efficiency of some Low Impact Development techniques implemented in SWMM₅, a sensitivity analysis was carried out. The three technologies analysed were rain barrel, drainage trench and permeable pavement. Each of them was applied to a notional catchment of 5 hectares, varying technological parameters and assessing their role under different rainfall inputs. The main objective of the analysis was to choose the best configurations to implement in Sesto Ulteriano (MI) for diffuse storage purpose. The input data that define the sensitivity analysis varied according to the technology, since each of them has different layer characteristics. However, all three have two main parameters in common, which are: berm height (assumed to vary between 10, 50 and 100 mm) that is maximum depth to which water can pond above the surface of the unit before overflow occurs and drainage time (assumed to vary between 1, 5, 10, 20 and 50 hours). For each combination of these two parameters, a flow rate value (mm/h) was obtained which represents the amount of water drained in the unit of time and is closely related to the flow coefficient, a parameter that characterizes the drain element of each infrastructure in SWMM₅. In this regard, the modeling of sustainable urban drainage systems in SWMM₅ takes place by defining the characteristics of the individual modules that make up each SuDS technology, which are generally: surface layer, soil layer, storage layer and drain.

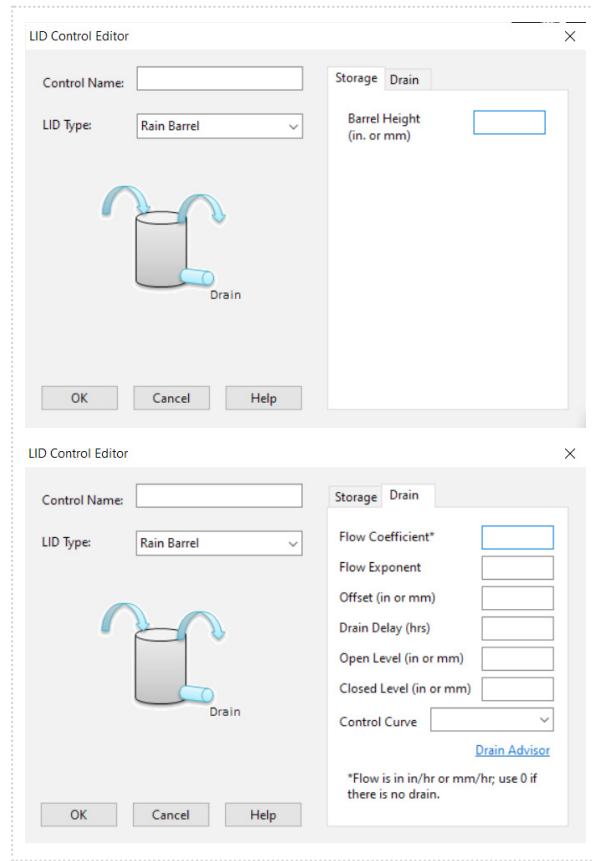
Rain Barrel

Rain barrels (or cisterns) are boxes that collect stormwater runoff releasing it in a larger period or storing it for future reuse during periods of drought. A rain barrel can be modelled as a single empty storage layer with a drain valve located at the bottom. In SWMM₅ this infrastructure is modelled through several parameters related to storage and drain (Fig. 3.17). Specifically, the storage section is only characterized by the Barrel Height parameter, identified as the depth of a rain barrel in which the water can be stored. The drain section is characterized by several parameters, such as:

- Flow coefficient C , calculated as suggested by SWMM₅ as the ratio between the drained flow rate (mm/h) and the height of the barrel raised to n (flow exponent)
- Flow exponent n , whose value, as recommended by SWMM₅, was set equal to 0.5 to ensure that the drain acts as an orifice
- Offset (mm), height from the drain, set equal to 0
- Drain delay (h), drain delay, set equal to 0
- Open level (mm), set equal to 0
- Closed level (mm), set equal to 0

The simulations (45) were carried out to test each configuration (berm and flow coefficient) under three rain inputs characterized by increasing severity: 2, 5 and 10 years return period. The idea was in fact to understand how the performance of rain barrel varies according to precipitation characteristics.

The output of each simulation allowed to obtain a hydrograph for each combination of Berm Height, Flow Coefficient and Return Period and to calculate the total volume discharged and,



Above Fig. 3.17 Rain Barrel parameters, screenshot from the modeling software;

On the right Fig. 3.18 Infiltration Trench parameters, screenshots from the modeling software

above all, the maximum flow rate, intended as the peak of the mentioned hydrograph. The output hydrograph were analysed in three different ways:

1. Under the same flow rate (mm/h) and return period (year) to assess the role of the berm height
2. Under the same berm height (mm) and return period (year) to assess the role of the flow rate
3. Under the same berm height (mm) and flow rate (mm/h) to assess the role of the return period

Infiltration Trench

Infiltration trenches are narrow ditches filled with gravel that intercept stormwater runoff. The drainage trench is a system that was created with the aim of dispersing rainwater in the subgrade, it is carried out with an excavation, generally with a rectangular section, filled with natural inert material with high permeability. In SWMM5

drainage trench is modelled as a single layer of draining soil characterized by several parameters related to surface, storage and drain (Fig. 3.18).

Specifically, the surface section is characterized by the following parameters:

- Berm Height (mm), identified as the depth of the surface storage
- Vegetation Volume Fraction, fraction of volume occupied by vegetation, set equal to 0
- Surface Roughness, set equal to 0.1
- Surface Slope (%), slope of the surface, set equal to 1

The storage section is characterized by the following parameters:

- Thickness (mm), thickness of the gravel layer set respectively equal to 250 mm and 500 mm
- Void ratio, volume of voids, set equal to 0.3
- Seepage rate, infiltration rate in the subgrade, set equal to 20 mm/h according to the characteristics of the subgrade and literature review
- Clogging factor, negligible.

The drain section is characterized by the following parameters:

- Flow coefficient C, calculated as suggested by SWMM5 as the ratio between the drained flow rate (mm/h) and the height of the barrel raised to n (flow exponent)
- Flow exponent n, whose value, as recommended by SWMM5, was set equal to 0.5 to ensure that the drain acts as an orifice
- Offset (mm), height from the drain, set equal to 0
- Drain delay (h), drain delay, set equal to 0
- Open level (mm), set equal to 0

The figure displays three sequential screenshots of the 'LID Control Editor' dialog box for an 'Infiltration Trench'. Each screenshot shows a 3D diagram of the trench with 'Surface', 'Storage', and 'Drain*' components. The 'Surface' tab includes parameters: Berm Height (in. or mm), Vegetation Volume Fraction, Surface Roughness (Mannings n), and Surface Slope (percent). The 'Storage' tab includes: Thickness (in. or mm), Void Ratio (Voids / Solids), Seepage Rate (in/hr or mm/hr), and Clogging Factor. The 'Drain' tab includes: Flow Coefficient*, Flow Exponent, Offset (in or mm), Open Level (in or mm), Closed Level (in or mm), and Control Curve. A 'Drain Advisor' link and a note '*Flow is in in/hr or mm/hr; use 0 if there is no drain.' are also present.

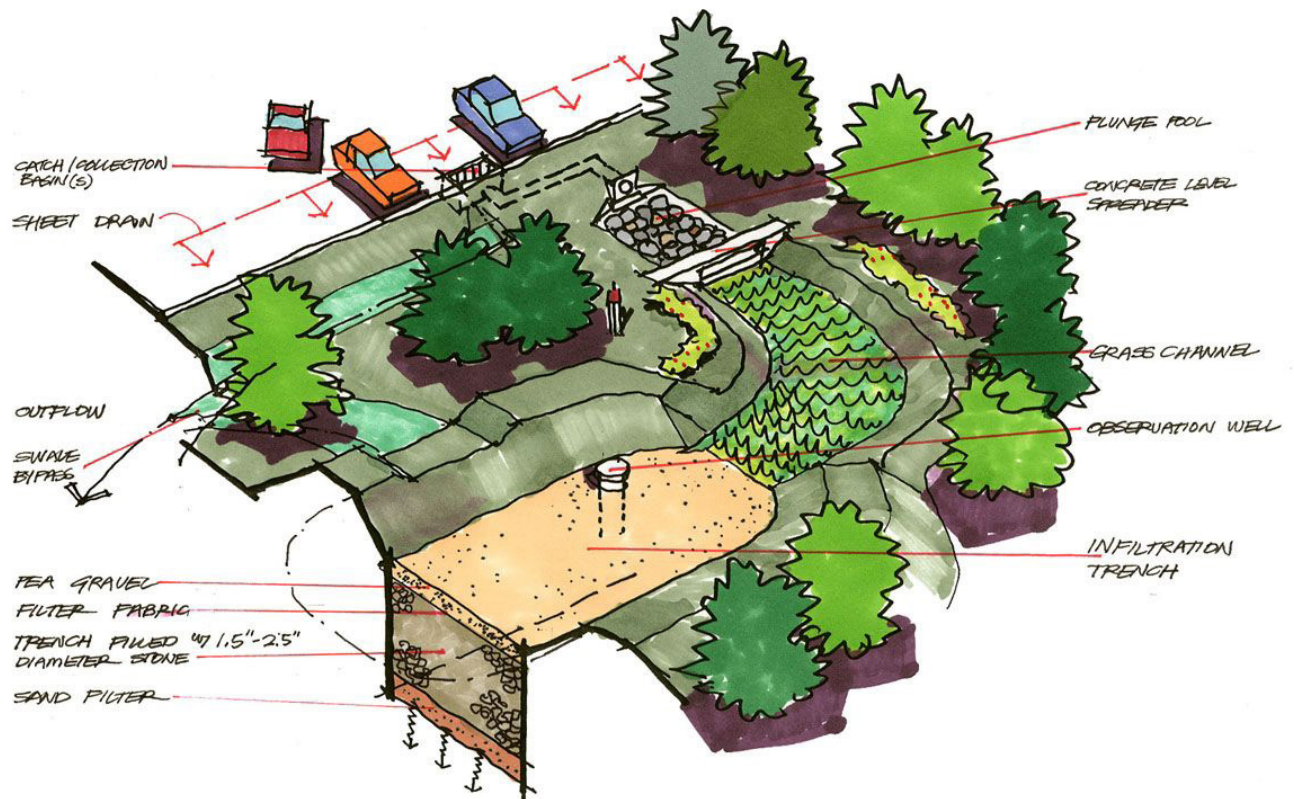
- Closed level (mm), set equal to 0

The simulations carried out on the draining trench take into account not only the variability of the berm height, the flow coefficient and the return period, but also of the storage layer, placed once equal to 250 mm and once equal to 500 mm. This procedure, which involves 90 short SWMM5 simulations, was implemented to understand if the thickness of the storage could somehow influence the behavior of the trench. The output of each simulation allowed to obtain a hydrograph for each combination of Berm Height, Flow Coefficient, Return Period and Storage height

and to calculate the total volume discharged and, above all, the maximum flow rate, intended as the peak of the mentioned hydrograph.

The output hydrograph were analysed for each of the Storage height (250/500 mm) in three different ways:

1. Under the same flow rate (mm/h) and return period (year) to assess the role of the berm height
2. Under the same berm height (mm) and return period (year) to assess the role of the flow rate
3. Under the same berm height (mm) and flow rate (mm/h) to assess the role of the return period



INFILTRATION TRENCH

INFILTRATION TRENCH SKETCH

<https://www.pinterest.it/pin/305189312223249922/>

Permeable Pavement

Permeable pavement systems are road areas or parking lots that are paved with a porous concrete or asphalt mix placed on top of a gravel storage layer. Rain passes through the pavement into the storage layer where it can infiltrate the site's native soil (SWMM Ref. Manual Vol.III). Permeable pavements allow pedestrians and vehicles to circulate and at the same time allow the infiltration of rainwater through the surface into the underlying layers. The water comes temporarily subsequently stored, a part infiltrates the ground and a part is discharged further downstream. This SuDS in SWMM₅ is characterized by several parameters related to surface, pavement, soil, storage and drain (Fig. 3.19 on the right and in the next page).

Specifically, the surface section is characterized by the following parameters:

- Berm Height (mm), identified as the depth of the surface storage
- Vegetation Volume, fraction of volume occupied by vegetation, set equal to 0
- Surface Roughness, set equal to 0.1
- Surface Slope (%), slope of the surface, set equal to 1

The pavement section is characterized by the following parameters:

- Thickness (mm), set equal to 100 mm
- Void ratio, set equal to 0.1
- Impervious Surface Fraction, equal to 0
- Permeability, variable according to the highest, the mean and the lowest value of the SWMM₅ Manual range (711.2-44450 mm/h)
- Clogging Factor, set equal to 0

The figure displays four screenshots of the LID Control Editor dialog box for Permeable Pavement. Each screenshot shows a different tab selected in the parameter list on the right, while the central diagram and other controls remain consistent.

Top Screenshot (Surface Tab): Parameters include Berm Height (in. or mm), Vegetation Volume Fraction, Surface Roughness (Mannings n), and Surface Slope (percent).

Second Screenshot (Pavement Tab): Parameters include Thickness (in. or mm), Void Ratio (Voids / Solids), Impervious Surface Fraction, Permeability (in/hr or mm/hr), Clogging Factor, Regeneration Interval (days), and Regeneration Fraction.

Third Screenshot (Soil Tab): Parameters include Thickness (in. or mm), Porosity (volume fraction), Field Capacity (volume fraction), Wilting Point (volume fraction), Conductivity (in/hr or mm/hr), Conductivity Slope, and Suction Head (in. or mm).

Bottom Screenshot (Storage Tab): Parameters include Thickness (in. or mm), Void Ratio (Voids / Solids), Seepage Rate (in/hr or mm/hr), and Clogging Factor.

Each screenshot includes a central diagram of the LID structure (Surface, Pavement, Soil*, Storage, Drain*) and a '*Optional' label below it. The dialog box also features 'Control Name', 'LID Type' (set to Permeable Pavement), and 'OK', 'Cancel', and 'Help' buttons.



CHICAGO PERMEABLE PAVEMENTS
Picture from the web

- Regeneration Interval (day), set equal to 0
- Regeneration Fraction, set equal to 0

The soil section is characterized by the following parameters:

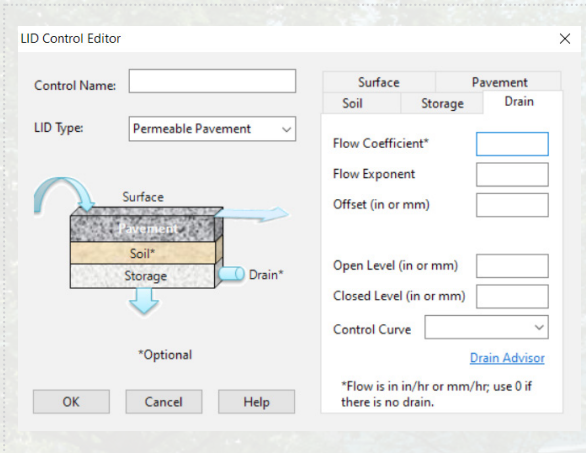
- Thickness (mm), set equal to 50 mm
- Porosity, set equal to 0.3
- Field capacity, set equal to 0.2
- Wilting Point, set equal to 0.01
- Conductivity (mm/h), variable according to the highest, the mean and the lowest value of the SWMM₅ Manual range (127-762 mm/h)
- Conductivity slope, set equal to 0
- Suction Head (mm), set equal to 76.2 mm

The storage section is characterized by the following parameters:

- Thickness (mm), thickness of the gravel layer set to 100 mm
- Void ratio, volume of voids, set equal to 0.3
- Seepage rate, infiltration rate in the subgrade, set equal to 20 mm/h according to the characteristics of the subgrade and literature review
- Clogging factor, negligible.

The drain section is characterized by the following parameters:

- Flow coefficient C, calculated as suggested by SWMM₅ as the ratio between the drained flow rate (mm/h) and the height of the barrel raised to n (flow exponent)
- Flow exponent n, whose value, as recommended by SWMM₅, was set equal to 0.5 to ensure that the drain acts as an orifice
- Offset (mm), height from the drain, set equal to 0



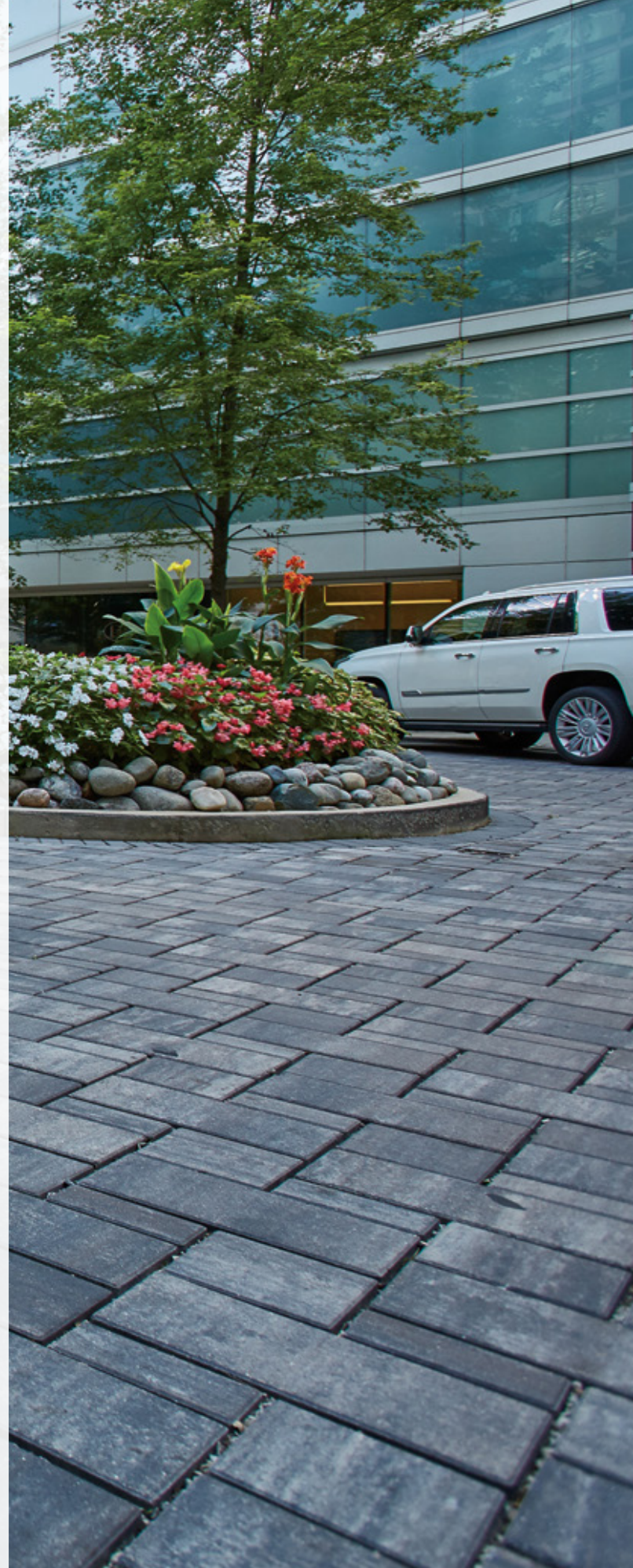
Above and in the previous page Fig. 3.19 Permeable Pavement parameters, screenshots from the modeling software

- Drain delay (h), drain delay, set equal to 0
- Open level (mm), set equal to 0
- Closed level (mm), set equal to 0

The output of each simulation allowed to obtain a hydrograph for each combination of Berm Height, Flow Coefficient, Return Period and Permeability/Conductivity scenario and to calculate the total volume discharged and, above all, the maximum flow rate, intended as the peak of the mentioned hydrograph.

The output hydrograph were analysed for each of Permeability/Conductivity scenario (High Infiltration, Mean infiltration and Low infiltration) again in three different ways:

1. Under the same flow rate (mm/h) and return period (year) to assess the role of the berm height
2. Under the same berm height (mm) and return period (year) to assess the role of the flow rate
3. Under the same berm height (mm) and flow rate (mm/h) to assess the role of the return period



SuDS implementation at the catchment scale aiming at a “Diffuse-Storage” scenario

Rain barrel and Permeable Pavements, both object of the sensitivity analyses, were individually implemented in the SWMM₅ drainage model of Sesto Ulteriano to assess the effectiveness of floodable streets and squares in the reduction of stormwater peak flows and volumes discharged. Drainage trenches were excluded from the catchment-scale analysis. This kind of infrastructure was investigated in the sensitivity analysis just because it was halfway between the modeling simplicity of rain barrels and the complexity of pervious pavements. The parameterization of rain barrels and permeable pavements were inferred from the sensitivity analysis. However, additional remarks were done about the Berm Height and the draining time of these infrastructures. For both the infrastructure, in fact a Berm Height of 100 mm was chosen because it was the most realistic and the effective one. The thicknesses of 10 and 50 mm were discarded because would have lead to fewer benefits in the reduction of urban flooding phenomena. As regard the draining time, two different values were tested: 10 hours, representative of the “worst condition”, and 50 hours, representative of the “better condition”. Values lower than 10 hours were discharged because considered unrealistic if compared with the concentration time of the catchment. Sustainable drainage infrastructure implementation focused on the industrial catchments A, C and E for their suitability in the realization of floodable streets and squares. Therefore, the residential catchment were excluded from the analyses.

CHEONGGYECHEON PARK IN SEOUL, SOUTH KOREA
Picture from ArchDaily

Diffuse-storage with Rain Barrels

The first scenario provides for the modelling of floodable street and squares in the industrial areas of Sesto Ulteriano through the implementation of the “Rain Barrel” SWMM₅ SuDS module. As already mentioned, two different drainage times were investigated: 10 h (worst condition) and 50 h (best condition). Each configuration was tested under 2-years, 5-years and 10-years return



period rainfalls. The rain barrels were modelled in SWMM₅ as follows: The Barrel Height parameters was set equal to 100 mm while the flow coefficient C was set equal to 1 for obtaining the drainage in 10 hours and equal to 0.2 for the 50-hours drainage. All the other parameters were set according to the parameterization discussed in the sensitivity analysis. SWMM₅ simulations (6) were carried out and the output data were processed in terms of:

1. Peak flow, understood as the maximum flow rate value in the flood hydrogram (Q_{max});
2. Total volume, calculated as the area underlying the hydrograph extended over time (V_{tot});
3. Volume to be discharged into drainage tanks (V_{lam}), calculated as the volume in the flood hydrograph that exceeds the limit value of 40 l / s per hectare of impervious surface.

Diffuse-storage with Permeable Pavements

The second scenario provides for the modelling of floodable street and squares in the industrial areas of Sesto Ulteriano through the implementation of the “Permeable Pavement” SWMM₅ SuDS module. As already mentioned, two different drainage times were investigated: 10 h (worst condition) and 50 h (best condition). Each configuration was tested under 2-years, 5-years and 10-years return period rainfalls. The permeable pavements were modelled in SWMM₅ as follows: The Berm Height parameters was set equal to 100 mm while the flow coefficient C was set equal to 1 for obtaining the drainage in 10 hours and equal to 0.2 for the 50-hours drainage. All the other parameters were set according to the parameterization discussed in the sensitivity analysis. SWMM₅ simulations (6) were carried out and the output data were processed in terms of:

1. Peak flow, understood as the maximum flow rate value in the flood hydrogram;
2. Total volume, calculated as the area underlying the hydrograph extended over time;
3. Volume to be discharged into drainage tanks, calculated as the volume in the flood hydrograph that exceeds the limit value of 40 l / s per hectare of impervious surface.



Results

The project of detention tanks in the “Central-Storage” scenario

Volumes of the detention tanks in the “Central-Storage” scenario are reported in Table 3.7, 3.8., 3.9 for each of the investigated rainfall event. Even for slight rains (T=2 years), an activation of several CSOs (Outfalls in the following tables) can be

observed (especially in the industrial catchment A, C, E) with over 3000 m³ to be discharged into the tanks (V_{Lam}). This is symptomatic of the significant flood-related criticalities that affect the urban fabric of Sesto Ulteriano. This condition worsens with the increase of the severity of rainfall events (T=5, T=10).

T=2							
Tank	CSO	Aimp (ha)	Q _{max} (m ³ /s)	V _{tot} (m ³)	Q _{Law} (l/s)	Q _{Law} (m ³ /s)	V _{Lam} (m ³)
A	1019	51.2	3.5668	25590.384	2048	2.048	1776.504
B	3132	7.4	0.00162	10.068	296	0.296	0
	3127	2.9	0.00133	8.256	116	0.116	0
	3275	2.4	0.00163	3.738	96	0.096	0
C	2862	4.8	0.01863	42.6	192	0.192	0
	2852	5.93	0.25458	731.4	237.2	0.2372	10.428
	J7	19.3	1.44864	2982.03	772	0.772	577.638
	3155	0.3	0.03347	40.896	12	0.012	18.696
	2861	1.1	0.02959	252.486	44	0.044	0
D	140	3.2	0.04709	416.214	128	0.128	0
	137	0.2	0.04967	356.916	8	0.008	186.384
	127	0.7	0.02146	158.172	28	0.028	0
	191	0.8	0.02157	176.664	32	0.032	0
	3150	0.7	0.02082	168.198	28	0.028	0
	3099	0.9	0.03031	219.57	36	0.036	0
E	2863	12.3	0.122	317.1	492	0.492	0
	3520	14.7	1.11015	8004.348	588	0.588	835.194

Tab. 3.7 Identification of volumes to be discharged into detention tanks in occasion of 2-year return period rainfall events according to limitation imposed by Regional Law;

On the right from the top Tab. 3.8 Identification of volumes to be discharged into detention tanks in occasion of 5-year return period rainfall events according to limitation imposed by Regional Law;

Tab. 3.9 Identification of volumes to be discharged into detention tanks in occasion of 10-year return period rainfall events according to limitation imposed by Regional Law

T=5

Tank	CSO	Aimp (ha)	Q _{max} (m ³ /s)	V _{tot} (m ³)	Q _{Law} (l/s)	Q _{Law} (m ³ /s)	V _{Lam} (m ³)
A	1019	51.2	6.31375	41358.912	2048	2.048	8309.712
B	3132	7.4	0.24117	345.924	296	0.296	0
	3127	2.9	0.00856	21.48	116	0.116	0
	3275	2.4	0.00254	6.12	96	0.096	0
C	2862	4.8	0.33435	287.964	192	0.192	85.41
	2852	5.93	0.70154	1861.722	237.2	0.2372	542.16
	J7	19.3	2.28651	7351.302	772	0.772	2685.57
	3155	0.3	0.05053	114.834	12	0.012	78.228
	2861	1.1	0.11629	590.784	44	0.044	111.66
D	140	3.2	0.1723	875.31	128	0.128	26.58
	137	0.2	0.21773	877.104	8	0.008	692.034
	127	0.7	0.10564	381.222	28	0.028	84.816
	191	0.8	0.08003	407.994	32	0.032	71.262
	3150	0.7	0.07821	379.56	28	0.028	66.894
	3099	0.9	0.0978	480.366	36	0.036	76.338
E	2863	12.3	0.15919	781.578	492	0.492	0
	3520	14.7	2.26911	13707.666	588	0.588	3781.62

T=10

Tank	CSO	Aimp (ha)	Q _{max} (m ³ /s)	V _{tot} (m ³)	Q _{Law} (l/s)	Q _{Law} (m ³ /s)	V _{Lam} (m ³)
A	1019	51.2	7.45348	52741.794	2048	2.048	14716.632
B	3132	7.4	0.68247	1329.558	296	0.296	527.298
	3127	2.9	0.02048	38.916	116	0.116	0
	3275	2.4	0.17123	178.152	96	0.096	57.474
C	2862	4.8	1.72428	1568.664	192	0.192	1148.1
	2852	5.93	1.47965	2983.758	237.2	0.2372	1287.504
	J7	19.3	3.12528	10247.334	772	0.772	3857.202
	3155	0.3	0.07585	160.914	12	0.012	112.962
	2861	1.1	0.3369	898.296	44	0.044	307.116
D	140	3.2	0.4865	1346.244	128	0.128	274.77
	137	0.2	0.44744	1410.966	8	0.008	1226.19
	127	0.7	0.22929	564.858	28	0.028	197.85
	191	0.8	0.22936	618.21	32	0.032	201.828
	3150	0.7	0.22628	593.856	28	0.028	208.944
	3099	0.9	0.29398	768.342	36	0.036	271.08
E	2863	12.3	0.33539	1261.044	492	0.492	0
	3520	14.7	2.71051	17311.452	588	0.588	5632.842

Sensitivity Analysis Low Impact Development modules: rain barrels, drainage trenches and pervious pavements

Rain Barrel

1. Under the same flow rate (mm/h) and varying return periods to assess the role of the berm height: Figure 3.20 represent the flow discharged from the rain barrel for the same flow rate (10 mm/h) and different rainfall severities. Increasing the berm height from 10 mm to 100 mm, it is possible to observe a significant reduction and delay of the peak flow. No great differences can be underlined switching from a 50 to a 100 mm berm height. With the increase of the severity of rainfall event, only rain barrels with 10-mm berm height reach higher peak flows. For the others the peak flow seems not to be influenced by the return period of the rainfall events. It should be remembered that these assumption could somehow be influenced by the characteristics of the notional study model.

2. Under varying berm heights and the same return period to assess the role of the flow rate: Figure 3.21 represent the flow discharged from the rain barrel for the same return period (T=2) and different berm heights. With the increase of the drainage time, it is possible to underline a peak flow reduction. However, the peak flow increases with the reduction of the berm height.

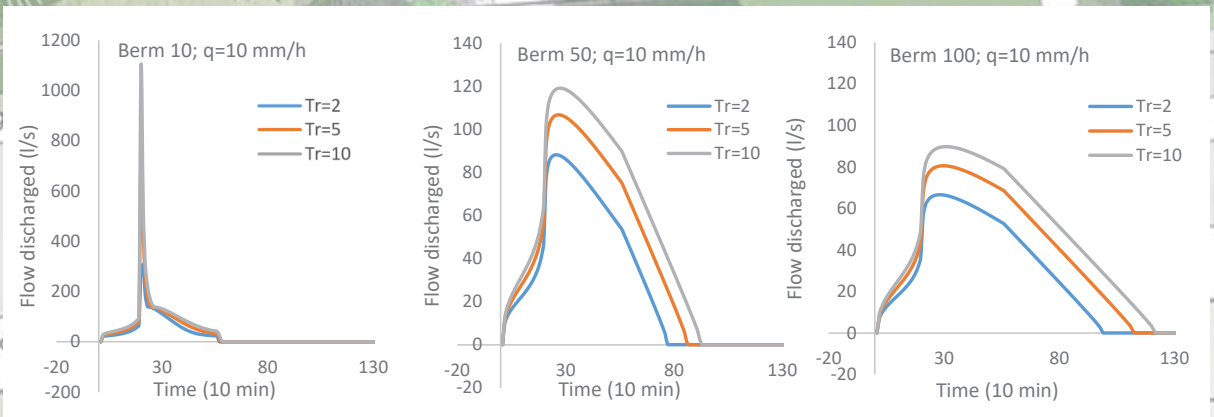
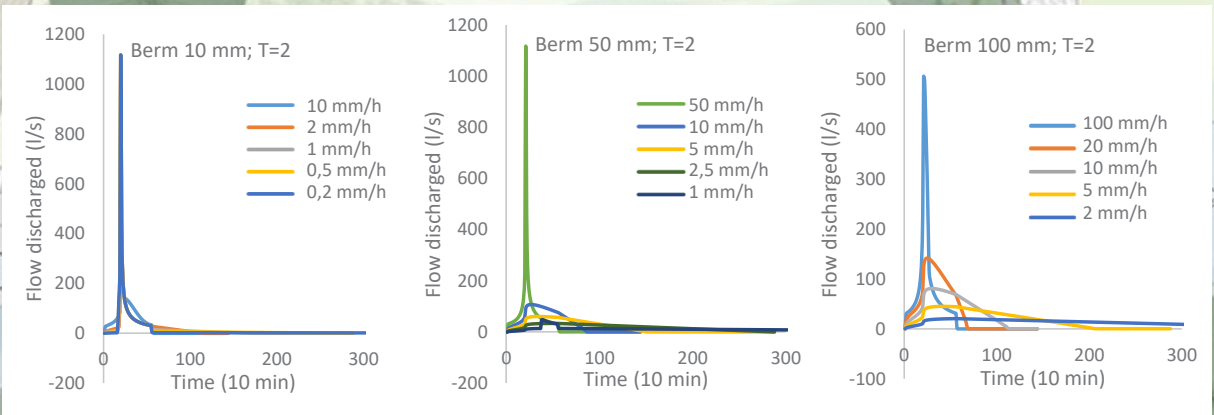
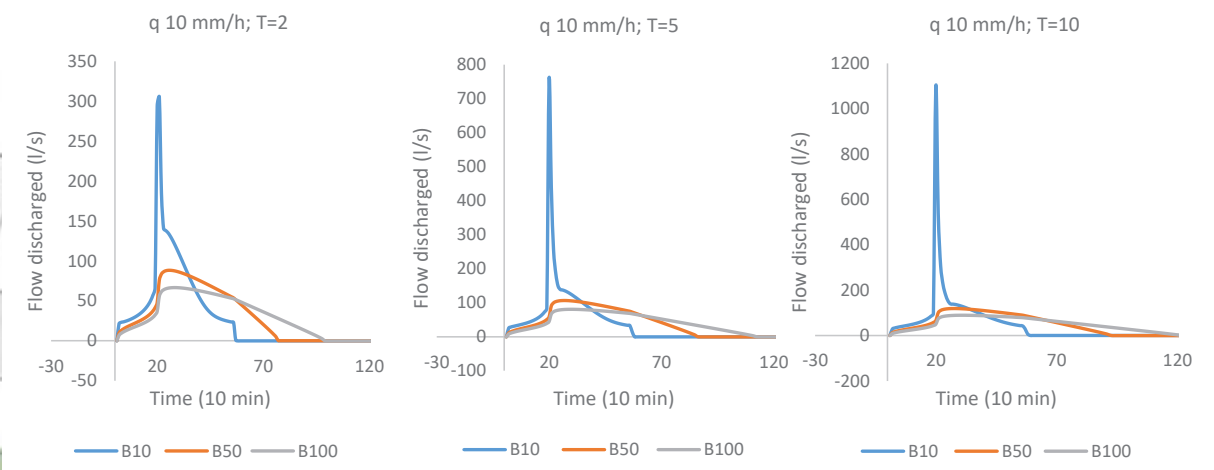
3. Under the same flow rate (10 mm/h) and varying berm heights to assess the role of the return period: The peak of the hydrograph increases along with the increase of the rainfall severity (Fig. 3.22). The differences that occur with the different rain inputs, however, tend to decrease for lower berm heights and for larger drainage times.

On the right from the top Fig. 3.20 Flow discharged from the outfall under the same flow rate and varying return periods to assess the role of the berm height;

Fig. 3.21 Flow discharged from the outfall under varying berm heights and the same return period to assess the role of the flow rate;

Fig.3.22 Flow discharged from the outfall under the same flow rate (10 mm/h) and varying berm heights to assess the role of the return period

BARKARBY MADER, BARKARBY, STOCKHOLM, SWEDEN
Picture from LANDEZINE



Drainage Trench

The storage depth turned out to be irrelevant; the results reported in the following are the same for 250-mm and 500-mm depth.

1. Under the same flow rate (10 mm/h) and varying return periods to assess the role of the berm height: Figure 3.23 represent the flow discharged from the drainage trench for the same flow rate (10 mm/h) and different rainfall severities. Increasing the berm height from 10 mm to 100 mm, it is possible to observe a significant reduction of the peak flow. However, differently from the rain barrel, there is not a delay of the peak flow. No great differences can be underlined switching from a 50 to a 100 mm berm height. The peak flow seems not to be influenced by the severity of the rainfall events but what changes is the duration of the peak and consequently the volume of the hydrograph.

2. Under varying berm heights and the same return period to assess the role of the flow rate: Figure 3.24 represent the flow discharged from the drainage trench for the same return period (T=2) and different berm heights. With the increase of the drainage time, it is possible to underline a peak flow reduction. However, the peak flow increases with the reduction of the berm height.

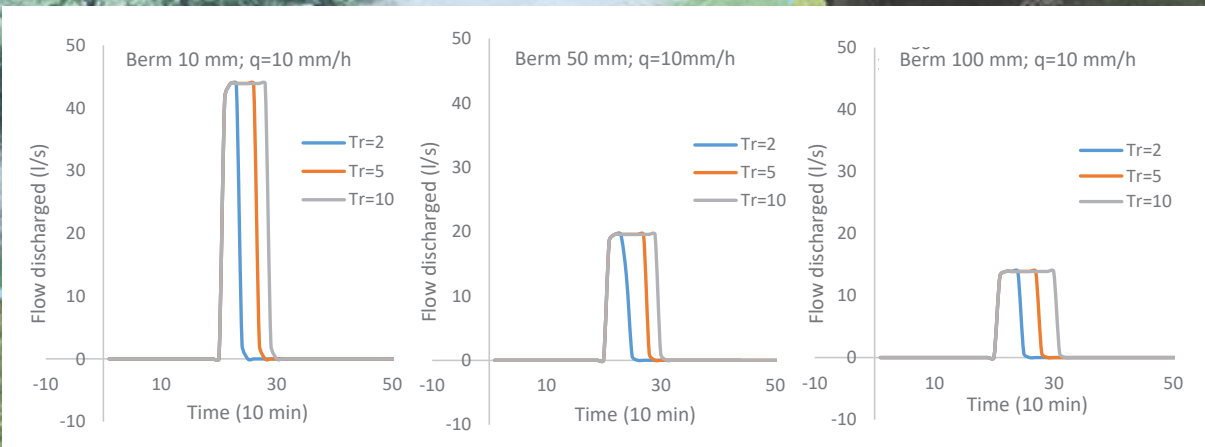
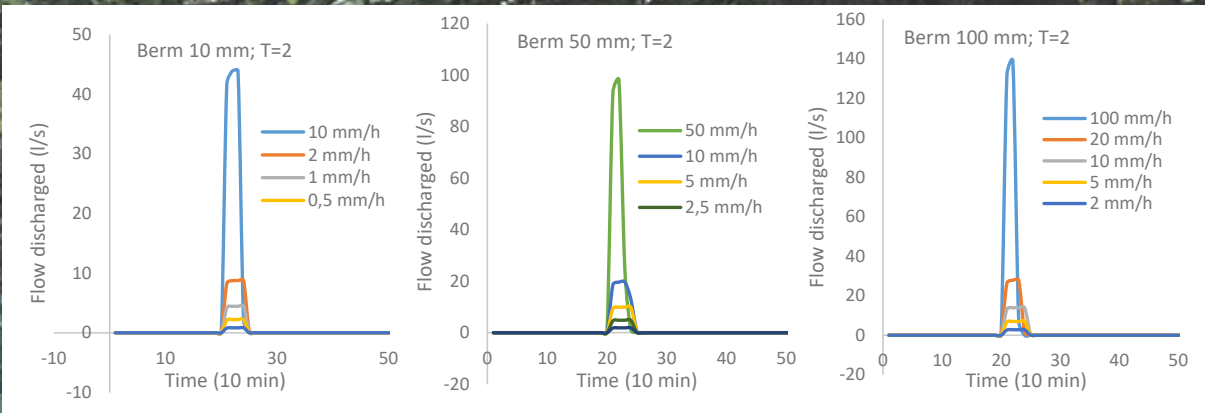
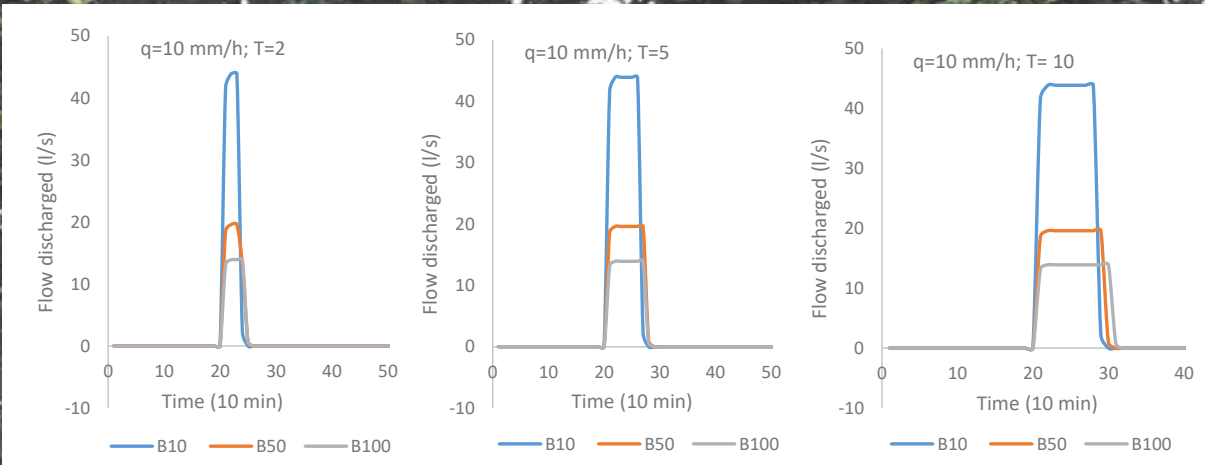
3. Under the same flowrate (10 mm/h) and varying berm heights to assess the role of the return period: The peak of the hydrograph seems not influenced by the increase of the rainfall severity (Fig. 3.25) for all flow rate and the berm heights investigated. As mentioned before, what changes is the duration of the peak and the volume of the hydrograph (whose values increase with the increase of the rainfall intensity). Independently from the return period of the rainfall, berm heights of 50 and 100 mm both lead to good reduction of the peak flow.

On the right from the top Fig. 3.23 Flow discharged from the outfall under the same flow rate and varying return periods to assess the role of the berm height;

Fig. 3.24 Flow discharged from the outfall under varying berm heights and the same return period to assess the role of the flow rate;

Fig.3.25 Flow discharged from the outfall under the same flow rate (10 mm/h) and varying berm heights to assess the role of the return period

FLOODABLE PARK,
GOTHENBURG, SWEDEN
<https://ramboll.com/media/rgr/strategic-cloudburst-management-plan-will-bring-blue-green-infrastructure-to-gothenburg>



Permeable Pavement

The output data obtained from the simulations with the three different permeability conditions (high, medium and low) resulted identical to each other. This could be linked to the reference values provided by the manual, actually not representative of the reality. Downstream of this consideration, only the high permeability condition will be reported, which will also be representative of the other two.

1. Under the same flow rate (10 mm/h) and varying return periods to assess the role of the berm height: Figure 3.26 represent the flow discharged from the permeable pavement for the same flow rate (10 mm/h) and different rainfall severities. The berm height seems to be irrelevant for the modelled permeable pavement under rainfall characterized by T=2. Under such rainfall input the infrastructure is able to retain a large part of stormwater, minimizing the flow discharged. Increasing the severity of the rainfall, the effect of the berm height is much more visible. Increasing the berm height from 10 mm to 100 mm it is possible to observe a significant reduction and short delay of the peak flow.

2. Under varying berm heights and the same return period to assess the role of the flow rate: Figure 3.27 represent the flow discharged from the permeable pavement for the same return period (T=5) and different berm heights. With the increase of the drainage time, it is possible to underline again a peak flow reduction. However, the peak flow increases with the reduction of the berm height.

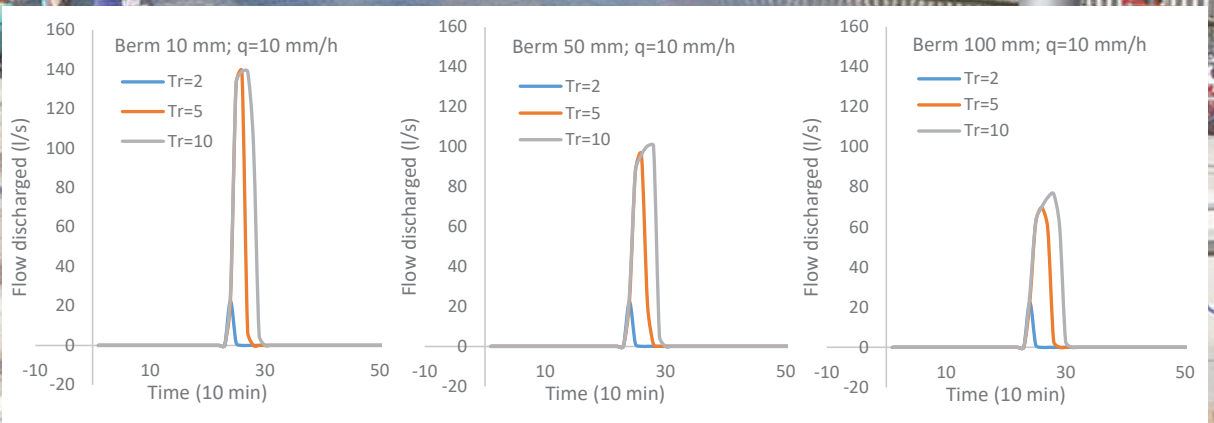
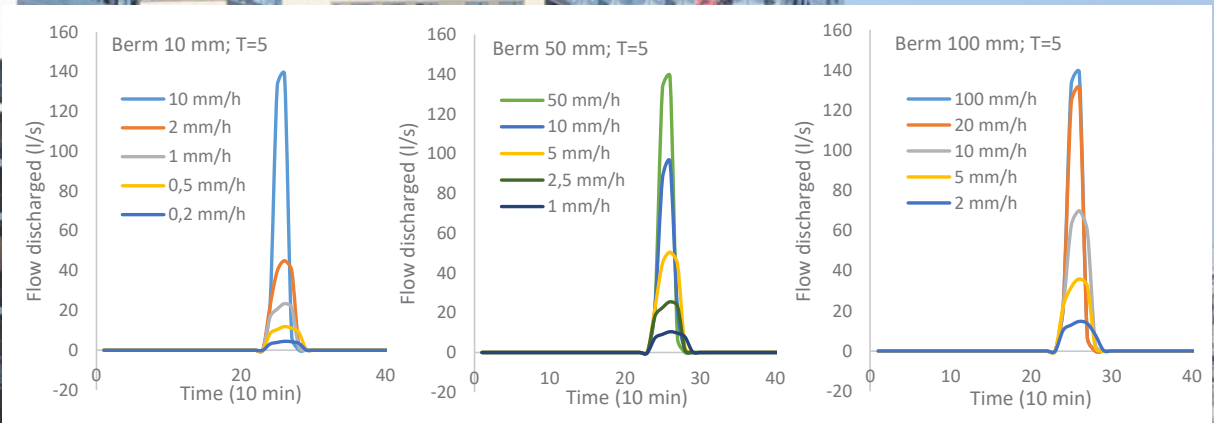
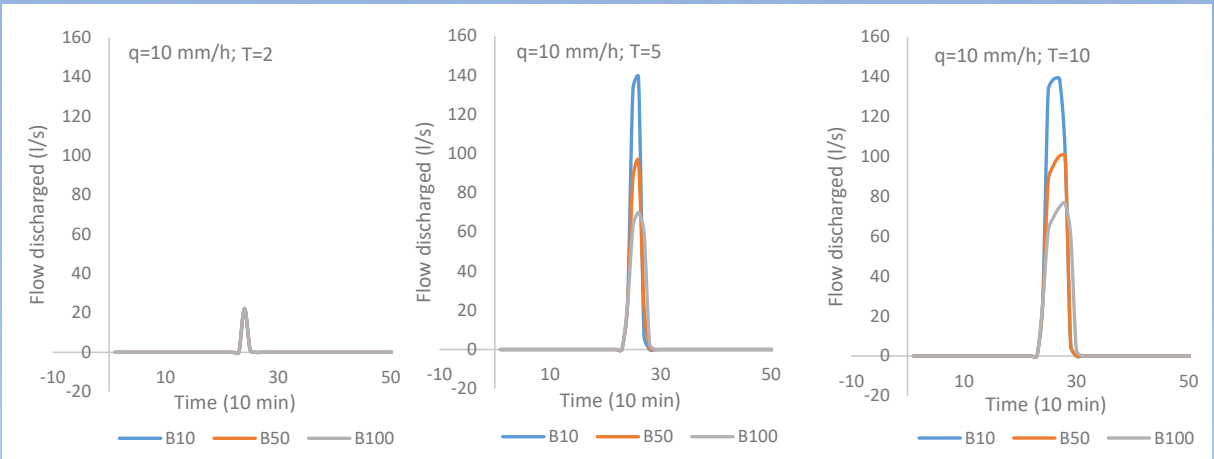
3. Under the same flow rate (10 mm/h) and varying berm heights to assess the role of the return period: The peak of the hydrograph seems influenced by the increase of the rainfall severity from T=2 to T=5; however no great differences can be observed switching from T=5 to T=10(Fig. 3.28). As mentioned before, what changes is the duration of the peak and the volume of the hydrograph (whose values increase with the increase of the rainfall intensity). Independently from the return period of the rainfall, berm heights of 50 and 100 mm both lead to good reduction of the peak flow.

On the right from the top Fig. 3.26 Flow discharged from the outfall under the same flow rate and varying return periods to assess the role of the berm height;

Fig. 3.27 Flow discharged from the outfall under varying berm heights and the same return period to assess the role of the flow rate;

Fig.3.28 Flow discharged from the outfall under the same flow rate (10 mm/h) and varying berm heights to assess the role of the return period

FLOODABLE PUBLIC SPACES,
HAMBURG, GERMANY
<https://www.arquine.com/hafen-city-public-space-de-embt-benedetta-tagliabue/>



Comparison between the analysed technologies

The sensitivity analyses was essential also to compare the performances of each system. The rain barrel is able to detain stormwater and discharge it in a longer time interval. Differently from the rain barrel, the drainage trench and the permeable pavement are also able to retain stormwater that infiltrate through the substrate into the native soil, reducing not only the peak flow but also the total volume discharged. Their behaviour is, for this reason, similar but permeable pavement, as well as rain barrels, for their traditional use in the urban context are definitely closer to the systems traditionally used in the pursuit of the concept of “floodable” cities.

HUNTER'S POINT SOUTH PARK,
NY, USA

<https://www.azuremagazine.com/article/hunters-point-south-park-queens-resilience/>



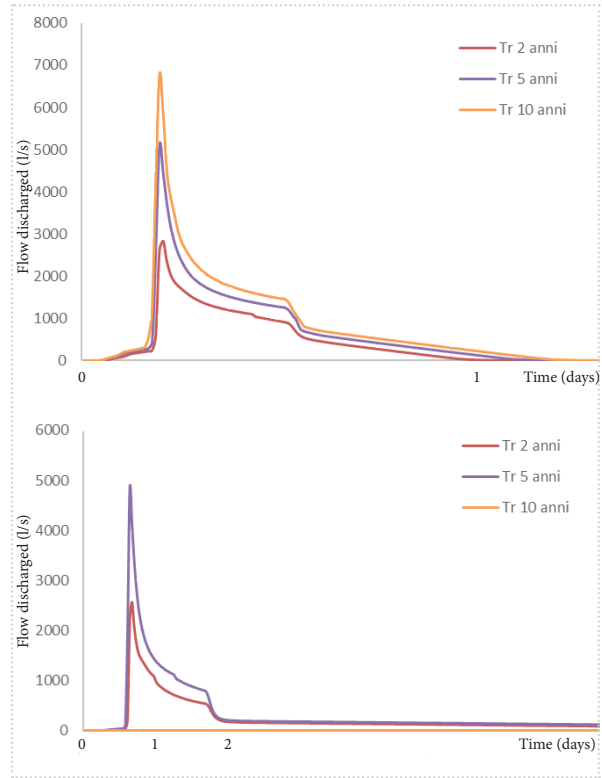


SuDS implementation at the catchment scale aiming at a “Diffuse-Storage” scenario: results

Diffuse-storage with Rain Barrels (RB)

Looking at Table 3.10 (a, b, c) as the rainfall severity increases, the volume to be discharged into detention tanks becomes larger and larger. This phenomenon is even more visible by referring to the hydrograph of each CSO of the sewer. In Figure 3.29 the hydrograph of a strategic outfall (node 1019) is reported for each of the analysed T.

With the increase of the drainage time of the rain barrels (50 h) a good reduction of peak flows, total volumes and volumes to be discharged according to regional regulations into detention tanks can be observed (Table 3.11 a, b, c). Also in this case the hydrographs of node 1019 for all the rainfall inputs investigated are plotted in Figure 3.30.



a.

T=2

Tank	CSO	A _{imp} (ha)	Q _{Law} (m ³ /s)	Q _{Max} (m ³ /s)	V _{Tot} (m ³)	V _{Lam} (m ³)
A	1019	51.2	2.048	2.82745	39373.536	988.68
B	3132	7.4	0.296	0.00157	9.978	0
	3127	2.9	0.116	0.00129	8.172	0
	3275	2.4	0.096	0.00139	3.57	0
C	2862	4.8	0.192	0.00776	72.51	0
	2852	5.93	0.2372	0.1747	906.462	0
	J7	19.3	0.772	1.2503	2918.478	426.378
	3155	0.3	0.012	0.02663	24.018	9.018
	2861	1.1	0.044	0.0331	442.02	0
D	140	3.2	0.128	0.04855	419.634	0
	137	0.2	0.008	0.04704	362.4	193.026
	127	0.7	0.028	0.01979	156.648	0
	191	0.8	0.032	0.02256	176.508	0
	3150	0.7	0.028	0.02247	167.028	0
E	3099	0.9	0.036	0.02933	217.248	0
	2863	12.3	0.492	0.06534	414.582	0
	3520	14.7	0.588	0.89419	10965.342	381.462

From above Fig. 3.29 and 3.30 Hydrograph of a strategic outfall (node 1019) for each of the analysed T and for 10 h and 50 h of discharging time;

On the left Tab. 3.10 a Volume to be discharged into the detention tanks in occasion of a T=2 year rainfall (10 hours discharging time) - Diffuse-Storage with Rain Barrels;

On the right from above Tab. 3.10 b and c Volume to be discharged into the detention tanks in occasion of a T=5 year and a T=10 year rainfall respectively (10 hours discharging time) - Diffuse-Storage with Rain Barrels;

b.

T=5

Tank	CSO	A _{imp} (ha)	Q _{Law} (m ³ /s)	Q _{Max} (m ³ /s)	V _{Tot} (m ³)	V _{Lam} (m ³)
A	1019	51.2	2.048	5.23254	58530.918	6938.232
B	3132	7.4	0.296	0.43712	614.982	102.612
	3127	2.9	0.116	0.00767	20.82	0
	3275	2.4	0.096	0.00234	5.976	0
C	2862	4.8	0.192	0.28028	278.208	52.968
	2852	5.93	0.2372	0.5586	1983.822	259.704
	J7	19.3	0.772	1.92318	7338.006	1526.88
	3155	0.3	0.012	0.04771	98.868	67.962
	2861	1.1	0.044	0.14719	859.854	134.664
D	140	3.2	0.128	0.20907	983.466	95.07
	137	0.2	0.008	0.2659	1012.086	827.514
	127	0.7	0.028	0.12562	403.572	104.886
	191	0.8	0.032	0.12517	451.218	111.564
	3150	0.7	0.028	0.11414	431.508	115.674
	3099	0.9	0.036	0.15694	562.608	154.416
E	2863	12.3	0.492	0.18122	971.742	0
	3520	14.7	0.588	1.68627	17511.234	3031.866

c.

T=10

Tank	CSO	A _{imp} (ha)	Q _{Law} (m ³ /s)	Q _{Max} (m ³ /s)	V _{Tot} (m ³)	V _{Lam} (m ³)
A	1019	51.2	2.048	6.79816	72446.796	11868.834
B	3132	7.4	0.296	0.74504	1228.344	417.762
	3127	2.9	0.116	0.20818	150.246	55.308
	3275	2.4	0.096	0.15605	182.478	61.452
C	2862	4.8	0.192	0.48018	493.386	172.908
	2852	5.93	0.2372	0.81955	2859.45	599.256
	J7	19.3	0.772	2.27512	10866.498	2731.992
	3155	0.3	0.012	0.05342	144.12	97.104
	2861	1.1	0.044	0.20637	1116.036	232.014
D	140	3.2	0.128	0.31601	1317.27	221.976
	137	0.2	0.008	0.34464	1418.286	1232.796
	127	0.7	0.028	0.17633	547.164	177.084
	191	0.8	0.032	0.17487	609.99	189.066
	3150	0.7	0.028	0.16504	588.204	198.372
	3099	0.9	0.036	0.22381	765.06	261.438
E	2863	12.3	0.492	0.27401	1360.098	0
	3520	14.7	0.588	2.19686	22034.106	5019.834

a.

T=2

Tank	CSO	A _{imp} (ha)	Q _{Law} (m ³ /s)	Q _{Max} (m ³ /s)	V _{Tot} (m ³)	V _{Lam} (m ³)
A	1019	51.2	2.048	2.56441	40307.688	421.164
B	3132	7.4	0.296	0.00157	9.978	0
	3127	2.9	0.116	0.00129	8.172	0
	3275	2.4	0.096	0.00139	3.564	0
C	2862	4.8	0.192	0.00707	46.578	0
	2852	5.93	0.2372	0.14619	619.098	0
	J7	19.3	0.772	1.14744	1887.006	305.634
	3155	0.3	0.012	0.0203	14.358	4.98
	2861	1.1	0.044	0.02683	328.752	0
D	140	3.2	0.128	0.04855	419.634	0
	137	0.2	0.008	0.04704	362.4	193.026
	127	0.7	0.028	0.0198	156.642	0
	191	0.8	0.032	0.02256	176.508	0
	3150	0.7	0.028	0.02247	167.028	0
	3099	0.9	0.036	0.02933	217.254	0
	E	2863	12.3	0.492	0.06281	337.152
	3520	14.7	0.588	0.79311	8588.532	217.116

b.

T=5

Tank	CSO	A _{imp} (ha)	Q _{Law} (m ³ /s)	Q _{Max} (m ³ /s)	V _{Tot} (m ³)	V _{Lam} (m ³)
A	1019	51.2	2.048	4.87781	61224.72	5383.026
B	3132	7.4	0.296	0.43659	612.486	100.5
	3127	2.9	0.116	0.00767	20.82	0
	3275	2.4	0.096	0.00234	5.976	0
C	2862	4.8	0.192	0.21592	190.77	14.352
	2852	5.93	0.2372	0.52135	1379.412	220.032
	J7	19.3	0.772	1.86221	4707.966	1159.02
	3155	0.3	0.012	0.04794	86.814	57.684
	2861	1.1	0.044	0.14064	681.6	118.896
D	140	3.2	0.128	0.20907	983.502	95.082
	137	0.2	0.008	0.26594	1012.08	827.508
	127	0.7	0.028	0.12582	403.686	105
	191	0.8	0.032	0.12516	451.218	111.564
	3150	0.7	0.028	0.11415	431.52	115.686
	3099	0.9	0.036	0.15695	562.62	154.422
	E	2863	12.3	0.492	0.17205	818.034
	3520	14.7	0.588	1.57342	13854.474	2234.628

C.

T=10

Tank	CSO	A _{imp} (ha)	Q _{Law} (m ³ /s)	Q _{Max} (m ³ /s)	V _{Tot} (m ³)	V _{Lam} (m ³)
A	1019	51.2	2.048	6.58145	76582.074	9238.092
B	3132	7.4	0.296	0.74487	1225.71	416.682
	3127	2.9	0.116	0.20506	148.374	53.436
	3275	2.4	0.096	0.15611	180.252	59.484
C	2862	4.8	0.192	0.44883	397.71	154.098
	2852	5.93	0.2372	0.78803	2053.116	507.114
	J7	19.3	0.772	2.21953	7077.528	2262.162
	3155	0.3	0.012	0.05328	118.842	82.872
	2861	1.1	0.044	0.19665	885.054	203.922
D	140	3.2	0.128	0.31597	1317.264	221.958
	137	0.2	0.008	0.34465	1418.13	1232.64
	127	0.7	0.028	0.17656	547.29	177.21
	191	0.8	0.032	0.17485	609.948	189.018
	3150	0.7	0.028	0.16505	588.21	198.378
	3099	0.9	0.036	0.22382	765.066	261.444
E	2863	12.3	0.492	0.26455	1155.408	0
	3520	14.7	0.588	2.09918	17350.092	3794.874

On the left and above Tab. 3.11 a, b and c Volume to be discharged into the detention tanks in occasion of a T=2 year, 5 year and 10 year rainfall (50 hours discharging time) - Diffuse-Storage with Rain Barrels;

Diffuse-storage with Permeable Pavements (PP)

As for the scenario with the rain barrel and as expected, with the increase of rainfall severity the volume to be discharged into detention tanks becomes larger and larger (Table 3.12 a, b and c). With the increase of the drainage time of the permeable pavements (50 h) again a good reduction of peak flows, total volumes and volumes to be discharged into detention tanks. can be observed (Table 3.13 a, b, c).



a.

T=2

Tank	CSO	A _{imp} (ha)	Q _{Law} (m ³ /s)	Q _{Max} (m ³ /s)	V _{Tot} (m ³)	V _{Lam} (m ³)
A	1019	51.2	2.048	2.48466	18838.77	261.996
B	3132	7.4	0.296	0.00157	9.978	0
	3127	2.9	0.116	0.00129	8.172	0
	3275	2.4	0.096	0.00139	3.564	0
C	2862	4.8	0.192	0.00685	17.988	0
	2852	5.93	0.2372	0.13933	453.216	0
	J7	19.3	0.772	1.10746	1753.002	256.158
	3155	0.3	0.012	0.01747	11.268	3.282
D	2861	1.1	0.044	0.02505	207.186	0
	140	3.2	0.128	0.04855	419.64	0
	137	0.2	0.008	0.04704	362.388	193.014
	127	0.7	0.028	0.01979	156.648	0
	191	0.8	0.032	0.02257	176.514	0
	3150	0.7	0.028	0.02247	167.028	0
E	3099	0.9	0.036	0.02933	217.248	0
	2863	12.3	0.492	0.0612	239.898	0
	3520	14.7	0.588	0.72115	5955.168	150.09

On the left Tab. 3.12 a Volume to be discharged into the detention tanks in occasion of a T=2 year rainfall (10 hours discharging time) - Diffuse-Storage with Permeable Pavements;

On the right from above Tab. 3.12 b and c Volume to be discharged into the detention tanks in occasion of a T=5 year and a T=10 year rainfall respectively (10 hours discharging time) - Diffuse-Storage with Permeable Pavements.

b.

T=5

Tank	CSO	A _{imp} (ha)	Q _{Law} (m ³ /s)	Q _{Max} (m ³ /s)	V _{Tot} (m ³)	V _{Lam} (m ³)
A	1019	51.2	2.048	4.84115	32510.772	5373.792
B	3132	7.4	0.296	0.43693	612.042	100.596
	3127	2.9	0.116	0.00767	20.82	0
	3275	2.4	0.096	0.00234	5.976	0
C	2862	4.8	0.192	0.18172	138.708	0
	2852	5.93	0.2372	0.48557	1183.2	186.876
	J7	19.3	0.772	1.83372	4667.394	1090.848
	3155	0.3	0.012	0.04362	83.148	54.798
	2861	1.1	0.044	0.13518	545.964	112.872
D	140	3.2	0.128	0.20907	983.502	95.082
	137	0.2	0.008	0.26593	1012.062	827.49
	127	0.7	0.028	0.12561	403.56	104.874
	191	0.8	0.032	0.12518	451.224	111.57
	3150	0.7	0.028	0.11415	431.514	115.68
	3099	0.9	0.036	0.15694	562.62	154.416
	E	2863	12.3	0.492	0.16947	711.234
	3520	14.7	0.588	1.51045	10983.366	2246.292

c.

T=10

Tank	CSO	A _{imp} (ha)	Q _{Law} (m ³ /s)	Q _{Max} (m ³ /s)	V _{Tot} (m ³)	V _{Lam} (m ³)
A	1019	51.2	2.048	6.48957	42360.264	9573.612
B	3132	7.4	0.296	0.74397	1226.778	415.944
	3127	2.9	0.116	0.20438	147.966	53.028
	3275	2.4	0.096	0.15612	179.592	58.908
C	2862	4.8	0.192	0.44095	354.642	149.37
	2852	5.93	0.2372	0.78637	1845.552	473.184
	J7	19.3	0.772	2.20767	7121.07	2164.092
	3155	0.3	0.012	0.05238	117.84	83.022
	2861	1.1	0.044	0.19384	743.796	202.92
D	140	3.2	0.128	0.31598	1317.27	221.964
	137	0.2	0.008	0.34465	1418.346	1232.856
	127	0.7	0.028	0.17647	547.236	177.156
	191	0.8	0.032	0.17486	609.942	189.018
	3150	0.7	0.028	0.16506	588.216	198.384
	3099	0.9	0.036	0.22383	765.072	261.45
	E	2863	12.3	0.492	0.26167	1049.514
	3520	14.7	0.588	2.06826	14298.612	3950.13

a.

T=2						
Tank	CSO	A _{imp} (ha)	Q _{Law} (m ³ /s)	Q _{Max} (m ³ /s)	V _{Tot} (m ³)	V _{Lam} (m ³)
A	1019	51.2	2.048	2.48466	18795.42	261.996
B	3132	7.4	0.296	0.00157	9.978	0
	3127	2.9	0.116	0.00129	8.172	0
	3275	2.4	0.096	0.00139	3.564	0
C	2862	4.8	0.192	0.00685	17.832	0
	2852	5.93	0.2372	0.13933	449.706	0
	J7	19.3	0.772	1.10746	1729.278	256.158
	3155	0.3	0.012	0.01747	11.268	3.282
	2861	1.1	0.044	0.02505	206.496	0
D	140	3.2	0.128	0.04855	419.64	0
	137	0.2	0.008	0.04704	362.388	193.014
	127	0.7	0.028	0.01979	156.648	0
	191	0.8	0.032	0.02257	176.514	0
	3150	0.7	0.028	0.02247	167.028	0
	3099	0.9	0.036	0.02933	217.248	0
	E	2863	12.3	0.492	0.0612	239.418
	3520	14.7	0.588	0.72115	5941.266	150.09

b.

T=5						
Tank	CSO	A _{imp} (ha)	Q _{Law} (m ³ /s)	Q _{Max} (m ³ /s)	V _{Tot} (m ³)	V _{Lam} (m ³)
A	1019	51.2	2.048	4.86319	31942.644	5078.292
B	3132	7.4	0.296	0.43693	612.036	100.59
	3127	2.9	0.116	0.00767	20.82	0
	3275	2.4	0.096	0.00234	5.976	0
C	2862	4.8	0.192	0.18172	136.422	0
	2852	5.93	0.2372	0.48557	1136.778	186.582
	J7	19.3	0.772	1.83372	4345.122	1088.328
	3155	0.3	0.012	0.04362	82.878	54.828
	2861	1.1	0.044	0.13518	536.31	112.872
D	140	3.2	0.128	0.20907	983.502	95.082
	137	0.2	0.008	0.26593	1012.05	827.478
	127	0.7	0.028	0.12561	403.566	104.88
	191	0.8	0.032	0.12518	451.224	111.57
	3150	0.7	0.028	0.11415	431.52	115.686
	3099	0.9	0.036	0.15694	562.614	154.416
	E	2863	12.3	0.492	0.16947	697.038
	3520	14.7	0.588	1.51045	10799.34	2065.482

C.

T=10

Tank	CSO	A _{imp} (ha)	Q _{Law} (m ³ /s)	Q _{Max} (m ³ /s)	V _{Tot} (m ³)	V _{Lam} (m ³)
A	1019	51.2	2.048	6.4818	41418.678	8795.376
B	3132	7.4	0.296	0.74414	1226.988	416.142
	3127	2.9	0.116	0.20426	147.894	52.956
	3275	2.4	0.096	0.15612	179.568	58.854
C	2862	4.8	0.192	0.44095	349.512	149.37
	2852	5.93	0.2372	0.78634	1772.004	473.802
	J7	19.3	0.772	2.20732	6606.546	2156.562
	3155	0.3	0.012	0.05238	117.264	83.016
	2861	1.1	0.044	0.19384	726.924	198.246
D	140	3.2	0.128	0.31598	1317.27	221.964
	137	0.2	0.008	0.34465	1418.358	1232.868
	127	0.7	0.028	0.17647	547.23	177.156
	191	0.8	0.032	0.17486	609.948	189.018
	3150	0.7	0.028	0.16506	588.216	198.384
	3099	0.9	0.036	0.22383	765.072	261.45
E	2863	12.3	0.492	0.26167	1023.354	0
	3520	14.7	0.588	2.06826	13976.634	3627.21

On the left and above Tab. 3.13 a, b and c Volume to be discharged into the detention tanks in occasion of a T=2 year, 5 year and 10 year rainfall (50 hours discharging time) - Diffuse-Storage with Permeable Pavements.

“Central-Storage” scenario vs “Diffuse-Storage” scenario

Peak Flow

From Tables 3.14 (a, b), 3.15 (a, b), 3.16 (a, b) and from Figure 3.31 (*), which represents the average reductions in peak flow as the drainage and precipitation scenario changes, it is clear that both the implementation of rain barrels and permeable pavements in the urban context of Sesto Ulteriano seem to significantly reduce the maximum flow of the “Central-Storage” scenario. Greater reductions can be observed in the scenario with permeable pavement with a drainage time of 50 hours, capable of absorbing a part of the rainwater and releasing the remainder in a fairly long period of time, and in the case of rains with a return time 2 years.

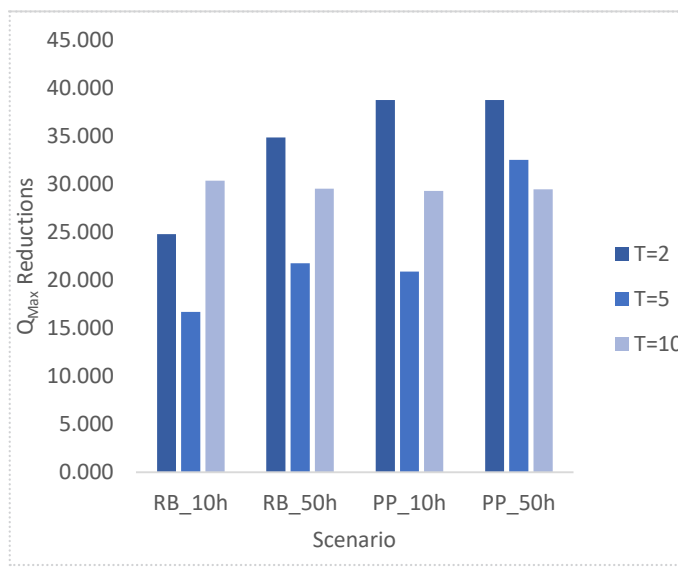


Fig. 3.31 Q_{Max} average reductions for each “Diffuse-Storage” scenario investigated and for each return period

		Q_{Max} (m^3/s); T=2				
Tank	CSO	Central-Storage	RB_10h	RB_50h	PP_10h	PP_50h
A	1019	3.567	2.827	2.564	2.485	2.485
	2862	0.019	0.008	0.007	0.007	0.007
	2852	0.255	0.175	0.146	0.139	0.139
C	J7	1.449	1.250	1.147	1.107	1.107
	3155	0.033	0.027	0.020	0.017	0.017
	2861	0.030	0.033	0.027	0.025	0.025
E	2863	0.122	0.065	0.063	0.061	0.061
	3520	1.110	0.894	0.793	0.721	0.721
Q_{Max} Reductions under T=2 Rainfall						
Tank	CSO		RB_10h	RB_50h	PP_10h	PP_50h
A	1019		20.729	28.103	30.339	30.339
	2862		58.347	62.050	63.231	63.231
	2852		31.377	42.576	45.271	45.271
C	J7	Peak Flow percentages of reduction with the implementation of each "Diffuse-Storage" scenario	13.691	20.792	23.552	23.552
	3155		20.436	39.349	47.804	47.804
	2861		-11.862	9.327	15.343	15.343
E	2863		46.443	48.516	49.836	49.836
	3520		19.453	28.558	35.040	35.040
Mean			24.827	34.909	38.802	38.802

On the left from the top Tab. 3.14 a Q_{Max} discharged from the sewer's CSOs for each “Diffuse-Storage” scenario investigated and for 2-year return period rainfall and 3.14 b Q_{Max} reductions obtained in each CSO thanks to the implementation of “Diffuse-Storage” scenarios for a 2-year return period rainfall

* In the following tables and plots “RB” represents the scenarios with Rain Barrels, “PP” represents the scenarios with Permeable Pavements while 10h and 50h represent the investigated draining time.

Q _{Max} (m ³ /s); T=5						
Tank	CSO	Central-Storage	RB_10h	RB_50h	PP_10h	PP_50h
A	1019	6.314	5.096	4.823	4.738	4.683
	2862	0.334	0.229	0.204	0.231	0.188
	2852	0.702	0.509	0.470	0.479	0.431
C	J7	2.287	1.845	1.741	1.778	1.724
	3155	0.051	0.048	0.047	0.048	0.048
	2861	0.116	0.114	0.102	0.102	0.096
E	2863	0.159	0.147	0.146	0.145	0.150
	3520	2.269	1.759	1.639	1.560	0.000

Q _{Max} Reductions under T=5 Rainfall						
Tank	CSO		RB_10h	RB_50h	PP_10h	PP_50h
A	1019		19.287	23.614	24.960	25.829
	2862		31.649	39.121	31.030	43.912
	2852	Peak Flow	27.387	32.938	31.744	38.514
C	J7	percentages of	19.308	23.860	22.257	24.603
	3155	reduction with the	4.492	6.313	4.413	4.453
	2861	implementation of	1.694	12.262	12.710	17.138
E	2863	each "Diffuse-Storage"	7.469	8.474	8.857	5.917
	3520	scenario	22.461	27.759	31.246	100.000
Mean			16.718	21.793	20.902	32.546

On the left from the top Tab. 3-15 a Q_{Max} discharged from the sewer's CSOs for each "Diffuse-Storage" scenario investigated and for 5-year return period rainfall and 3-15 b Q_{Max} reductions obtained in each CSO thanks to the implementation of "Diffuse-Storage" scenarios for a 5-year return period rainfall

Q _{Max} (m ³ /s); T=10						
Tank	CSO	Central-Storage	RB_10h	RB_50h	PP_10h	PP_50h
A	1019	7.453	6.779	6.050	6.252	6.353
	2862	1.724	0.000	0.575	0.578	0.578
	2852	1.480	0.692	0.661	0.673	0.659
C	J7	3.125	2.337	2.210	2.143	2.143
	3155	0.076	0.071	0.068	0.069	0.069
	2861	0.337	0.271	0.267	0.265	0.265
E	2863	0.335	0.264	0.254	0.259	0.253
	3520	2.711	2.486	2.423	2.363	2.363

Q _{Max} Reductions under T=10 Rainfall						
Tank	CSO		RB_10h	RB_50h	PP_10h	PP_50h
A	1019		9.049	18.834	16.118	14.760
	2862		100.000	66.664	66.494	66.494
	2852	Peak Flow percentages	53.250	55.316	54.499	55.441
C	J7	of reduction with the	25.230	29.295	31.446	31.446
	3155	implementation of	6.632	10.758	9.216	9.216
	2861	each "Diffuse-Storage"	19.495	20.760	21.214	21.214
E	2863	scenario	21.286	24.249	22.899	24.551
	3520		8.295	10.608	12.810	12.810
Mean			30.405	29.560	29.337	29.492

On the left from the top Tab. 3-16 a Q_{Max} discharged from the sewer's CSOs for each "Diffuse-Storage" scenario investigated and for 10-year return period rainfall and 3-16 b Q_{Max} reductions obtained in each CSO thanks to the implementation of "Diffuse-Storage" scenarios for a 10-year return period rainfall

Total Volume

The total volume show a particular trend. The “Diffuse-Storage” scenarios with rain barrels is characterized by runoff volumes higher than those reached in the “Central-Storage” scenario or similar. The reason behind this behavior could be ascribed to the technology itself that is not able to retain stormwater but only to delay it in a longer period of time. In addition, if widely implemented at the catchment scale, these systems do not allow the water to be treated by the pervious areas available. However, it should be remember the importance of rain barrel in the reduction of peak flows. As for the permeable pavements, significant total volumes reductions were registered, especially in occasion of less severe rainfalls.

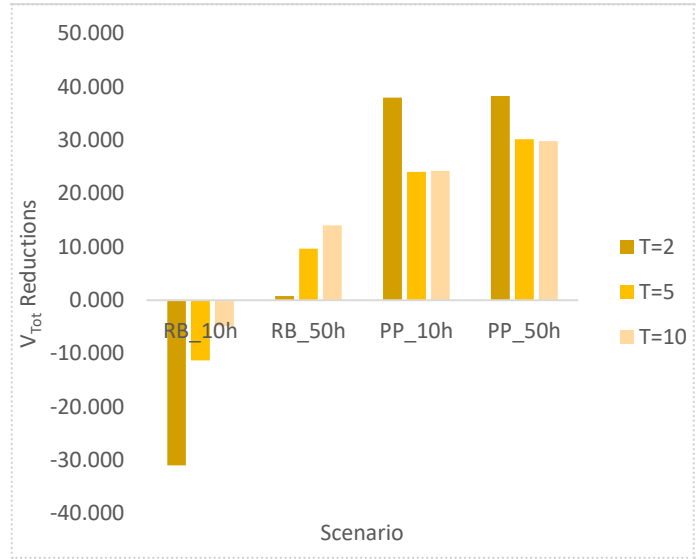


Fig. 3.32 V_{Tot} average reductions for each “Diffuse-Storage” scenario investigated and for each return period

		V_{Tot} (m ³); T=2				
Tank	CSO	Central-Storage	RB_10h	RB_50h	PP_10h	PP_50h
A	1019	25590.384	39373.536	40307.688	18838.770	18795.420
	2862	42.600	72.510	46.578	17.988	17.832
	2852	731.400	906.462	619.098	453.216	449.706
C	J7	2982.030	2918.478	1887.006	1753.002	1729.278
	3155	40.896	24.018	14.358	11.268	11.268
	2861	252.486	442.020	328.752	207.186	206.496
E	2863	317.100	414.582	337.152	239.898	239.418
	3520	8004.348	10965.342	8588.532	5955.168	5941.266
		V_{Tot} Reductions under T=2 Rainfall				
Tank	CSO		RB_10h	RB_50h	PP_10h	PP_50h
A	1019		-53.861	-57.511	26.383	26.553
	2862		-70.211	-9.338	57.775	58.141
	2852	Peak Flow	-23.935	15.354	38.034	38.514
C	J7	percentages of reduction with the implementation of each "Diffuse-Storage" scenario	2.131	36.721	41.214	42.010
	3155		41.271	64.891	72.447	72.447
	2861		-75.067	-30.206	17.942	18.215
E	2863		-30.742	-6.324	24.346	24.498
	3520		-36.992	-7.298	25.601	25.775
Mean			-30.926	0.786	37.968	38.269

On the left from the top Tab. 3.17 a V_{Tot} discharged from the sewer's CSOs for each “Diffuse-Storage” scenario investigated and for 2-year return period rainfall and 3.17 b V_{Tot} reductions obtained in each CSO thanks to the implementation of “Diffuse-Storage” scenarios for a 2-year return period rainfall

* In the following tables and plots “RB” represents the scenarios with Rain Barrels, “PP” represents the scenarios with Permeable Pavements while 10h and 50h represent the investigated draining time.

V _{Tot} (m ³); T=5						
Tank	CSO	Central-Storage	RB_10h	RB_50h	PP_10h	PP_50h
A	1019	41358.912	57821.298	60536.340	32406.084	31310.844
	2862	287.964	239.040	184.116	170.028	141.582
	2852	1861.722	1962.054	1352.964	1229.028	1157.016
C	J7	7351.302	7364.688	4801.434	5078.976	4613.382
	3155	114.834	94.152	81.906	96.462	79.188
	2861	590.784	817.446	636.774	509.064	490.056
E	2863	781.578	893.232	741.396	654.810	611.286
	3520	13707.666	17413.974	13766.712	11103.492	10759.836
V _{Tot} Reductions under T=5 Rainfall						
Tank	CSO		RB_10h	RB_50h	PP_10h	PP_50h
A	1019		-39.804	-46.368	21.647	24.295
	2862		16.990	36.063	40.955	50.833
	2852	Peak Flow	-5.389	27.327	33.984	37.852
C	J7	percentages of reduction with the implementation of each "Diffuse-Storage" scenario	-0.182	34.686	30.911	37.244
	3155		18.010	28.674	15.999	31.041
	2861		-38.366	-7.785	13.832	17.050
E	2863		-14.286	5.141	16.219	21.788
	3520		-27.038	-0.431	18.998	21.505
Mean			-11.258	9.663	24.068	30.201

V _{Tot} (m ³); T=10						
Tank	CSO	Central-Storage	RB_10h	RB_50h	PP_10h	PP_50h
A	1019	52741.794	72205.362	75941.436	42719.988	41255.100
	2862	1568.664	833.262	655.260	669.822	619.392
	2852	2983.758	2882.838	2060.154	1939.782	1797.006
C	J7	10247.334	10842.480	7076.874	7394.226	6708.060
	3155	160.914	141.924	119.478	149.316	120.168
	2861	898.296	1129.050	901.416	774.270	747.690
E	2863	1261.044	1327.188	1118.670	1036.068	993.108
	3520	17311.452	22014.552	17360.520	14544.486	14046.582
V _{Tot} Reductions under T=10 Rainfall						
Tank	CSO		RB_10h	RB_50h	PP_10h	PP_50h
A	1019		-36.904	-43.987	19.002	21.779
	2862		46.881	58.228	57.300	60.515
	2852	Peak Flow	3.382	30.954	34.989	39.774
C	J7	percentages of reduction with the implementation of each "Diffuse-Storage" scenario	-5.808	30.939	27.842	34.538
	3155		11.801	25.750	7.208	25.322
	2861		-25.688	-0.347	13.807	16.766
E	2863		-5.245	11.290	17.840	21.247
	3520		-27.168	-0.283	15.983	18.860
Mean			-4.843	14.068	24.246	29.850

On the left from the top Tab. 3.18 a V_{Tot} discharged from the sewer's CSOs for each "Diffuse-Storage" scenario investigated and for 5-year return period rainfall and 3.18 b V_{Tot} reductions obtained in each CSO thanks to the implementation of "Diffuse-Storage" scenarios for a 5-year return period rainfall

On the left from the top Tab. 3.19 a V_{Tot} discharged from the sewer's CSOs for each "Diffuse-Storage" scenario investigated and for 10-year return period rainfall and 3.19 b V_{Tot} reductions obtained in each CSO thanks to the implementation of "Diffuse-Storage" scenarios for a 10-year return period rainfall

Volumes discharged into detention tanks

The assessment of the reduction of the volumes to be discharged into the detention tanks and, consequently, the reduction of the dimensions of the latter is certainly one of the most interesting points of this part of the research. As can be seen from the tables and Figure 3.33, it is clear that the implementation of “Diffuse-Storage” strategies is essential for the reduction of the volumes to be discharged into tanks produced in the “Central-Storage” Scenario. Permeable pavements once again proved to be more performing. Overall the increase in the severity of the rain event involves the activation of additional of CSOs and an increase in the volume to be treated by detention tanks.

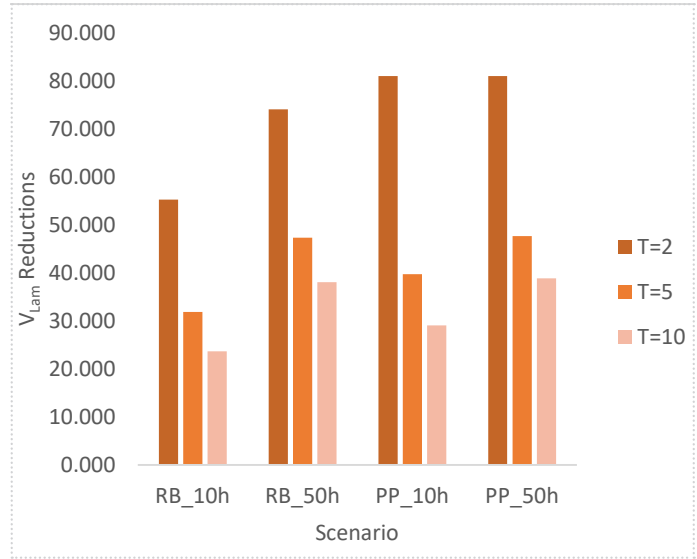


Fig. 3.33 V_{Tot} average reductions for each “Diffuse-Storage” scenario investigated and for each return period

		$V_{Lam}(m^3); T=2$				
Tank	CSO	Central-Storage	RB_10h	RB_50h	PP_10h	PP_50h
A	1019	1776.504	988.680	421.164	261.996	261.996
	2862	0.000	0.000	0.000	0.000	0.000
	2852	10.428	0.000	0.000	0.000	0.000
C	J7	577.638	426.378	305.634	256.158	256.158
	3155	18.696	9.018	4.980	3.282	3.282
	2861	0.000	0.000	0.000	0.000	0.000
E	2863	0.000	0.000	0.000	0.000	0.000
	3520	835.194	381.462	217.116	150.090	150.090
		V_{Lam} Reductions under T=2 Rainfall				
Tank	CSO		RB_10h	RB_50h	PP_10h	PP_50h
A	1019		44.347	76.293	85.252	85.252
	2862		-	-	-	-
	2852		100.000	100.000	100.000	100.000
C	J7	Peak Flow percentages of reduction with the implementation of each "Diffuse-Storage" scenario	26.186	47.089	55.654	55.654
	3155		51.765	73.363	82.445	82.445
	2861		-	-	-	-
E	2863		-	-	-	-
	3520		54.327	74.004	82.029	82.029
Mean			55.325	74.150	81.076	81.076

On the left from the top Tab. 3.20 a V_{Lam} to be discharged into detention tanks for each “Diffuse-Storage” scenario investigated and for 2-year return period rainfall and 3.20 b V_{Lam} reductions thanks to the implementation of “Diffuse-Storage” scenarios for a 2-year return period rainfall

* In the following tables and plots “RB” represents the scenarios with Rain Barrels, “PP” represents the scenarios with Permeable Pavements while 10h and 50h represent the investigated draining time.

V _{Lam} (m ³); T=10						
Tank	CSO	Central-Storage	RB_10h	RB_50h	PP_10h	PP_50h
A	1019	14716.632	11972.112	8951.154	10481.676	8981.388
	2862	1148.100	429.678	324.348	343.014	325.158
	2852	1287.504	655.686	547.500	583.422	524.748
C	J7	3857.202	2800.644	2375.736	2709.474	2337.888
	3155	112.962	97.800	85.482	103.788	85.812
	2861	307.116	250.764	225.720	247.614	225.024
E	2863	0.000	0.000	0.000	0.000	0.000
	3520	5632.842	5073.702	3873.840	4271.922	3768.570
V _{Lam} Reductions under T=10 Rainfall						
Tank	CSO		RB_10h	RB_50h	PP_10h	PP_50h
A	1019		18.649	39.177	28.777	38.971
	2862		-	-	-	-
	2852	Peak Flow	49.073	57.476	54.686	59.243
C	J7	percentages of	27.392	38.408	29.755	39.389
	3155	reduction with the	13.422	24.327	8.121	24.035
	2861	implementation of	-	-	-	-
E	2863	each "Diffuse-	-	-	-	-
	3520	Storage" scenario	9.926	31.228	24.160	33.096
Mean			23.693	38.123	29.100	38.947

V _{Lam} (m ³); T=5						
Tank	CSO	Central-Storage	RB_10h	RB_50h	PP_10h	PP_50h
A	1019	8309.712	6335.844	4507.614	5404.758	4265.688
	2862	85.410	21.918	6.930	23.160	0.000
	2852	542.160	228.492	161.220	181.440	172.908
C	J7	2685.570	1671.516	1334.190	1486.554	1363.182
	3155	78.228	63.348	55.236	64.296	55.470
	2861	111.660	98.604	79.824	85.530	74.022
E	2863	0.000	0.000	0.000	0.000	0.000
	3520	3781.620	2979.684	2215.332	2461.254	2135.670
V _{Lam} Reductions under T=5 Rainfall						
Tank	CSO		RB_10h	RB_50h	PP_10h	PP_50h
A	1019		23.754	45.755	34.959	48.666
	2862		-	-	-	-
	2852	Peak Flow	57.855	70.263	66.534	68.108
C	J7	percentages of	37.759	50.320	44.647	49.240
	3155	reduction with the	19.021	29.391	17.809	29.092
	2861	implementation of	-	-	-	-
E	2863	each "Diffuse-	-	-	-	-
	3520	Storage" scenario	21.206	41.418	34.915	43.525
Mean			31.919	47.430	39.773	47.726

On the left from the top Tab. 3.21 a V_{Lam} discharged from the sewer's CSOs for each "Diffuse-Storage" scenario investigated and for 5-year return period rainfall and 3.21 b V_{Lam} reductions thanks to the implementation of "Diffuse-Storage" scenarios for a 5-year return period rainfall

On the left from the top Tab. 3.22 a V_{Lam} discharged from the sewer's CSOs for each "Diffuse-Storage" scenario investigated and for 10-year return period rainfall and 3.22 b V_{Lam} reductions thanks to the implementation of "Diffuse-Storage" scenarios for a 10-year return period rainfall

Final discussions

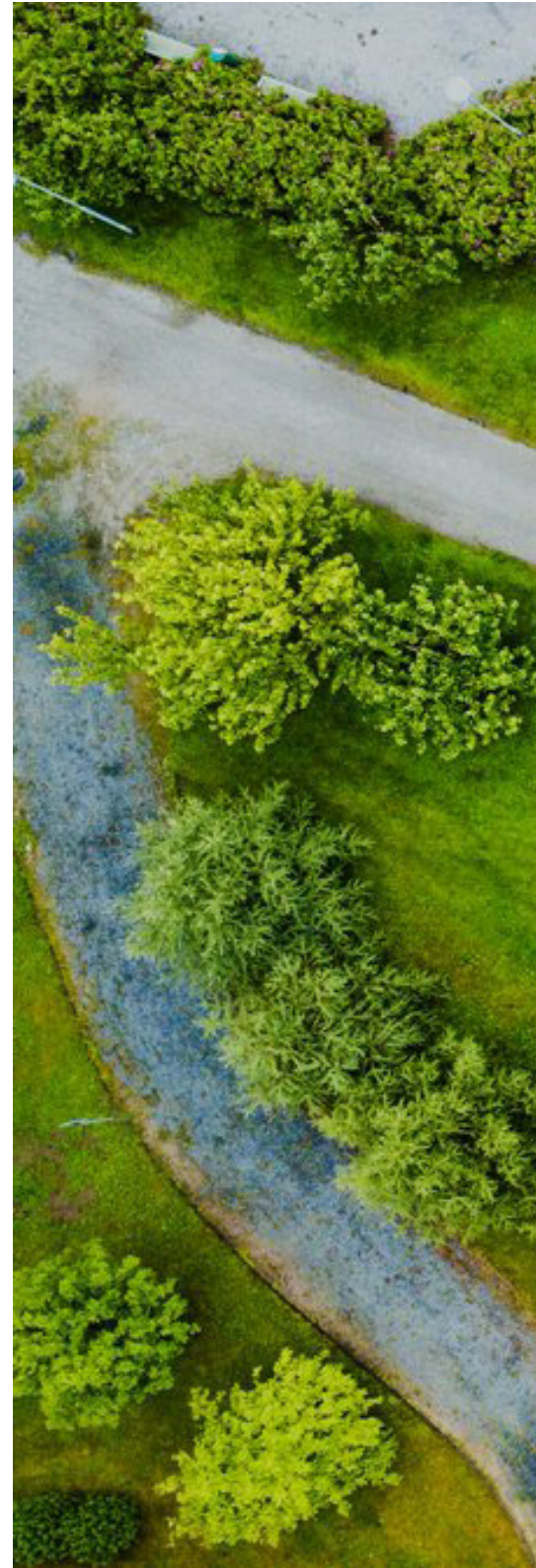
This part of the research assessed the hydraulic and hydrological benefits deriving from the implementation of detailed SuDS retrofitting project in Sesto Ulteriano (MI), a consolidated urban context affected by several criticalities related to the stormwater management. In particular, thanks to a comprehensive retrofitting design of SuDS choice and localization, this research aspired to compare typically potential or model-based SuDS retrofitting scenarios with feasible or design-based ones to understand whether and to what extent their results could affect the general opinion of decision-makers upon the efficiency of sustainable infrastructures. In addition, considering SuDS relation with the urban context another key element, land use role and optimal localization of these systems were also investigated. To the purpose, several event scale and long-term scale SWMM₅ simulations were performed to compare SuDS design-based and model-based retrofitting scenarios with different spatial distributions and areal extension with an hard-technology scenario, without SuDS. The analyses mainly focused on the reduction of maximum flow and total volume discharged from the CSOs and the decrease of the number of nodes above a fixed filling degree threshold. Generally, as expected, both hydrological and hydraulic analysis pointed out that major differences between SuDS-based and hard-technology scenarios occurred for the larger areal SuDS implementation such as 8.3% and 4.2% and for the lower intensity events. Although different in their methodology, SuDS choice and localization, climatic conditions, several modeling studies support this idea (Palla & Gnecco, 2015; Hua et al., 2020; Samouei & Ozger, 2020). Moreover, whatever the climate scenario is, no significant variability in maximum flow reduction moving from 100% to 50% SuDS implementation scenarios was highlighted. In particular, both in terms of total volume and peak flow reduction, model-based scenarios, that provided for implementation of SuDS practices even in areas where design-based scenario would not foresee such retrofitting, showed a higher hydrological performance, with reduction of total volume discharged from the CSOs reaching up on average to 70%. If compared to the existing literature, these results seem somewhat higher. In Hua et al. (Hua et al., 2020) a maximum runoff reduction of 41% was founded retrofitting about the 9% of the catchment area





Tracey Whitefoot for National Geographic - CENTRAL PARK, NEW YORK (USA)

with different typology of SuDS while in Palla & Gnecco (Palla & Gnecco, 2015) the runoff volume reduced of 23% at most after the implementation of green roofs and permeable parking lots. However, these varying results were for sure expectable and are mainly attributable to the obvious differences in the research studies. Major differences were accounted for catchments B and D, both intended for residential use. The reason behind this behaviour lies just up to uniform spatial distribution of SuDS that experience equal spatial distribution of CSOs loads and consequently a uniform retention in terms of peak flow and runoff volume. This effect appeared particular evident in the case of the continuous simulation and for what concerns the runoff volume reduction. Overall, the hydrological analysis highlighted that both design-based and model-based scenarios, especially for higher implementations, successfully reduced the number of flooded nodes over time even in the occurrence of severe rainfall, thus improving the performance of the drainage network of Sesto Ulteriano. However, model-based scenarios always registered better performances. Field studies conducted so far are also valuable to confirm obtained results (Avellaneda et al., 2017; Jiang et al., 2020). Even if featuring low SuDS implementation percentages (0.7%), the study carried out by Avellaneda et al. (Avellaneda et al., 2017) demonstrated that SuDS can reach the 9% of surface runoff reduction. Actually, considerably higher are the results in terms of stormwater management of single sustainable drainage infrastructure analysed on their own (Jiang et al., 2020). Land use also seemed to affect the catchment hydrological performance. Specifically, in residential catchments, even if featured by the lowest percentage of impervious area and for this reason by the lowest percentage of SuDS retrofitting, peak flow and volume reduction appeared the most effective. For a given percentage of retrofitting, the presence of SuDS affected on balance at the same extent both continuous and event scale simulations. In addition, at the event scale, the rainfall return period seemed not to significantly affect the maximum flow reduction. Major differences were registered for the low percentage of retrofitting implementation (10%). Hence, being aware of the actual retrofitting potential of an urban catchment seems essential to predict the effectiveness of SuDS projects in the mitigation of flooding risk. Each urban system has its own structure, land use, organization, population, localization and nature of criticalities. A good knowledge of these features makes sure that measures undertaken in a specific urban context succeed in improving its hydrological and hydraulic resilience. Generic projects and strategical solutions based on fixed and unaware retrofitting percentages, would inevitably result





Picture of SRN Sustainability Research Network

in misleading analysis, unsuccessful interventions, unsolved issues and high financial costs for both administrations and citizens.

Moreover, within the same study, the benefits of the implementation of the floodability concept in Sesto Ulteriano were assessed. Diffuse-storage scenarios (floodable streets and squares+Hard-Technology storage) were compared with the centralized-storage scenario in which only storage tanks downstream were provided to identify whether and to what extent centralized storage tanks volumes could be reduced. Results, assessed in terms of peak flow, total volume discharged and excess stormwater, again showed that integrated approaches, involving the use of both SuDS and Hard-Technology, could be a great solution for a sustainable stormwater management. In particular, if used for the modeling of floodable streets and squares, both rain barrels and permeable pavements significantly reduce the maximum flow of the “Central-Storage” scenario. The latter showed the best performance reaching a 40% peak flow mean reduction. Great performances of pervious pavements were registered also in terms of mean total volumes reductions (maximum 40% with lowest values never below 20%). The same cannot be said for the rain barrels that, as discussed, are unable to retain stormwater but only to delay it in a longer period of time. Finally, the best results were reached in terms of the reduction of the volumes to be discharged into detention tanks. Permeable pavements once again proved to be more performing with a maximum mean reduction of about 80%. Lowest mean reductions, never below 20%, were registered in the rain barrel scenario and under severe rainfalls (T=10).

Overall, findings achieved so far suggest that these infrastructures are actually able to mitigate the effects deriving from urbanization and soil sealing. Although few are the retrofittable surfaces in developed urban context, such infrastructures are nevertheless a valid aid for traditional drainage systems in the management of stormwater, providing besides numerous additional benefits for human beings and nature. For sure, in planning such interventions, it must also be taken into account that the effect of climate changes can counteract their efficiency. Detailed research studies on climate change, therefore, are needed in order to understand the performance of SuDS systems over time. Efforts towards interdisciplinary research and integrated planning strategies are also needed to support local authorities in their decisions and furthermore, key stakeholders and communities should also be involved in the complex process toward sustainable (re)development of urban ecosystems.

Chapter 4

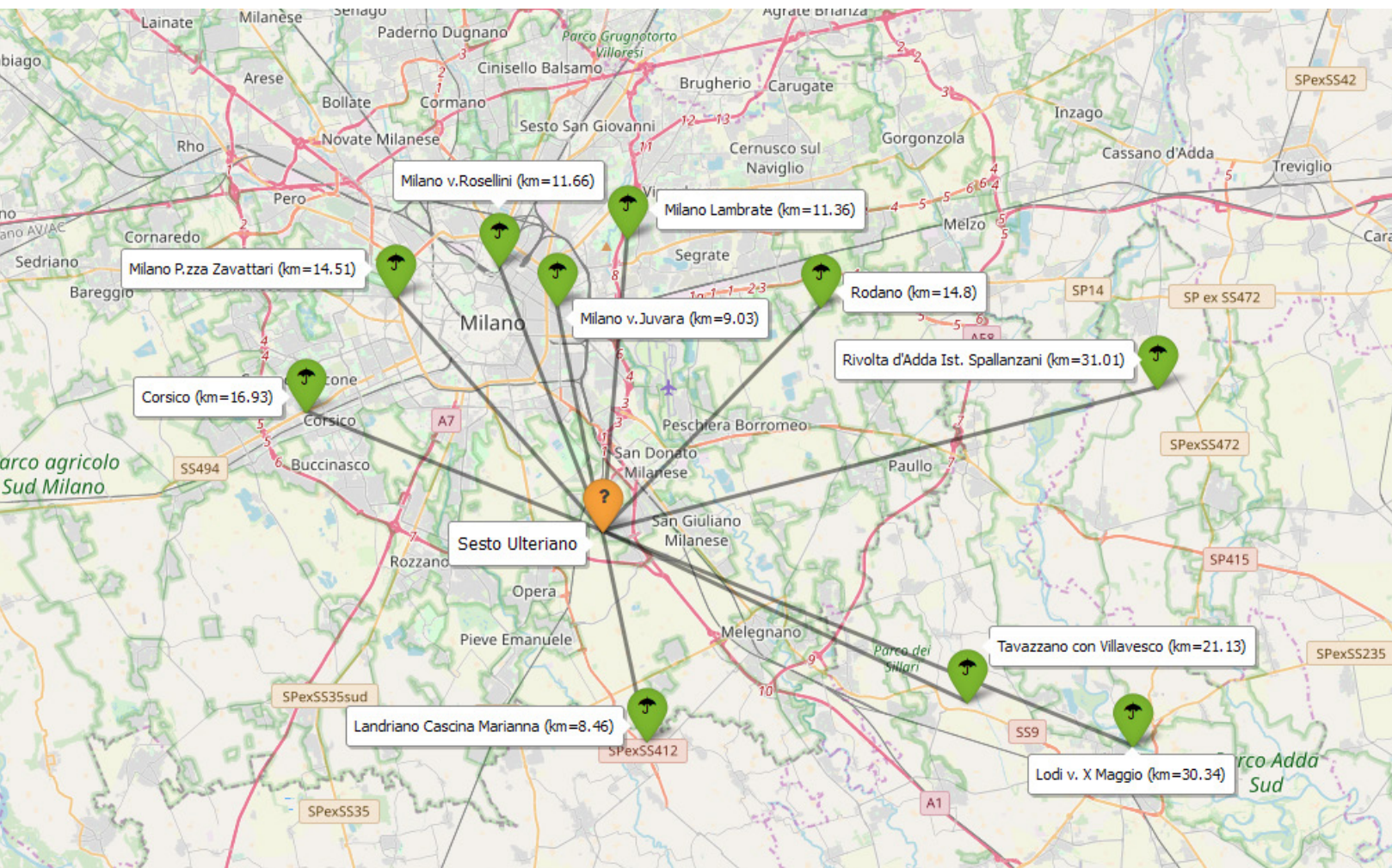
Historical precipitations analysis

Preliminary studies applied to the Sesto Ulteriano urban catchment

Historical rainfall in the Sesto Ulteriano urban area

Interpolation methodology for obtaining historical rainfall data

The availability of rainfall data, essential for several hydrological studies, is a factor that presents great variability over time and space. A first reason lies in the fact that weather stations are not distributed evenly throughout the territory. Furthermore, it is necessary to consider that rainfall data collection systems can, inevitably and for various reasons, present problems of missing data. Measurement of rain amount is therefore a procedure subject to both systematic and random errors (Larson & Peck, 1974; Vieux, 2001). Water losses during a measurement are among the most common systematic errors in the measurements of the rain gauges. In many situations, however, it is also possible to completely lose data in a precise interval of time or recording errors due to a malfunction of the measuring systems. These errors are particularly critical because they invalidate the continuity of rainfall data and influence the results of rain models that use rain as input (Teegavarapu & Chandramouli, 2005). As for the case study area presented in the previous chapter, the problem consisted mainly in the fact that we were dealing with discontinuous rainfall datasets, furthermore not characteristic of Sesto Ulteriano. The nearest weather stations, in fact were located about 8 km away, so it was difficult to predict, without geostatistical applications, historical precipitations. In the absence of detailed information, it was deemed appropriate to apply an interpolation methodology that would allow us, from precipitations collected by all weather stations closest to Sesto Ulteriano, to identify typical, complete and reliable rainfall datasets. The first phase of work therefore foresaw the identification of the rain gauges closest to the study area. In particular, it was decided to take into account those within a 30 km radius or about (Figure 4.1). In Figure 4.1 the weather stations closest to the study area are represented on the map (Corsico, Landriano Cascina Marianna, Lodi v. X Maggio, Milano v. Juvara, Milano Lambrate, Milano v. Rosellini, Milano p.zza Zavattari, Rivolta d'Adda Ist. Spallanzani, Rodano, Segrate Milano Due, Tavazzano con Villavesco Enel suolo). For greater perception of distances, the kilometres separating each rain gauge from the Sesto Ulteriano basin have also been explained. The data of the different weather stations were acquired by the Regional Agency for Environmental Protection (ARPA) of the Lombardy Region (IT) through a specific request on the dedicated web page (https://www.arpalombardia.it/Pages/ARPA_Home_Page.aspx). In particular, data from the 10 weather stations identified concerning rain heights and other meteorological and climatic characteristics were collected for a period of 10 years (from 2009 to 2018). A first check was then carried out in order to verify the actual availability of the information (Table 4.1). Analysing the single extracts, then, it was possible to highlight that for some years the data recorded in the files were not significant because in their place there was a code “-999” to indicate “missing or invalid value”. From a more in-depth analysis of the available data, it was noted that in the years 2009-2013 there is less information available (many non-functioning sensors) and in any case different values missing in the individual days. It was decided, therefore, to proceed, at least in a first phase, using only the data of the last 5 years (2014-2018), more complete and more reliable, as shown in the summary table in Table 4.2 in which the number of functioning rain gauges on an hourly scale and for each year is reported.



Above Fig. 4.1 Weather Station around Sesto Ulteriano;
On the right (upside-down):

Tab. 4.1 Availability analysis of rainfall data;

SENSOR	Distance (Km)	2009	2010	2011	2012	2013	2014	2015	2016	2017	2018
Corsico	16.93	✓	✓	✓	✓	X	✓	✓	✓	✓	✓
Landriano	8.46	✓	✓	✓	✓	✓	✓	✓	✓	✓	✓
Lodi	30.34	✓	✓	✓	✓	X	✓	✓	✓	✓	✓
Milano Juvara	9.03	✓	✓	✓	✓	X	✓	✓	✓	✓	✓
Milano Lambrate	11.36	✓	✓	✓	✓	✓	✓	✓	✓	✓	✓
Milano Rosellini	11.66	X	X	X	✓	X	✓	✓	✓	✓	✓
Milano Zavattari	14.51	✓	✓	✓	✓	X	✓	✓	✓	✓	✓
Rivolta	31.01	✓	✓	✓	✓	✓	✓	✓	✓	✓	✓
Rodano	14.80	✓	✓	✓	✓	X	✓	✓	✓	✓	✓
Tavazzano	21.13	✓	✓	✓	✓	X	✓	✓	X	X	X

Tab. 4.2 Number of active wether stations per year of analysis . Along with the statistics, also a detail of the number of the overall measurements for each sensor in each year is reported.

Year	Number of Active Sensors											Min	Max	Mean	
	0	1	2	3	4	5	6	7	8	9	10				
2009	0	0	70	1686	6981	0	0	0	0	0	0	0	2	4	3.8
2010	0	0	0	238	8499	0	0	0	0	0	0	0	3	4	4.0
2011	0	0	0	691	6797	1249	0	0	0	0	0	0	3	5	4.1
2012	0	0	0	9	231	2146	6375	0	0	0	0	0	3	6	5.7
2013	0	0	25	8712	0	0	0	0	0	0	0	0	2	3	3.0
2014	0	0	0	0	2	129	3933	1	5	285	4382	4	10	8.1	
2015	0	0	0	0	0	0	0	4	80	4773	3880	7	10	9.4	
2016	0	0	0	0	0	0	0	63	1169	7529	0	7	9	8.9	
2017	0	0	0	0	0	0	0	2	393	8342	0	7	9	9.0	
2018	0	0	0	0	0	0	0	8	407	8322	0	7	9	9.0	

Inverse distance weighting method and results verification

The choice of the methodological approach to be used for the interpolation fell, following some tests carried out with different deterministic interpolation methods, on the Inverse Distance Weighting. For its reasonable computational cost and replicability in other contexts, this method certainly proved to be particularly suitable in this research activity. Inverse Distance Weighting usually indicates a family of methods that work on the basic concept of the inverse relationship between the contribution or weight of the elements and the distance from the point for which an evaluation is necessary. In short, therefore, the attributes of the most distant points appear to contribute in a less significant way, with respect to those closer to them, to the identification of the value sought. Therefore, in order to obtain continuous rainfall data sets of Sesto Ulteriano, the methodology established the determination of each rainfall value as the sum of the products of the different rain heights for the relative distances from the centre of Sesto Ulteriano divided by the sum of the distances. In particular, after some experimental checks, a value of $a=1$ was chosen which represents the speed at which the weights decrease as a function of distance. To verify the reliability of the interpolation algorithms experienced, historical weather forecasts of Sesto Ulteriano were acquired from some web portals and compared to the interpolated dataset. The forecasts of specialized weather sites are carried out according to statistical models that take into account unpublished information that include satellite images, historical series, orography of the territory, wind direction, and other available parameters. Unfortunately, these time series are

often fee charging (e.g. military aeronautical service), except for a few cases in which they are publicly available but on an hourly time scale. Registered just few hours before the happening of atmospheric events (the archive data correspond to the latest forecasts carried out) and typical of a specific area, therefore precipitation forecasts have a high degree of reliability and can reasonably be considered as a reference to choose and verify the interpolation methods implemented. Unfortunately, free-of-charge forecasts collect data on a daily basis and do not always report the exact amount of rain. We find general information such as "rain, storm, snow, etc.". Hence, from historical weather forecasts and for each day of the year, it was determined, whether that day it rained (1) or not (0). Then, looking at the rainfall data sets obtained from interpolation, for each day of the year, a value of 1 was assigned if the total of millimetres of rain for that day was > 0.2 mm (threshold value obtained experimentally), 0 otherwise. These values were compared with the previous ones obtained from the weather forecasts and the code "1" was assigned if the values coincided (rain or no rain) and "0" if they were different. The total of the coincident values, identified with the code "1" was then divided by 365 (total number of days per year) to understand what was the percentage/ degree of reliability of the interpolation method. Specifically, Sesto Ulteriano rainfall data, obtained from the aforementioned Inverse Distance Weighting interpolation methodology, showed a 91% match with downloaded forecasts and for this reason considered sufficiently reliable for the following analyses.

Analysis of rainfall data of Sesto Ulteriano obtained from interpolation



Fig. 4.2 Rainfall Analysis: a. Rainfall time series 2014-2018 (the rainfall is expressed in millimeters); b. Barplot of number of rainfall events by intensity 2014-2018; c. Monthly total rainfall 2014-2018; d. Rainy days per month 2014-2018

Analysis and detection of the most significant precipitation scenarios of the last 10 years

The need to identify interesting or “critical” precipitation scenarios, continuous or short term, is basically explained by the need to evaluate the performance of design-based SuDS scenarios (identified as “GREEN” in the previous chapter), during significant historical rainfall periods or events and to compare it with the hard-technology scenario, without SuDS. It must be added that, in this case as in the previous analysis, the need to extract information from such large data sets, to carry out exploratory analyses, to identify recurrent “patterns”, to aggregate data, to reconcile them, and compare various processing approaches, required the creation of scripts in R language and more generally the use of analysis tools and interactive environments (i.e. RStudio) typical of the world of Data Science. Therefore, obtained from interpolation the complete precipitation dataset (2009-2018), the first analyses were conducted in order to carry out statistics that could identify the annuity of interest for the purpose of continuous simulation. The importance of completeness of data sets in the case of long-period simulations, led to considering, in this first phase, only the last 5 years of data (2014-2018), less affected by systematic errors. In particular, it was decided to take into consideration the year 2014, characterized by the maximum precipitation amount (1515.57 mm). As regards the short-term simulations, and therefore on an event scale, it was decided to identify three types of events: I) rainfall event characterized by maximum intensity in an hour (5.23 mm/h), II) rainfall event characterized by maximum intensity (7.36 mm/h) and III) rainfall event characterized from maximum return period (5 years with a 6.87 mm/h intensity). Since, in this case, it was considered that the “completeness” of the rain series could not significantly affect the result at the event scale, it was decided to use and, therefore, to analyse the data relating to the complete database (10 years). It is important to underline that while the latter can be considered an almost “critical” rainfall event, the previous two despite the intensity are characterized by “common” values of total rainfall volume and duration. For completeness, a heat map representing the daily rainfall value for each of the 10 year of analysis is represented in Figure 4.4. In order, therefore, to identify the event of rain characterized by maximum hourly intensity, having a database with values available at a resolution of 10 min, we proceeded by aggregation of the same and identification of the maximum value sought. From this, in order to create a series of data to be given as input for the simulation in SWMM5, the rain event characterized by that maximum hourly intensity value was isolated. As regards, instead, the identification of the event of rain characterized by maximum intensity in the last ten years, the different rain events were extracted from the database through the use of the R Studio software. It was decided to consider as separate those rainfall events characterized by an Antecedent Dry Water Period of at least 6 hours. For each of the identified events, the rain intensity was then calculated as the ratio between the cumulated rainfall of the event itself and the duration. At this point, the maximum intensity rain event was chosen. Finally, more steps were necessary to identify the event with maximum return period (T_{max}). In this regard, according to the information provided by ARPA Lombardia, the intensity-duration curves for the territory of Sesto Ulteriano (MI) were built for assigned return periods. The ten most intense rain events were then extracted from the previously constructed database. Known both the rainfall heights and the duration of these events, these points have been included in the graph for the graphic evaluation of the return periods of each (Figure 4.3). From a simple first reading of the graph it was possible to observe that nine rain events did not exceed

a return period of two years and only one was characterized by a return period of five years. The latter was chosen for the subsequent analysis. Overall, this study expected the development of eight simulations. In fact, for both scenarios (with and without SuDS), one simulation was carried out with annual rainfall to verify the long term performance of drainage systems and three were carried out under historical event-scale rainfall inputs.

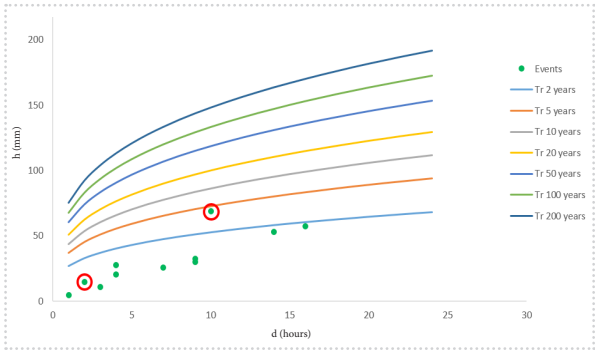


Fig. 4.3 IDF curves Sesto Ulteriano with identification of maximum return period event and maximum intensity event

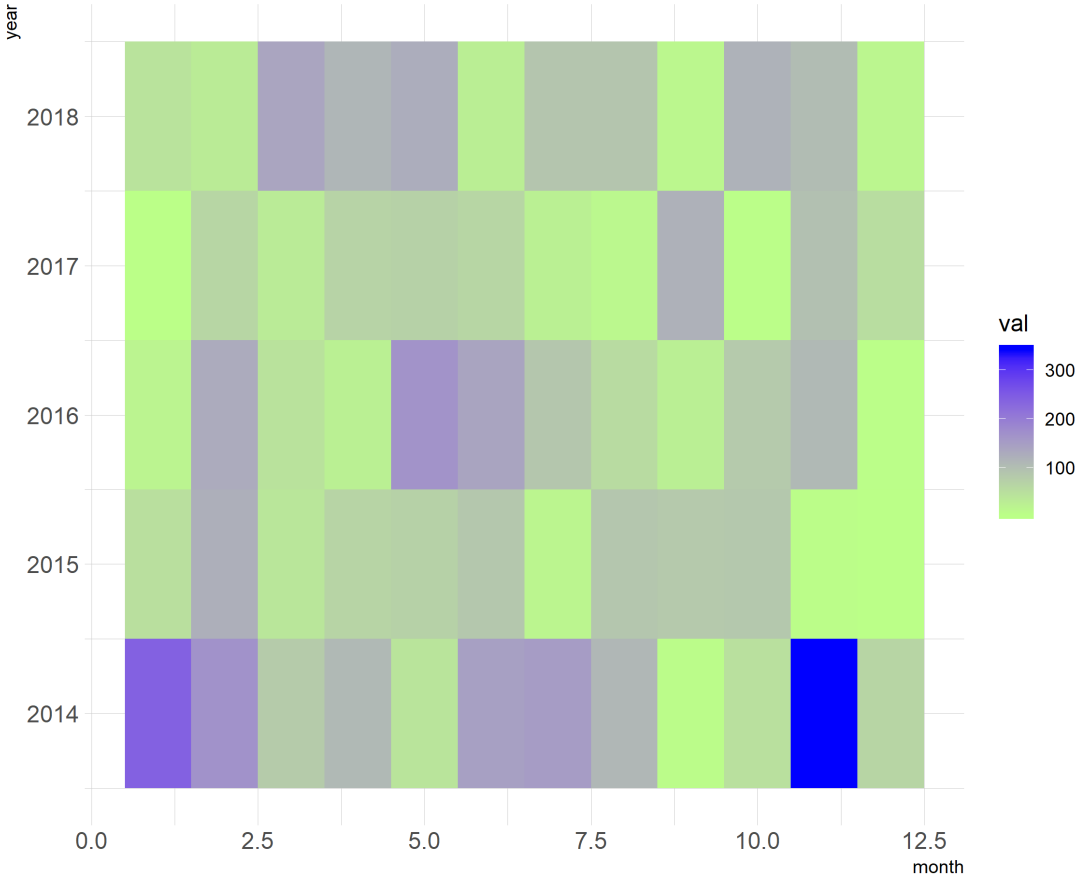


Fig. 4.4 Heatmap of rainfall monthly amount (mm) 2014-2018

SuDS performance under historical rainfall

This research merged in a conference paper entitled “Assessing the performance of Sustainable Drainage Systems (SuDS) in urban context using SWMM₅ modelling scenarios: the example of a typical industrial area in Lombardia Region, northern Italy” presented at EGU General Assembly 2020 (D’Ambrosio, Schmalz & Longobardi, 2020)

SWMM₅ modelling allowed a comparison of the performance of the drainage system of Sesto Ulteriano (MI), without integrated strategies, with a design-based scenario, involving SuDS, under the mentioned historical real rainfalls. The design-based scenario chosen for this analysis is the “GREEN 100%”, presented in the third chapter and representative of an overall retrofitting surface of 8.34%. The results, assessed in terms of reduction of Maximum Flow (Q_{max}) and Total Volume (V_{tot}) in the outfalls of the drainage system following the implementation of SuDS, confirm that these sustainable infrastructures could have given a real contribution in the management of historical precipitation stormwater, both event scale and annual. Once again, it is essential to remember that only the T=5 rainfall event can be considered an almost “critical” one. The other, despite the intensities, can be defined as “common” precipitations. Figure 4.5 and 4.6 represent reductions of Maximum Flow and Total Volume discharged from the network Combined Sewer Overflows (O1-O27) following SuDS retrofitting under the different historical rainfall scenarios.

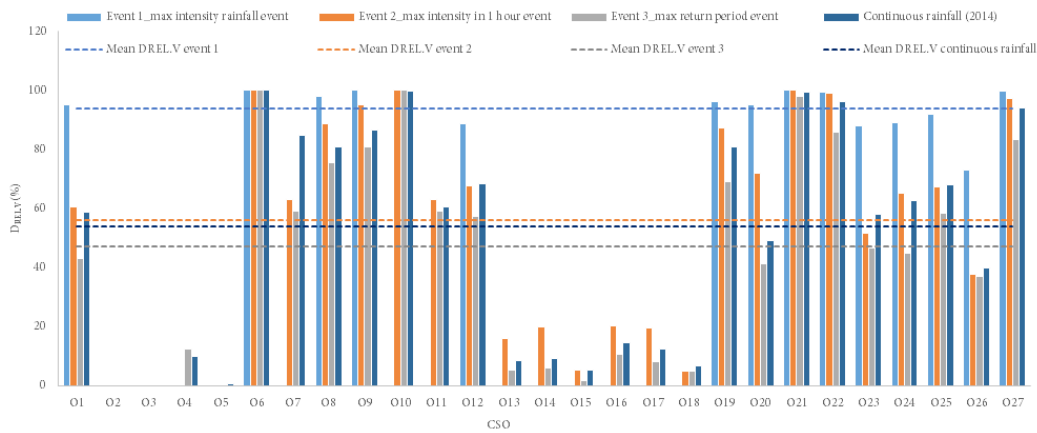


Fig. 4.5 Reductions of V_{tot} in the drainage system CSOs following the implementation of SuDS

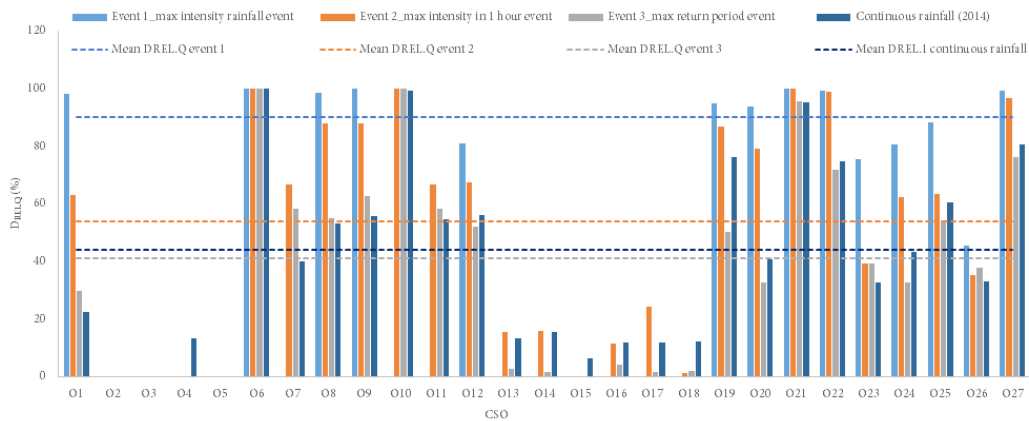


Fig. 4.6 Reductions of Q_{max} in the drainage system CSOs following the implementation of SuDS

**Rain! Whose soft
architectural hands have
power to cut stones,
and chisel to shapes
of grandeur the very
mountains.**

(Henry Ward Beecher)

Chapter 5

SuDS adaptation to Climate Change

SuDS as an adaptation strategy to climate change consequences: A methodological approach experienced for Sesto Ulteriano urban catchment

Urban sprawl and climate change effects, as already mentioned in the previous chapters, are the leading cause of flooding phenomena within the urban environment (Albano et al., 2014; Pistocchi et al., 2015; Alfieri et al., 2016;; D'Ambrosio et al., 2019;; Palermo et al., 2020;).

During the past century, the scientific community gave particular attention to global climate change. Precipitation patterns are changing due to the global warming, dramatically affecting the hydrological cycle and, consequently, both flood-related criticalities and the availability of water resources (Liuzzo et al., 2016). The stationarity typical of rainfall statistics and stochastic models used in support of urban drainage studies is tackled more in general by a changing world and specifically in a changing climate perspective. Several studies were conducted all over the world to detect rainfall trends, both accounting for empirical data and climate models (Piervitali et al., 1998; Brunetti et al., 2001; Brunetti et al., 2004; Zahmatkesh et al., 2014; Cannon & Innocenti, 2019). Coupled Model Intercomparison Project Phase 5 (CMIP5) modelled on average project a gradual increase in global precipitation over the 21st century (AR5 IPCC, 2013). Specifically, studies conducted in Europe in the last twenty years pointed out an heavy winter precipitation increase in central and northern Europe, an heavy summer precipitation increase in north-eastern Europe and an extension of Mediterranean droughts which start earlier in the year and last longer (Frei et al., 2006; Beniston et al., 2007; Madsen et al., 2014; Arahuetes & Olcina Cantos, 2019). Research conducted in Italy confirmed great precipitation-trend variability. Nevertheless, rainfall intensity showed statistically significant temporal increases in the north and in the central area of the peninsula (Vallebona et al., 2015) among with a general decrease of the number of rainy days and annual rainfall amounts (Acquaotta et al., 2018).

Urban stormwater management systems are usually designed to meet performance standards based on historical climate data. However, considering the possible impact of climate change on rainfall intensities and consequently on stormwater runoff peak flow and volumes, it is essential to start assessing flood risk adaptation strategies under future climate conditions (Semadeni-Davies, 2012; Zahmatkesh et al., 2014; Liu et al., 2018; Andimuthu et al., 2019).

For this reason, recently researchers assessed climate change impact on stormwater runoff in urban catchments (Alfieri et al., 2016; Andimuthu et al., 2019; Zhou et al., 2019) and some of them also focused on the effectiveness of sustainable drainage systems in the mitigation of potential flooding risk increase (Semadeni-Davies et al., 2008; Zahmatkesh et al., 2014; Rodríguez-Sinobas et al., 2018; Liu et al., 2018). Overall, findings suggest that the implementation of SuDS generally have a positive effect on the mitigation of flooding risk and that robustness, adaptability and cost effectiveness are fundamental for sustainable drainage under deep uncertainty of climate change (Semadeni-Davies, 2008; Semadeni-Davies, 2012; Xu et al., 2019).



Marcus Yam/LA Times via Getty - FLOODS IN USA CAUSED BY HURRICANE HARVEY, 2017

Nevertheless, uniqueness and variability of the results does not allow extracting from the analysis conducted so far universally valid remarks.

This is due to the presence, in these kind of studies, of a combination of structural (urban layouts, infrastructures, criticalities), climatic and design variables (type of intervention, SuDS choice, localization and parameterization) specifically related to the case study and the objectives of the research.

Focusing again on the Sesto Uleriano (MI) urban context, presented in the third chapter, this part of the research specifically aims at understanding if the “GREEN 100%” SuDS project can ensure high performance during the whole life span of these infrastructures, meeting the expectations under climatic conditions that deviates from the historical ones.

Statistical analyses on historical rainfall data sets recorder for the study area, spanning from 1858 to 2019, provided identification of temporal trends in precipitation extremes in order to design potential climate scenario within the medium range of the next 30 years.

Current and future rainfall scenarios were used to force the combined hydraulic-hydrological model of the urban drainage network, both accounting for a hard-technology scenario, where no SuDS practices are considered, and a SuDS-based scenario, where instead a number of green facilities were planned.

Results, assessed in terms of reduction of maximum discharge and total volume discharged from the combined sewer overflow of the network, pointed out that the implementation of SuDS techniques has beneficial effects on the mitigation of urban flooding risk. However, the resilience they provide in terms of stormwater management issue seems to be much more sensitive to climate input in the next future.



Sesto Uleriano view from Google Earth

CLIMATE CHANGE AND THE ENVIRONMENT

CANADA has received **16%** more precipitation in the past six decades

Annual average air temperature has warmed **1.5°C** in the past six decades

The **ARCTIC** is warming twice as fast as the south

2001-2010: warmest decade on record

Warmer temperatures increase water evaporation, leading to bigger and more dangerous storms

Temperature over land is **WARMING** faster than over oceans

PERMAFROST temperatures across the country have increased

There is a great loss of snow cover in the Spring and summer

Melting permafrost releases **GREENHOUSE GASES**

MELTING GLACIERS contribute to rising sea levels

RIVER FLOW has decreased over the past few decades in southern Canada but increased in northern Canada

Each decade, **SEA ICE** is shrinking more and more

STRATIFICATION is the formation of different layers of water in the ocean

OCEAN ACIDIFICATION Too much CO₂ is absorbed into the water, making it difficult for some species to build shells and skeletal structures. Some waters are already considered "corrosive" to these organisms.

GLOBAL WARMING stops these layers from mixing properly, impacting the exchange of nutrients, heat and CO₂

In some areas, there is a lack of oxygen in the water, which is harmful to **MARINE LIFE**

WHERE AMERICANS STAND ON CLIMATE CHANGE

AS FIREFIGHTERS STRUGGLED to contain the wildfires that tore through the West Coast throughout September — hitting growers and nurseries in California and Oregon — the issue of climate change continues to be a hot-button topic circulating among politicians, news outlets and social media spheres. While there is no denying the catastrophic damage of global warming, it's important to note how Americans view important environmental issues. We rounded up some key findings from "The Pew Research Center from their April 21 article, "How Americans see climate change and the environment in 7 charts." Here are some of the notable points Pew discovered:



68% Believe the government isn't doing enough to protect water quality in **LAKES, RIVERS, STREAMS**

67% don't believe the government is doing enough to protect **AIR QUALITY**

63% of Americans believe stricter **ENVIRONMENTAL REGULATIONS** are worth the cost

30% believe that **GREEN LAWS REGULATIONS** would cost too many jobs and hurt the economy



There has been an increase of support for environmental prioritization in the U.S. Since 2011, and 64% of Americans believe that environmental protection should be a high priority for the president and Congress.



believe global climate change should be a **TOP PRIORITY** for **THE PRESIDENT** and **CONGRESS**

PARTISAN POLITICS FACTOR INTO PLAY WHEN IT COMES TO CLIMATE POLICIES in regard to the environment and the economy. In a October 2019 survey, Pew found that while 67% of Americans did not believe the government was doing enough to combat climate change, there were stark divides between parties.



71% OF DEMOCRATS believed such policies would be beneficial for the environment.

34% OF REPUBLICANS believe that climate change policies will help the environment.



CLIMATE CHANGE

Asia and the Pacific

...because of rising greenhouse gas emissions that might show the impacts of climate change in

For the whole Canada in a Changing Climate report visit Adaptation.NRCan.gc.ca

70% percentage of the region's emissions that comes from the People's Republic of China. The country's per capita emissions, however, is only about 50% of the developed world's average.

2030 the year when developing Asia's share in global energy-related emissions could reach about

45% without greater use of renewable energy and improved energy efficiency.

20 million number of Bangladeshis who will be displaced by a 1-meter rise in sea level in 2050.

More than > 60% number of the region's population working in agriculture, fisheries, and forestry, the sectors most at risk to climate change.

300 million to 410 million estimated increase of Asian urban dwellers at risk of coastal flooding by 2025. In inland areas, the number of people at risk will rise from 245 million to 341 million by 2025.

\$40 billion budget required annually to help Asia and the Pacific transition to low-carbon and climate-resilient economies.

\$7 billion approximate amount of ADB investment in clean energy related projects since 2008, with **\$2.1 billion** in 2011 alone.

invest in solutions that reduce other environmental stresses.



Productivity could be a 80% decline in the

Sea level rise The Coral Triangle may experience a

CAUSES

GREENHOUSE EFFECT

GLOBAL WARMING

1.1-1.6°F (0.6-0.9°C)

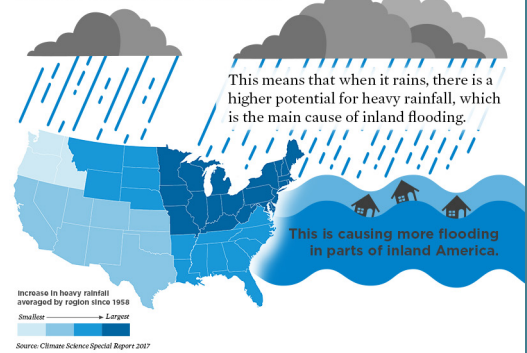
EFFECTS

SOLUTIONS

Why Is Inland America Flooding?

More Frequent, Heavier Rainfall

With rising global temperatures due to increased heat-trapping emissions, more water evaporates from the land and oceans. The warmer atmosphere can hold more water vapor.



Our Rapidly Changing Landscape

Modern land use practices have left our landscape less able to accommodate heavy rainfall, increasing the risk of floods and exacerbating their impacts.

- Increased development in floodplains
- Increased use of impermeable surfaces (e.g. asphalt)
- Destruction of natural areas

What Can We Do? Solutions at the local, state, and federal levels can give communities the best chance to stay above water.

Hard-technology versus SuDS scenario

Modeling approach was again pursued to understand the impact of the SuDS project in Sesto Ulteriano. To this end the scenario “GREEN 100”, mentioned in the third chapter and characterized by the highest percentage of retrofitting (8.34% for a total of 31.7 ha), was compared with the hard-technology scenario, representative of the drainage network of the case study area without SuDS implementation. Both were tested under event scale and continuous historical and future climate inputs

Historical rainfall statistical analysis and climate scenarios

Both event scale analysis and a continuous long-term analysis were performed. Precipitation data from the weather stations, new and historical, closest (within a 30 km radius) to the case study area were collected and analysed. Among them, those characterized by the highest operating ranges (> 30 year) were chosen: Lodi, Milano Brera, Monza and Pavia (Figure 5.1).

The selected rainfall stations are included in the rainfall network managed by the National Environmental Protection Agency (ARPA) of the Lombardia Region. For each station, the distance from the centre of the study area, the operating range, the characteristics of the data available and the completeness of the data sets were reported in Table 5.1.



Fig. 5.1 Location of the four weather stations

Weather Station	ID	TYPE	Province	Distance (km)	operativity range_from	operativity range_to	operativity range (years)	functioning (%)
Lodi	3	historical	Lodi	18.74	01/01/1972	31/12/2005	34	82
Lodi // v.X Maggio	8113	new	Lodi	18.74 ± 0.669	18/02/2003	31/12/2019	17	100
Milano Brera	1	historical	Milano	11.48	01/01/1858	31/12/2005	147	100
Milano // v. Brera	19373	new	Milano	11.48 ± 0.763	11/07/2016	31/12/2019	3	100
Monza	8	historical	Monza Brianza	22.03	31/12/1912	31/12/2006	94	93
Monza // v. Monte Generoso	30533	new	Monza Brianza	22.03 ± 0.427	26/09/2014	31/12/2019	5	100
Pavia	12	historical	Pavia	22.87	01/01/1873	30/12/2005	132	89
Pavia // v. Falperti	6694	new	Pavia	22.87 ± 0.533	01/06/2002	31/12/2019	18	100

Tab. 5.1 Weather stations characterization

To verify the statistical homogeneity between the historical and new data series, a preliminary analysis was carried out through the T-Student statistical test.

The test expresses a judgment on the significance of the difference in the average values of the two series, with a fixed probability. Considering a probability that the mean value falls outside the confidence interval equal to 5% and having defined the parameters useful for the analysis (mean, standard deviation, variance and number of the data series), the interval of confidence and statistical value *t* are defined.

The latter, compared with the critical values categorized in function of the probability of exceeding this value and the degree of freedom, defines the samples “statistically homogeneous” if the value of the statistics is lower than the critical value. Results of this preliminary analysis, due to the presence of missing data and the unreliability of the recorded data, showed that historical and recent rainfall datasets collect events with different statistical characteristics, as they do not fall within the confidence interval defined.

This result means that and therefore the data series recorded by the measurement stations they measure events with different statistical

characteristics even though they belong to the same monitoring area, as they cannot therefore be aggregated.

Even if this analysis suggested the data of the historical and new weather stations (located in the same place) should not be aggregated, considering the typical uncertainty of the statistical test and the absence (as mentioned in the following) of a clear sign of climate change, it was decided to merge them, obtaining in this way longer data ranges.

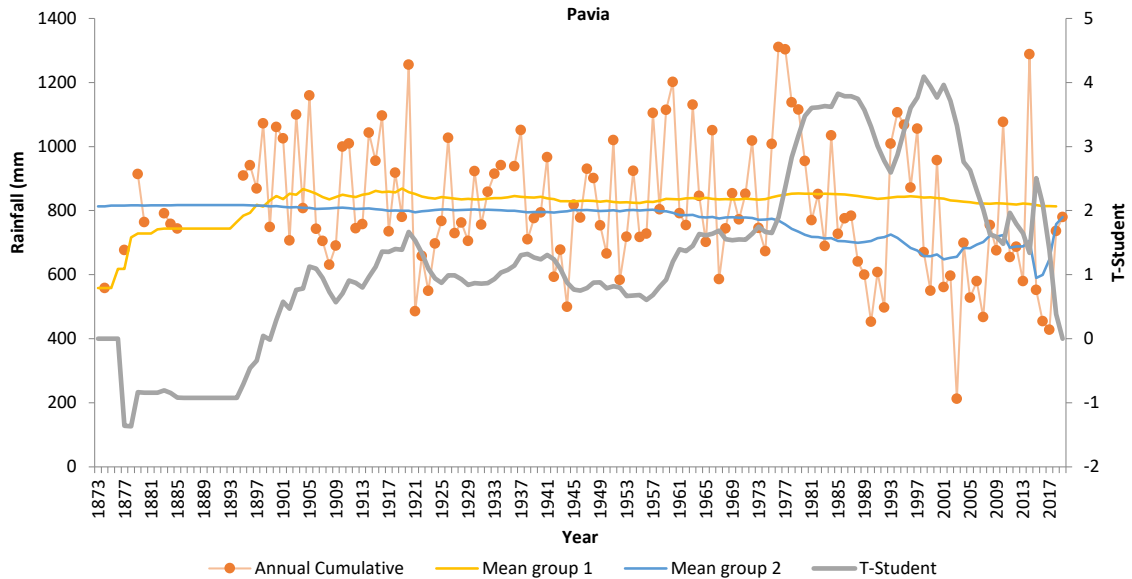
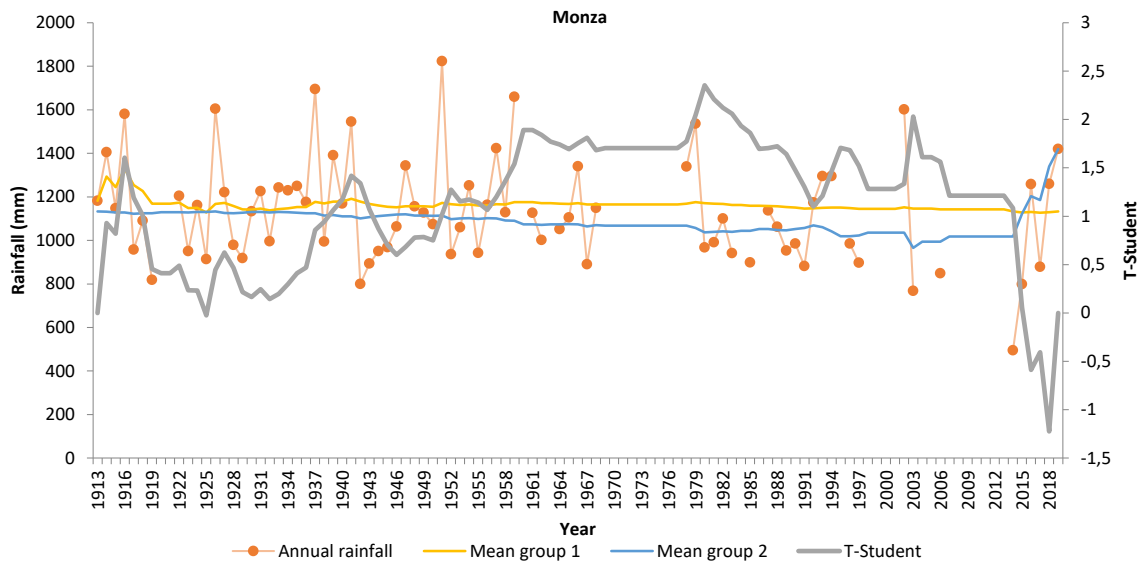
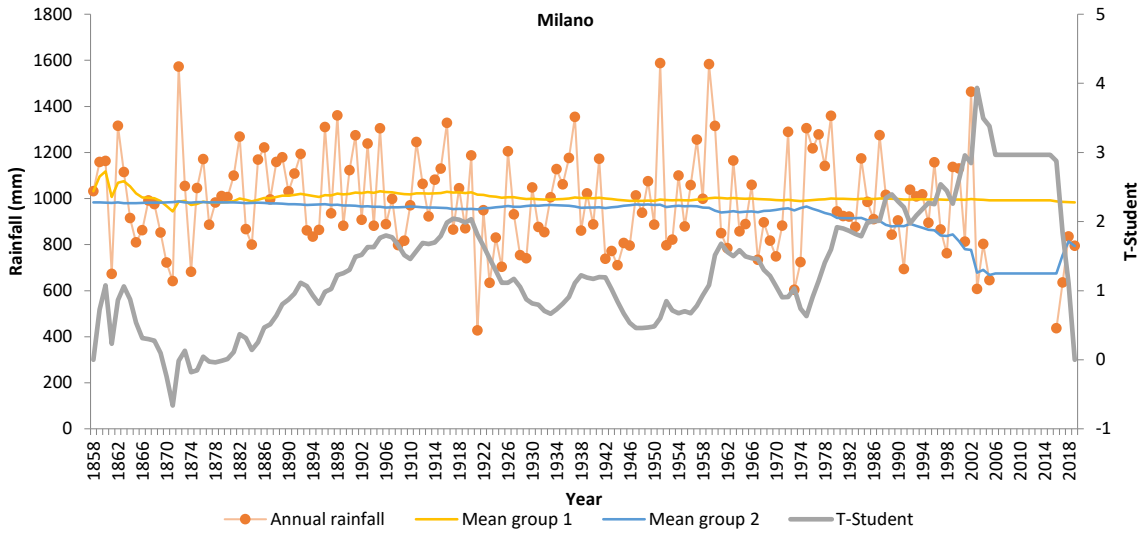
Moreover, to detect the possible presence of Break Points, representative of variations in the data sets statistics and related to the existence of a climate change or structural change of the rainfall observation, statistical analyses were performed. Three different statistical methods were here carried out to detect one or more break points in the data sample representative of the annual cumulative rainfall for each of the four weather stations: T-Test, CUMulative SUM test (CUMSUM) and PETTITT test (Figure 5.2, 5.3, 5.4).

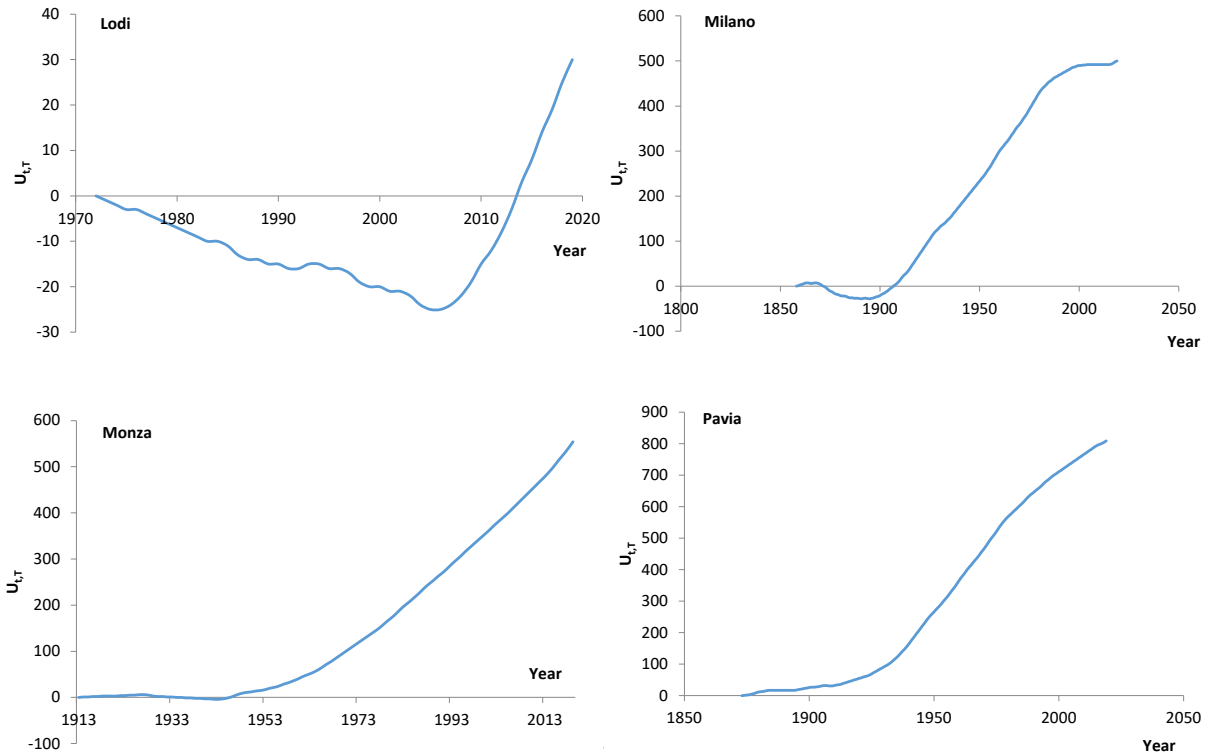
The variability found in the results (Table 5.2) suggests that the analyses carried out at this scale, also due to the numerous missing data, were not able to uniquely and reliably identify changes in the precipitation regime.

HISTORICAL CHANGES IN RAINFALL REGIME

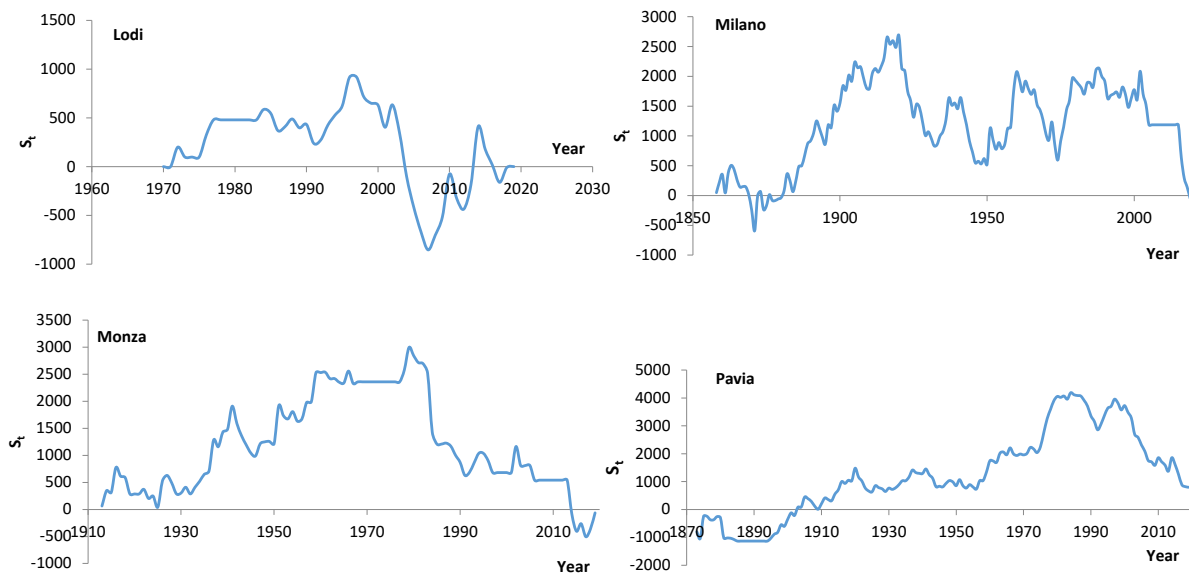
	Lodi	Milano	Monza	Pavia
T.test	-	1985	1960	1977
PETTITT.test	2006	-	-	-
CUMSUM.test	1997	-	1979	1985

Tab. 5.2 Identification of Break Points with different Statistical Approaches





On the left Fig. 5.2 T-Student statistical implementation for the identification of Break Points: plots for Milano, Monza and Pavia weather stations - Group 1 and 2 represent the two samples of rainfall data compared in each step; Above Fig. 5.3 PETTITT test implementation for the identification of Break Points: plots for Lodi, Monza, Milano and Pavia wather stations; Below Fig. 5.4 CUMulative SUM test implementation for the identification of Break Points: plots for Lodi, Monza, Milano and Pavia wather stations.



Hence, in order to detect trends in the precipitation extremes, data obtained from the weather station characterized by the highest completeness, Lodi, were aggregated at 30 minute, 1 hour and 24 hour time steps and the maximum values for each year were identified. The results were plotted and trend line were designed and analysed. In particular, the slope of the trend lines were used to predict rainfall extremes at 2050 (+30). These values were then compared with the mean historical value to obtain a percentage of variation V_{rain} (increase or decrease) as follows:

$$V_{rain(0.5, 1, 24)} (\%) = (R_{Predicted(0.5, 1, 24)} - MeanR_{Historical(0.5, 1, 24)}) / (MeanR_{Historical(0.5, 1, 24)}) * 100$$

Where:

$R_{Predicted(0.5, 1, 24)}$ = Predicted value of Maximum rainfall at 30 minute, 1 hour and 24 hour in 2050.

$MeanR_{Historical(0.5, 1, 24)}$ = Mean Historical value of Maximum rainfall at 30 min, 1 hour and 24 hour in 2050.

The obtained percentages of variation were used to build Intensity-Duration-Frequency (IDF) curves (2-year, 5-year and 10-year return period) at 2050. IDF designed according to historical rainfall were collected from ARPA web sites for the Lodi weather station. The maximum at 30 minute, 1 hour and 24 hours were adjusted according to the predicted percentage of variation and the obtained values were interpolated to trace the new IDF curves. The parameters of the curves, obtained from the equations, were used to design Chicago hyetographs with duration of 9-hour.

As for the continuous simulations (annual), even if some featured years of missing data, all the weather station were used. Annual cumulative rainfalls of Lodi, Monza, Pavia and Milano were plotted and trend line were again designed and analysed. In particular, the slope of the trend lines were used to predict rainfall annual amount at 2050 (+30) for each weather station. These values were then compared with the mean historical value to obtain a percentage of variation of annual cumulative V_{rain} (increase or decrease) as follows:

$$V_{a.rain(L, M, P, MI)} (\%) = (R_{a.Predicted(L, M, P, MI)} - MeanR_{a.Historical(L, M, P, MI)}) / (MeanR_{a.Historical(L, M, P, MI)}) * 100$$

Where:

$R_{a.Predicted(L, M, P, MI)}$ = Predicted value of rainfall amount in 2050 for Lodi (L), Monza (M), Pavia (P) and Milano (MI)

$MeanR_{a.Historical(30, 1, 24)}$ = Mean Historical value of rainfall amount for Lodi (L), Monza (M), Pavia (P) and Milano (MI)

The percentages of variation were used to adjust an annual rainfall typical of the case study area, obtained in a previous step through interpolation methodology and characteristic of the year 2014, which experienced the maximum rainfall amount within the last ten years.

Output of the simulations: extraction and analysis of the key parameters

The assessment of SuDS behaviour in the studied catchment aimed at identifying their impact on both peak flow and total volume under historical and future rainfall conditions. To this end several SWMM5

simulation were performed and both “Climate Change analysis” and “Drainage Network analysis” were carried out.

The first focused on the comparison of each of the drainage scenarios (hard-technology or SuDS) under historical and future rainfalls in order to identify the possible effects of climate changes on the hydrological parameters. To this end, the analyses provided the evaluation of the Peak Flow Maximum (Q_{max}) and Total Volume (V_{tot}) variations in the CSOs of the drainage network. The historical rainfall scenario was selected as the reference scenario and the increases in terms of maximum flow (I_V) and total volume (I_Q) were evaluated as in the following:

$$I_V (\%) = [(V_{TOT_CC-SCENARIO} - V_{TOT_HIST-SCENARIO}) / (V_{TOT_HIST-SCENARIO})] * 100$$

$$I_Q (\%) = [(Q_{MAX_CC-SCENARIO} - Q_{MAX_HIST-SCENARIO}) / (Q_{MAX_HIST-SCENARIO})] * 100$$

Where:

$V_{TOT_CC-SCENARIO}$ = Total Volume reached in the climate-change rainfall scenario calculated as the sum of the total volume of each CSO of the drainage network

$V_{TOT_HIST-SCENARIO}$ = Total Volume reached in the historical rainfall scenario calculated as the sum of the total volume of each CSO of the drainage network

$Q_{MAX_CC-SCENARIO}$ = Peak Flows Maximum reached in the CSOs in the climate-change scenario

$Q_{MAX_HIST-SCENARIO}$ = Peak Flows Maximum reached in the CSOs in the historical rainfall scenario

The “drainage network” analyses focused, instead, on the comparison of each of the rainfall scenarios (climate-change or historical) under hard-technology and design-based (SuDS) scenarios in order to identify the possible effects of SuDS on the hydrological parameters. To this end, the analyses provided again the evaluation of the Peak Flow Maximum (Q_{max}) and Total Volume (V_{tot}) variations in the CSOs of the drainage network. The hard-technology scenario was selected as the reference scenario and the reductions in terms of Total Volume (R_V) and Peak Flow (R_Q) were evaluated as in the following:

$$R_V (\%) = [(V_{TOT_HARD-T-SCENARIO} - V_{TOT_SUDS-SCENARIO}) / (V_{TOT_HARD-T-SCENARIO})] * 100$$

$$R_Q (\%) = [(Q_{MAX_HARD-T-SCENARIO} - Q_{MAX_SUDS-SCENARIO}) / (Q_{MAX_HARD-T-SCENARIO})] * 100$$

Where:

$V_{TOT_HARD-T-SCENARIO}$ = Total Volume reached in the hard technology scenario calculated as the sum of the total volume of each CSO of the drainage network

$V_{TOT_SUDS-SCENARIO}$ = Total Volume reached in the design-based (SuDS) scenario calculated as the sum of the total volume of each CSO of the drainage network

$Q_{MAX_HARD-T-SCENARIO}$ = Peak Flows Maximum reached in the CSOs in the hard technology scenario

$Q_{MAX_SUDS-SCENARIO}$ = Peak Flows Maximum reached in the CSOs in the design-based (SuDS) scenario.

Identification of potential rainfall scenarios at 2050

In Figure 5.5 (a, b, c) maximum values of 24-hour, 1-hour and 30-minutes rainfall for each of the observed year are plotted. The characteristics of the trend lines (slopes and intercepts) were used to predict rainfall extremes at 2050 and, through the comparison with the historical mean data, percentage of variation were detected. Results reported in Table 5.3 highlights that precipitation extremes at three different aggregation intervals would increase in the next years for the Lodi weather station. The maximum rainfall at 30-minutes showed the highest variation (+26.92%), the maximum rainfall at 1-hour the lowest (+6.55%). Even if affected by a large degree of uncertainty, due to the absence of continuous sub-hourly precipitation data sets, findings suggest an overall increase of the number of rainfall events with higher intensity as we it can be observed from Figure 5.6 (a, b, c). The latter collects picture of historical and predicted LSPP at 2-years, 5-years and 10-years return period (T) used to test at the event scale the mentioned drainage network models.

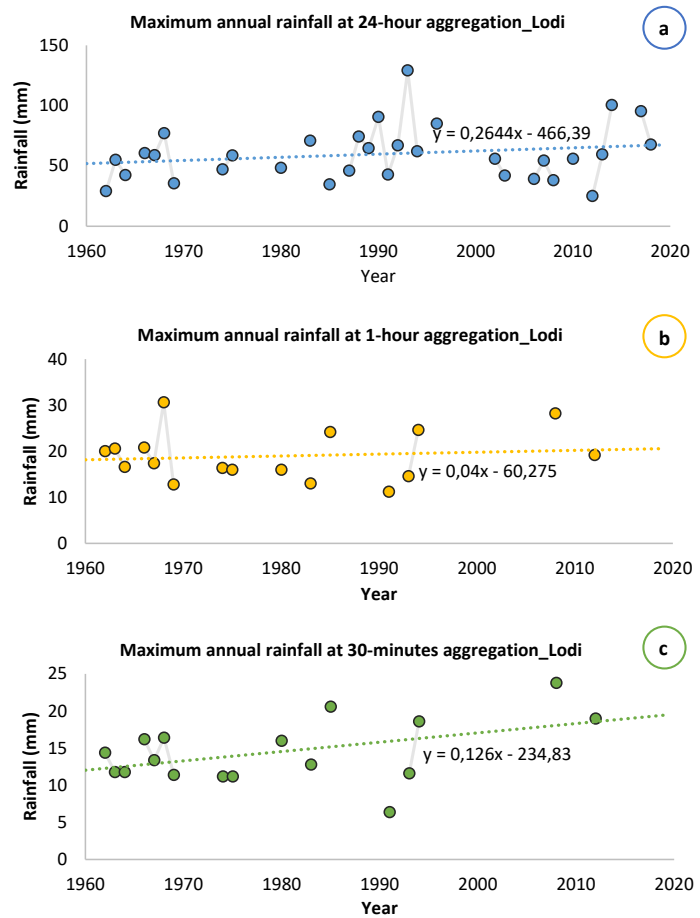


Fig. 5.5 24-hour (a), 1-hour (b) and 30-minutes (c) maximum rainfall for each of the observed year registered by the Lodi weather station

Lodi Weather Station						
	Slope	Intercept	$R_{\text{predicted at 2050}}$ (mm)	$\text{Mean}R_{\text{historical}}$ (mm)	V_{rain} (%)	
24 h	0.264	-466.4	68.00	59.81	13.70	
1 h	0.040	-60.3	20.19	18.95	6.55	
30 min	0.126	-234.8	18.41	14.51	26.92	

Tab. 5.3 above Variation of rainfall extremes for the Lodi weather station

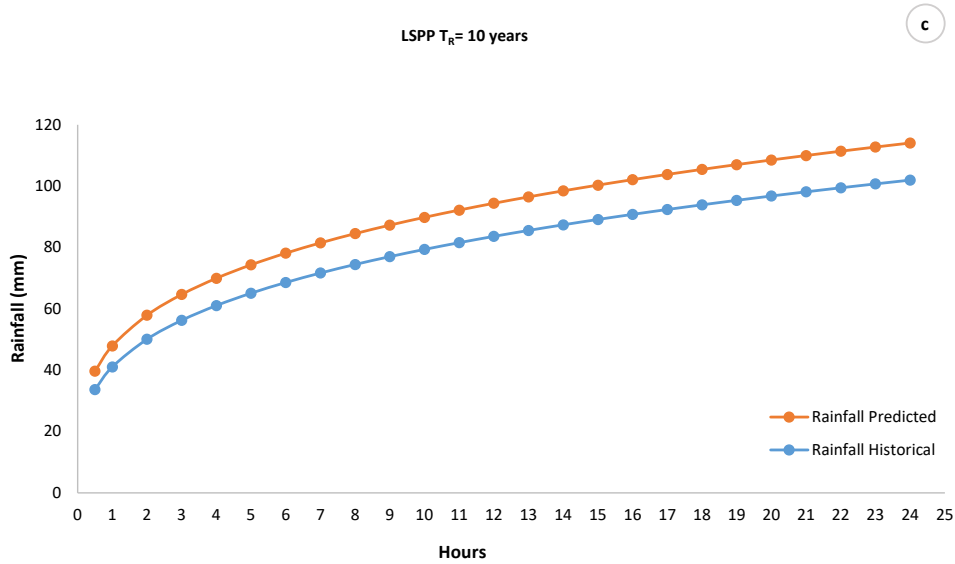
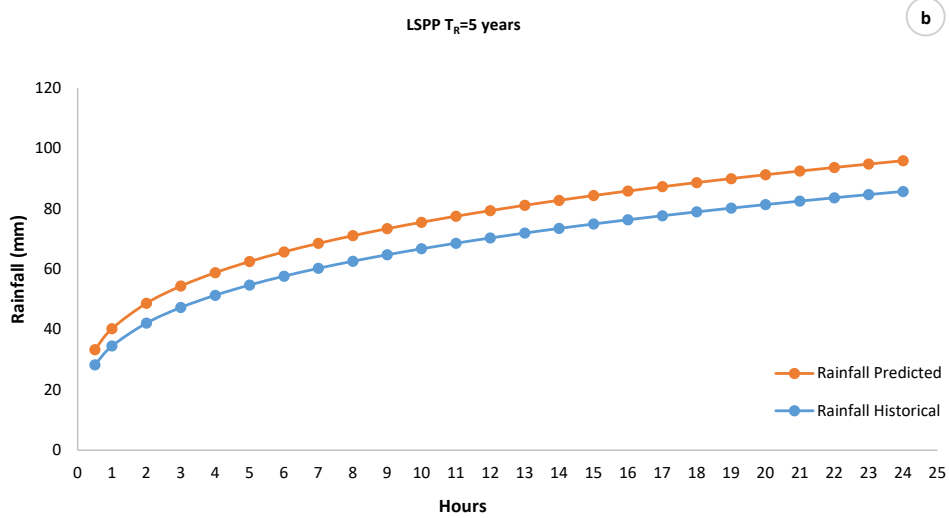
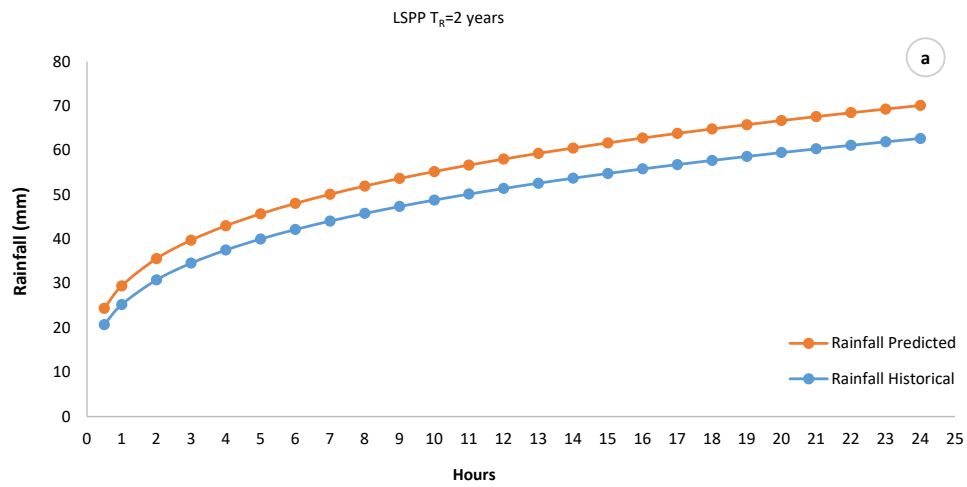


Fig. 5.6 Historical and predicted LSPP at 2-years (a), 5-years (b) and 10-years (c) return period (T)

In Figure 5.7 (a, b, c) annual cumulative rainfalls collected from Lodi, Monza, Pavia and Milano weather station are plotted. However, also in this case, incomplete datasets and period of missing data influenced the assessment increasing the randomness of the results (Table 5.4). With the exception of Lodi weather station (+1.20%), the others all registered an overall decrease of the annual rainfall amount (ranging from -2.54 % of Monza to -5.45 and -5.50 of Milano and Pavia).

Difference within the results can be also ascribed to the distance between the different weather stations analysed, due to the great space-time variability of the precipitation. The highest and the lowest percentages of variation (+1.20% and -5.50), along with two notional percentages (+5%, +10%) were used to adjust an annual rainfall typical of Sesto Ulteriano to test drainage system models under future long period precipitation.

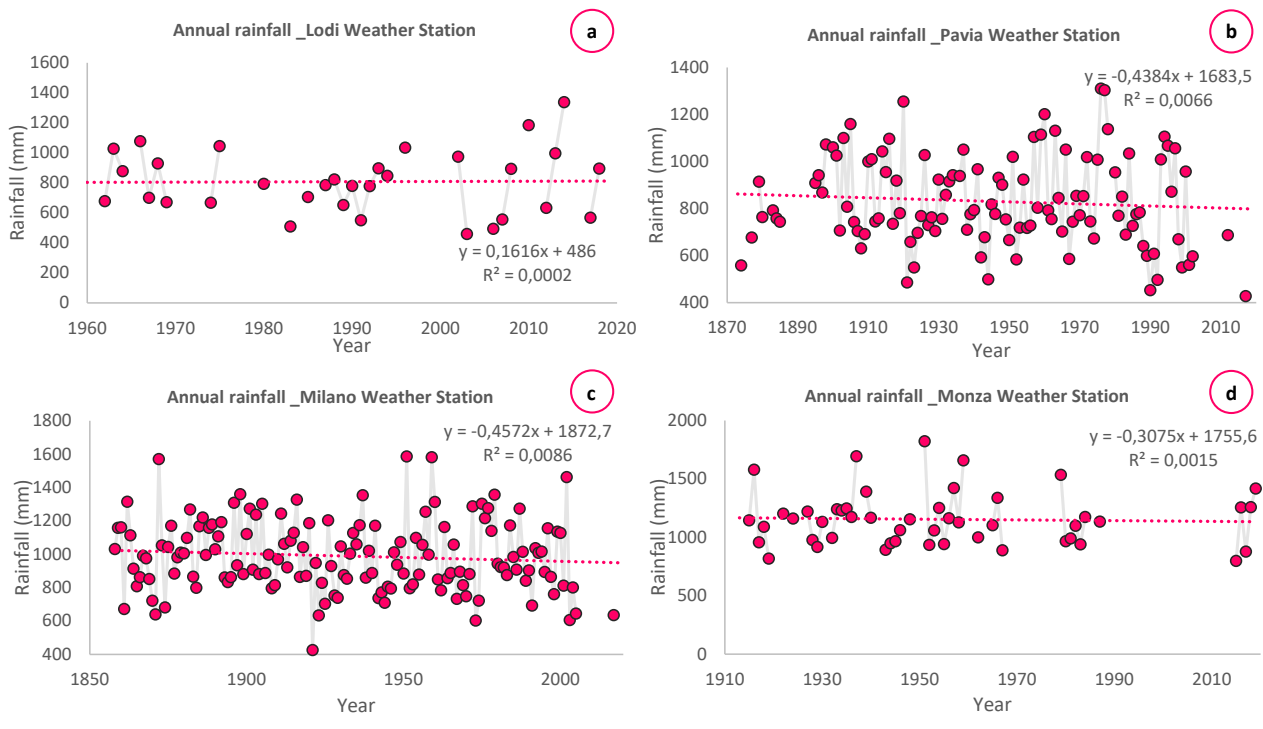


Fig. 5.7 Rainfall amount plotted for each year and for each weather station

	Slope	Intercept	R_{a,predicted} at 2050 (mm)	MeanR_{a,Historical} (mm)	V_{a,rain} (%)
Lodi	0.162	486.0	817.35	807.68	1.20
Pavia	-0.438	1683.5	784.87	830.57	-5.50
Milano	-0.457	1872.7	935.39	989.31	-5.45
Monza	-0.308	1755.6	1125.17	1154.52	-2.54

Tab. 5.4 Variation of annual rainfall amount for each weather station

Climate Change Analysis Results: assessing SWMM₅ drainage models performance focusing on climate change effects

The results of this analysis, aimed at comparing the drainage scenarios (hard-technology or design-based SuDS) under historical and future rainfalls, highlighted the possible impact of climate changes on Peak Flow and Total Volume discharged from the CSOs of the sewer. Table 5.5 (a, b) collects the results respectively of the SuDS-based scenario and the Hard-Technology scenario in terms of the aforementioned hydrological parameters and each percentage of increase obtained from the comparison of historical and potential event scale climate scenarios (T=2, 5, 10). Observing peak flows and total volumes in Table

5.5 (a, b), the SuDS-based scenario, independently from the return period of the rainfall event, is always characterized by values noticeably lower than the hard-technology scenario. For example, it reaches the maximum values of peak flow (1.92 m³/s) and total volumes (60373.40 m³) in the Climate Change Scenario with T= 10 years (worse condition). These values in the hard-technology scenario are yet reached for events with T<5 years. However, comparing the same drainage scenario under both historical and future rainfall inputs, results highlighted that SuDS-based scenario experienced, regardless of the rainfall intensity, higher increases in the hydrological parameters with differences from the hard-technology scenario reaching up 20 percentage points.

a. SuDS-based Scenario

SuDS-based Scenario (S)						
T _R	2 years		5 years		10 years	
Scenario	H	CC	H	CC	H	CC
Q _{max} [m ³ /s]	0.45	0.66	1.12	1.45	1.56	1.92
V _{tot} [m ³]	14953.05	21240.06	33111.72	42400.42	47986.80	60373.40
I _Q (%)	45		30		23	
I _V (%)	42		28		26	

b. Hard-Technology Scenario

Hard-Technology Scenario (H-T)						
T _R	2 years		5 years		10 years	
Scenario	H	CC	H	CC	H	CC
Q _{max} [m ³ /s]	1.60	1.91	2.66	2.89	2.94	3.13
V _{tot} [m ³]	41307.3	49783.2	70097.7	83004.2	91943.6	108244.5
I _Q (%)	20		8		6	
I _V (%)	21		18		18	

Tab. 5.5 Event scale Variations of Peak Flow and Total Volume discharged from the CSOs of the sewer in the SuDS-based Scenario (a) and in the Hard-Technology Scenario (b)

These findings pointed out that, even if SuDS are undoubtedly a great solution for the sustainable management of urban floods, they seem particularly sensitive to climate change effects. As regard the long period performance, results reported in Table 5.6 (a, b) pointed out again, this time less evidently, a larger susceptibility of SuDS-based drainage scenarios to climate changes.

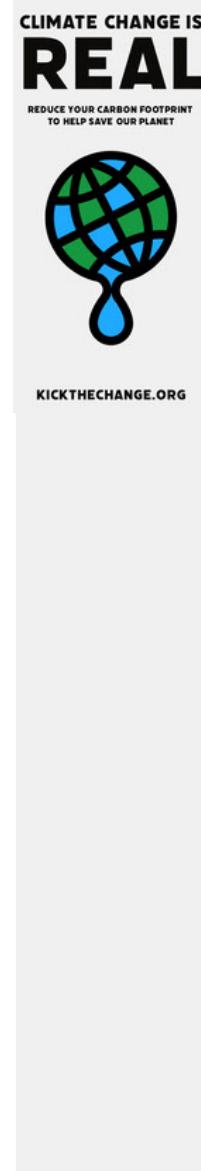
a. SuDS-based Scenario

SuDS-based Scenario (S)					
Scenario	H	CC_(-5.5%)	CC_(+1.2%)	CC_(+5.0%)	CC_(+10.0%)
Q_{max} [m ³ /s]	2.26	2.15	2.28	2.38	2.44
V_{tot} [m ³]	1004582.16	928767.37	1041171.77	1122561.35	1185729.21
I_Q (%)	-	-5	1	5	8
I_V (%)	-	-8	4	12	18

b. Hard-Technology Scenario

Hard-Technology Scenario (H-T)					
Scenario	H	CC_(-5.5%)	CC_(+1.2%)	CC_(+5.0%)	CC_(+10.0%)
Q_{max} [m ³ /s]	2.90	2.85	2.91	2.95	2.98
V_{tot} [m ³]	2190404.83	2047453.38	2264519.01	2423064.53	2543739.07
I_Q (%)	-	-2	0	2	3
I_V (%)	-	-7	3	11	16

Tab. 5.6 Long period variations of Peak Flow and Total Volume discharged from the CSOs of the sewer in the SuDS-based Scenario (a) and in the Hard-Technology Scenario (b)



Drainage Network Analysis Results: comparing under the same climate condition different SWMM₅ drainage models

Table 5.7 (a, b, c) compare under each rainfall event (respectively T=2, 5, 10) in both the historical and climate change scenarios peak flows and total volumes discharged from the CSOs of the SuDS-based and hard-technology drainage

modeling scenarios. It is clear again and more evidently, looking at the results, that SuDS are able to lower both peak flow and total volumes ranging between a maximum reduction of 72% and 64% respectively under the historical rainfall characterized by T=2 and a minimum reduction of 39% and 44% under the future rainfall with T=10. Despite this, observing SuDS performance under climate change, higher reduction

percentages were reached under the historical rainfall input, confirming that drainage systems that involve SuDS are much more sensitive to climate change as compared to traditional ones. As for the long period simulations (Table 5.8 a, b), little or no differences were registered between SuDS performances under historical

and future rainfall inputs. Just looking at the peak flow reduction it can be perceived a lowering of the SuDS performance with the worsening of climate scenarios (+5% and +10% rainfall increase). This would signify that in the long-term climate variation, though noticeable, seems not to affect the efficiency of SuDS in the study area.

a. T=2 years

Scenario	T _R = 2 years			
	Historical (H)		(Climate Change) CC	
	S	H-T	S	H-T
Q _{max} [m ³ /s]	0.45	1.60	0.66	1.91
V _{tot} [m ³]	14953.05	41307.3	21240.06	49783.2
R _Q (%)	72		66	
R _V (%)	64		57	

b. T=5 years

Scenario	T _R = 5 years			
	Historical (H)		(Climate Change) CC	
	S	H-T	S	H-T
Q _{max} [m ³ /s]	1.12	2.66	1.45	2.89
V _{tot} [m ³]	33111.72	70097.7	42400.42	83004.2
R _Q (%)	58		50	
R _V (%)	53		49	

c. T=10 years

Scenario	T _R = 10 years			
	Historical (H)		(Climate Change) CC	
	S	H-T	S	H-T
Q _{max} [m ³ /s]	1.56	2.94	1.92	3.13
V _{tot} [m ³]	47986.80	91943.6	60373.40	108244.5
R _Q (%)	47		39	
R _V (%)	48		44	

Tab. 5.7 comparison under T=2 rainfall event (a), T=5 rainfall event (b) and T=10 rainfall event (c) in both the historical and climate change scenarios of the peak flows and total volumes discharged from the CSOs of the SuDS-based and hard-technology drainage modeling scenarios.



a. studied trends

Scenario	Studied trends					
	Historical (H)		(Climate Change) CC_ _(-5.5%)		(Climate Change) CC_ _(+1.2%)	
	S	H-T	S	H-T	S	H-T
Q_{\max} [m ³ /s]	2.26	2.90	2.15	2.85	2.28	2.91
V_{tot} [m ³]	1004582.16	2190404.83	928767.37	2047453.38	1041171.77	2264519.01
R_Q (%)	22		25		22	
R_V (%)	54		55		54	

b. notional trends

Scenario	Notional trends					
	Historical (H)		(Climate Change) CC_ _(+5.0%)		(Climate Change) CC_ _(+10%)	
	S	H-T	S	H-T	S	H-T
Q_{\max} [m ³ /s]	2.26	2.90	2.38	2.95	2.44	2.98
V_{tot} [m ³]	1004582.16	2190404.83	1122561.35	2423064.53	1185729.21	2543739.07
R_Q (%)	22		19		18	
R_V (%)	54		54		53	

Tab. 5.8 Comparison under studied and notional annual rainfall trends in both the historical and climate change scenarios of the peak flows and total volumes discharged from the CSOs of the SuDS-based and hard-technology drainage modeling scenarios

Results discussion

Both under current and future potential climate conditions, the implementation of SuDS techniques resulted in a notable reduction of both maximum discharge and total volume.

As an example, with reference to short rainfall events and for return periods $T=5$ years, the maximum discharge and total volume reduction, in the case of the current scenario, is respectively about 80% and 75%.

However, in the case of the future potential climate scenario, the reduction percentages reduce to 70%, showing, at the same time, how SuDS can be valuable used to adapt to climate change conditions but that the resilience they provide in terms of stormwater management issue would be much more sensitive to climate input in the next future.



<https://www.groundsure.com/resources/sustainable-urban-drainage-systems-suds-a-proactive-approach-to-reducing-surface-flooding/>

“We are the first generation to feel the effect of climate change and the last generation who can do something about it.”

Barack Obama

Chapter 6

Discussion and Conclusions

This research aimed to understand the possibilities in the field of urban hydrology and specifically in the management of stormwater of sustainable drainage infrastructures, green roofs in particular and other types of “Nature-Based” solutions that can be implemented within the urban fabric. The presence of an experimental plant installed in 2017 outside the Maritime and Environmental Hydraulics laboratory of the University of Salerno, made it possible to study the behavior of two green roofs, both extensive but characterized by a different drainage layer, with specific reference to the relation between their retention capacity and the climatic and technological factors. This study allowed putting other pieces into the world research scenario that still sees this topic as particularly stimulating. Although the dependence of the retention capacity from the volume of water within the substrate layer did not appear strongly functional, it was considered fundamental for an a-priori identification of groups of rainfall-runoff events for which a relationship could be established between the retention capacity and the specific characteristics of the rainfall events. In particular, these results underlined a tendency to a reduction of retention properties for large events and mainly saw the rainfall cumulate depth as the best predictor for RC estimation. The differences between the two experimental green roofs in the group of event characterized by higher moisture contents led to the consideration of the important role played by the drainage layer in those conditions. Since they are almost identical, in fact, the differences can be attributed to the only element not in common: the drainage layer. Conversely, for the group of events with lower moisture contents little difference

was observed between the two investigated infrastructure, showing how vegetation and substrate layer, shared features, played a predominant role under these conditions. The severity of the rainfall events, as described by the return period, was only accidentally studied for the case study as only one of the thirty-five selected rainfall events is featured by a high return period, of 10 years. The characteristics of the rainfall events selected depend for sure on the site climate conditions but also on the length of the monitoring period (about 3 years), too short to observe numerous severe precipitations. Longer monitoring period and indoor experiments under controlled conditions would probably give the possibility to study the performance of these systems under severe rainfall ($T > 5$) to understand if the results discussed so far could also apply in that conditions. Once understood the behaviour and the potential of the green roofs, the subsequent steps aimed at answering these questions: Could these infrastructures really be able to solve the stormwater-related issues in urban areas? To what extent should they be implemented in order to substantially reduce flooding risk? Despite being a particularly addressed topic in existing literature, the difficulty here lies in the impossibility of identifying considerations universally true. Cities, in fact, already different in geomorphological and climatic context, experienced different urban and infrastructural development that make it difficult to extract from the catchment-based studies generally valid remarks. For this reason, this research focused on a study area included in the Sarno catchment that experienced between 1995 and 2016 an increase of the impervious fraction of 18% and consequently an enhancement of

flooding risk. Results showed that in order to make green roof retrofitting effective in the reduction of stormwater volumes and in the restoration of the natural pattern prior to the massive urbanization, a too large portion of the current waterproof surface should be retrofitted. Therefore, to improve city resilience against hydraulic risk, the preferable strategy is that of implementing a combined approach in which Green Roofs and other Sustainable Drainage Systems located within the urban context (i.e. drainage trenches, bioretention cells, pervious parking lots and rain gardens) support the traditional drainage systems in the management and reduction of urban flooding. These considerations led to undertake a modeling study for the assessment of hydraulic and hydrological benefits deriving from the implementation of detailed SuDS retrofitting project in Sesto Ulteriano (MI), a consolidated urban context affected by several criticalities related to the stormwater management. This task aimed to answer the following questions: What is the real importance of having a SuDS project implementation aware of the real retrofitting capabilities of the urban context? How a potential SuDS model scenario compares to the real feasibility of the project? Does localization affect SuDS performance? In particular, thanks to a comprehensive retrofitting design of SuDS choice and localization, this part of the research aspired to compare typically potential or model-based SuDS retrofitting scenarios with feasible or design-based ones to understand if their results could affect the general opinion of decision-makers upon the efficiency of sustainable drainage systems. It was understood that the degree of SuDS implementation (the more, the better) as well as

the characteristics of the rainfall event (the less severe, the better) are among the main factors for a successful retrofitting intervention. However, the identification of a threshold behavior in the percentage of implementation is also a fundamental result. Above a certain threshold, no great benefit can be observed due to the increase of SuDS retrofitting surface. Moreover, being aware of the actual retrofitting potential of an urban catchment seems essential to predict the effectiveness of SuDS projects in the mitigation of flooding risk. Generic projects and strategical solutions based on retrofitting percentages fixed and unaware of the features of the specific urban system would inevitably result in misleading analysis, unsuccessful interventions, unsolved issues and high financial costs. Within the same study, the benefits of the implementation of the floodability concept in Sesto Ulteriano were assessed. Diffuse-storage scenarios, involving floodable streets and squares along with the traditional storage systems, were compared with the centralized-storage scenario in which only storage tanks downstream were provided to identify a possible reduction of the centralized storage tanks volumes. Results again showed that integrated approaches, involving the use of SuDS, helped reducing stormwater discharged into detention tanks and consequently the volume of the traditional drainage infrastructures designed. Even under future potential climate conditions, the implementation of SuDS techniques resulted in a notable reduction of both maximum discharge and total volume. However, the resilience they provide in terms of stormwater management issue would be much more sensitive to climate input in the next future.



Epilogue

“No individual raindrop ever considers itself responsible for the flood” so stated John Ruskin, British writer, painter, poet and art critic. In the same way, man too is always led to think that a single action cannot be the cause of the exacerbation of certain natural phenomena: flooding and climate change just to keep to the subject! The construction of a single house does not alter the configuration of the catchment, it does not increase the impervious surface enough to exacerbate flooding phenomena in urban context. But what if the houses were two, ten, a hundred, a thousand? No one will feel brought into play on the occasion of a flood phenomenon, indeed everyone will be amazed. Unfortunately, even today we are still too often led to think as individuals and not as a community. It is time to start changing perspective, to join forces to face the challenges that we all have individually contributed to create!

It is also true that, in fact, as stated by the British writer Helen Keller, “Alone we can do so little, together we can do so much”. Humans are part of a great team able to fight against critical issues generated by individuals. Do you think that implementing a single green infrastructure may provide significant and visible benefits? But what if the green infrastructure were two, ten, a hundred, a thousand?



ST STEPHEN'S GREEN, CITY PARK, DUBLIN (IE)
https://en.wikipedia.org/wiki/Urban_park#/media/File:Dublin_Stephen's_Green-44_edit.jpg

References

- Acquaotta, F., Faccini, F., Fratianni, S., Paliaga, G., Sacchini, A. (2018). Rainfall intensity in the Genoa Metropolitan Area: secular variations and consequences. *Weather* 73, 356-362. <https://doi.org/10.1002/wea.3208>
- Akther, M., He J., Chu, A., Huang, J., van Duin, B. (2018). A Review of Green Roof Applications for Managing Urban Stormwater in Different Climatic Zones. *Sustainability* 10 (8), 2864. <https://doi.org/10.3390/su10082864>
- Albano, R., Sole, A., Sdao, F., Giosa, L., Cantisani, A., Pascale, S. (2014). A Systemic Approach to Evaluate the Flood Vulnerability for an Urban Study Case in Southern Italy. *Journal of Water Resources and Protection* 6(4), 351-362. <https://doi.org/10.4236/jwarp.2014.64037>
- Alferi, L., Feyen, L. & Di Baldassarre, G. (2016). Increasing flood risk under climate change: a pan-European assessment of the benefits of four adaptation strategies. *Climatic Change* 136, 507-521. <https://doi.org/10.1007/s10584-016-1641-1>
- Andimuthu, R., Kandasamy, P., Mudgal, B.V., Jeganathan, A., Balu, A., Sankar, G. (2019). Performance of urban storm drainage network under changing climate scenarios: Flood mitigation in Indian coastal city. *Scientific Reports* 9, 7783. <https://doi.org/10.1038/s41598-019-43859-3>
- Andreucci, M. B., (2017). *Progettare Green Infrastructure. Tecnologie, valori e strumenti per la resilienza urbana*. Wolters Kluwer Italia Srl, Milano. ISBN 978-88-217-6317-5
- Apollonio, C., Balacco, G., Novelli, A., Tarantino, E., Piccinni, A. F., (2016). Land Use Change Impact on Flooding Areas: The Case Study of Cervaro Basin (Italy). *Sustainability* 8, p. 996. <https://doi.org/doi:10.3390/su8100996>
- Arahetes, A., Olcina Cantos, J. (2019). The potential of sustainable urban drainage systems (SuDS) as an adaptive strategy to climate change in the Spanish Mediterranean, *International Journal of Environmental Studies* 76(5), 764-779. <https://doi.org/doi:10.1080/00207233.2019.1634927>
- Avellaneda, P.M., Jefferson, A.J., Grieser, J.M., Bush, S.A., (2017). Simulation of the cumulative hydrological response to green infrastructure. *Water Resources Research* 53(4), 3087-3101. <https://doi.org/10.1002/2016WR019836>
- Bai, Y., Li, Y., Zhang, R., Zhao, Na, Zeng, X., (2019). Comprehensive Performance Evaluation System Based on Environmental and Economic Benefits for Optimal Allocation of LID Facilities. *Water* 11, 341. <https://doi.org/10.3390/w11020341>
- Baryla, A.; Karczmarczyk, A.; Bus, A. (2018). Role of Substrates Used for Green Roofs in Limiting Rainwater Runoff. *Journal of Ecological Engineering* 19(5), 86-92. <https://doi.org/doi:10.12911/22998993/91268>
- Bell, S., (2018). *Urban Water Sustainability. Constructing Infrastructure for Cities and Nature*. Routledge, London and New York. ISBN 978-1-138-92990-6
- Beniston, M., Stephenson, D.B., Christensen, O.B. et al. (2007). Future extreme events in European climate: an exploration of regional climate model projections. *Climatic Change* 81, 71-95. <https://doi.org/10.1007/s10584-006-9226-z>
- Berndtsson, J. (2010). Green roof performance towards management of runoff water quantity and

quality: A review. *Ecological Engineering* 36(4), 351-360.

Bertilsson, L., Wiklund, K., de Moura Tebaldi, I., Moura Rezende, O., Pires Veról, A., Gomes Miguez, M. (2019). Urban flood resilience – A multi-criteria index to integrate flood resilience into urban planning. *Journal of Hydrology*, 573, 970-982. <https://doi.org/10.1016/j.jhydrol.2018.06.052>

Bertrand-Krajewski, J. L., Chebbo, G. (2002). Sizing Ratios for Stormwater Treatment Facilities. In: Ninth International Conference on Urban Drainage (gICUD). [https://doi.org/10.1061/40644\(2002\)54](https://doi.org/10.1061/40644(2002)54)

Borchardt, D., Sperling, F. (1997). Urban stormwater discharges: Ecological effects on receiving waters and consequences for technical measures. *Water Science and Technology* 36 (8-9), 173-178. [https://doi.org/10.1016/S0273-1223\(97\)00602-1](https://doi.org/10.1016/S0273-1223(97)00602-1)

Bouzouidja, R., Séré, G., Claverie, R., Ouvrard, S., Nuttens, L., Lacroix, D. (2018). Green roof aging: Quantifying the impact of substrate evolution on hydraulic performances at the lab-scale. *Journal of Hydrology* 564, 416-423. <https://doi.org/10.1016/j.jhydrol.2018.07.032>

Brandão, C., Cameira, M.D.R., Valente, F., Cruz de Carvalho, R, Paço, T.A. (2017). Wet season hydrological performance of green roofs using native species under Mediterranean climate. *Ecological Engineering* 102, 596-611.

Brandolini, P., Cevasco, A., Firpo, M., Robbiano, A., Sacchini, A. (2012). Geo-hydrological risk management for civil protection purposes in the urban area of Genoa (Liguria, NW Italy). *Natural Hazards and earth System Sciences*, 12, 943-959. <https://doi.org/10.5194/nhess-12-943-2012>

Brears, R. C. (2018). *Blue and Green Cities. The role of blue-green infrastructure in managing urban water resources.* Macmillan Publishers Ltd, London. <https://doi.org/10.1057/978-1-137-59258-3>

Brunetti, M., Maugeri, M., Nanni, T. (2001). Changes in total precipitation, rainy days and extreme events in northeastern Italy. *International Journal of Climatology* 21, 861-871. <https://doi.org/10.1002/joc.660>

Brunetti, M., Buffoni, L., Mangianti, F., Maugeri, M., Nanni, T. (2004). Temperature, precipitation and extreme events during the last century in Italy. *Global and Planetary Change* 40 (1-2), 141-149. [https://doi.org/10.1016/S0921-8181\(03\)00104-8](https://doi.org/10.1016/S0921-8181(03)00104-8)

Butler, D., McEntee, B., Onof, C., Hagger, A. (2007). Sewer storage tank performance under climate change. *Water Science & Technology* 56 (12), 29–35. <https://doi.org/10.2166/wst.2007.760>

Calabrò, P. S., Viviani, G. (2006). Simulation of the operation of detention tanks. *Water Research* 40(1), 83-90. <https://doi.org/10.1016/j.watres.2005.10.025>

Cannon, A. J., Innocenti S. (2019). Projected intensification of sub-daily and daily rainfall extremes in convection-permitting climate model simulations over North America: implications for future intensity–duration–frequency curves. *Natural Hazards and Earth System Sciences* 19, 421–440. <https://doi.org/10.5194/nhess-19-421-2019>

Chai, C.T., Putuhena, F.J., Selaman, O.S. (2017). A modelling study of the event-based retention performance of green roof under the hot-humid tropical climate in Kuching. *Water Science Technology* 76 (11), 2988-2999. <https://doi.org/10.2166/wst.2017.472>

Chenot, J., Gaget, E., Moinardeau, C., Jaunatre, R., Buisson, E., Dutoit, T. (2017). Substrate Composition and Depth Affect Soil Moisture Behavior and Plant-Soil Relationship on Mediterranean Extensive Green Roofs. *Water* 9(11), 817. <https://doi.org/10.3390/w9110817>

Clean Water Act Action Plan, US Environmental Protection Agency (2010). <https://www.epa.gov/sites/>

production/files/documents/actionplan101409.pdf

D'Ambrosio, R., Rizzo, A., Balbo, A., Longobardi, A. (2019). Assessing the Performance of SuDS in the Mitigation of Urban Flooding: The Industrial Area of Sesto Ulteriano (MI). *Proceedings* 48 (1). <https://doi.org/10.3390/ECWS-4-06449>

D'Ambrosio, R., Schmalz, B., Longobardi, A. (2020). Assessing the performance of Sustainable Drainage Systems (SuDS) in urban context using SWMM5 modelling scenarios: the example of a typical industrial area in Lombardia Region, northern Italy. In: *EGU General Assembly 2020*. <https://doi.org/10.5194/egusphere-egu2020-21377>

D'Ambrosio, R., Longobardi, A., Mobilia, M. (2020). Evaluation of green roofs evolution impact on substrate soil water content by FDR sensors calibration. In: *5th International Electronic Conference on Water Sciences session Water, Ecosystem Functioning and Services*. <https://doi.org/10.3390/ECWS-5-08028>

D'Ambrosio, R., Longobardi, A., Mobilia, M., Sassone, P. (2021). Sustainable strategies for flood risk management in urban areas. Enhancing city resilience with Green Roofs. *Journal of Urban Planning, Landscape & Environmental Design* 5(2), 87-98. <https://doi.org/10.6092/2531-9906/7759>

Di Matteo, M., Liang, R., Maier, H. R., Thyer, M. A., Simpson, A. R., Dandy, G. C., Ernst, B. (2019). Controlling rainwater storage as a system: An opportunity to reduce urban flood peaks for rare, long duration storms. *Environmental Modelling & Software* 111, 34-41. <https://doi.org/10.1016/j.envsoft.2018.09.020>

Dong, X., Guo, H., Zeng, S. (2017). Enhancing future resilience in urban drainage system: Green versus grey infrastructure. *Water Research* 124, 280-289. <https://doi.org/10.1016/j.watres.2017.07.038>

Eckart, K., McPhee, Z., Bolisetti, T. (2017). Performance and implementation of low impact development – A review. *Science of the Total Environment* 607–608, 413-432. <https://doi.org/10.1016/j.scitotenv.2017.06.254>

Ercolani, G., Chiardia, E. A., Gandolfi, C., Castelli, F., Masseroni, D. (2018). Evaluating performances of green roofs for stormwater runoff mitigation in a high flood risk urban catchment. *Journal of Hydrology* 566, 830-845. <https://doi.org/10.1016/j.jhydrol.2018.09.050>

EU Water Framework Directive, “Directive 2000/60/EC of the European Parliament and of the Council establishing a framework for the Community action in the field of water policy” (2000). *Official Journal (OJ L327)*.

Even, S., Mouchel, J. M., Servais, P., Flipo, N., Poulin, M., Blanc, S., Chabanel, M., Paffoni, C. (2007). Modelling the impacts of Combined Sewer Overflows on the river Seine water quality. *Science of the Total Environment* 375 (1–3), 140-151. <https://doi.org/10.1016/j.scitotenv.2006.12.007>

Everett, G., Lamond, J., Morzillo, A. T., Chan, F. K. S., Matsler, A. M. (2016). Sustainable drainage systems: helping people live with water. *Water Management* 169 (WM2). <http://dx.doi.org/10.1680/wama.14.00076>

Faccini, F., Paliaga, G., Sacchini, A., Watkins, C. (2016). The Bisagno stream catchment (Genoa, Italy) and its major floods: geomorphic and land use variations in the last three centuries. *Geomorphology* 273, 14-27. <https://doi.org/10.1016/J.GEOMORPH.2016.07.037>

Fahy, B., Chang, H. (2019). Effects of Stormwater Green Infrastructure on Watershed Outflow: Does Spatial Distribution Matter? *International Journal of Geospatial and Environmental Research* 6 (1),

Article 5.

- Ferrans, P., Rey, C. V., Pérez, G., Rodríguez, J. P., Diaz-Granados, M. (2018). Effect of Green Roof Configuration and Hydrological Variables on Runoff Water Quantity and Quality. *Water* 10(7), 960. <https://doi.org/10.3390/w10070960>
- Fletcher, T.D., Shuster, W., Hunt, W.F., Ashley, R., Butler, D., Arthur, S., Trowsdale, S., Barraud, S., Semadeni-Davies, A., Bertrand-Krajewski, J. L., Steen Mikkelsen, P., Rivard, G., Uhl, M., Dagenais, D., Viklander, M. (2015). SUDS, LID, BMPs, WSUD and more – The evolution and application of terminology surrounding urban drainage. *Urban Water Journal* 12(7), 525-542. <https://doi.org/10.1080/1573062X.2014.916314>
- Frei, C., Schöll, R., Fukutome, S., Schmidli, J., Vidale, P. L. (2006). Future change of precipitation extremes in Europe: Intercomparison of scenarios from regional climate models. *Journal of Geophysical Research Atmospheres* 111 (D6). <https://doi.org/10.1029/2005JD005965> Citations: 395
- Galea, S., Ertman, C. K., Vlahov, D. (2019). The Present and Future of Cities. In: *Urban Health*, 3-14. ISBN: 9780190915841
- Galupini, G., Quintilliani, C., Arosio, M., Barbero, G., Ghilardi, P., Manenti, S, Petaccia, G., Todeschini, S., Ciaponi, C., Martina, M.L.V., Creaco, E. (2020). A unified framework for the assessment of multiple source urban flash flood hazard: the case study of Monza, Italy. *Urban Water Journal* 17(1), 65-77, <https://doi.org/10.1080/1573062X.2020.1734950>
- Gimenez-Maranges, M., Breuste, J., Hof, A. (2020). Sustainable Drainage Systems for transitioning to sustainable urban flood management in the European Union: A review. *Journal of Cleaner Production* 255, 120191. <https://doi.org/10.1016/j.jclepro.2020.120191>
- Ghofrani, Z., Sposito, V., & Faggian, R. (2019). Modelling the impacts of blue-green infrastructure on rainfall runoff: a case study of Eastern Victoria, Australia. *International Journal of Water* 13(2), 151. <https://doi.org/10.1504/IJW.2019.10020979>
- Golden, H.E. and Hoghooghi, N. (2018). Green infrastructure and its catchment scale effects: an emerging science. *Wiley Interdisciplinary Reviews: Water* 5(1). <https://doi.org/10.1002/wat2.1254>
- Graziano, P., Rizzi, P., Piva, M., Barbieri, L. (2019). A Regional Analysis of Well-Being and Resilience Capacity in Europe. *Scienze Regionali*, 551-574. <https://doi.org/10.14650/94667>
- Guzzetti, F., Cipolla, F., Lolli, O., Pagliacci, S., Sebastiani, C., Tonelli, G. (2002). Information system on historical landslides and floods in Italy. *Urban Hazard Forum*. New York.
- Hernes, R. R., Gagne, A. S., Abdalla, E. M. H., Braskerud, B. C., Alfredsen, K., Muthanna, T. M. (2020). Assessing the effects of four SUDS scenarios on combined sewer overflows in Oslo, Norway: evaluating the low impact development module of the Mike Urban model. *Hydrology Research*. <https://doi.org/10.2166/nh.2020.070>
- Hiltner, R.N., Lawrence, T.M., Tollner, E.W. (2008). Modeling storm water runoff from green roofs with HYDRUS-1D. *Journal of Hydrology* 358, 288–293. <https://doi.org/10.1016/j.jhydrol.2008.06.010>
- Hua, P., Yang, W., Qi, X., Jiang, S., Xie, J., Gu, X., Li, H., Zhang, J., Krebs, P. (2020). Evaluating the effect of urban flooding reduction strategies in response to design rainfall and low impact development. *Journal of Cleaner Production* 242, 118515. <https://doi.org/10.1016/j.jclepro.2019.118515>
- Huang, G. (2019). A Revisit to Impact of Urbanization on Flooding. *Urban Planning and Water-related Disaster Management*, 43-56. https://doi.org/10.1007/978-3-319-90173-2_4

- Jiang, C., Li, J., Li, H., Li, Y., Zhang, Z. (2020). Low-impact development facilities for stormwater runoff treatment: Field monitoring and assessment in Xi'an area, China. *Journal of Hydrology* 585. <https://doi.org/10.1016/j.jhydrol.2020.124803>
- Johannessen, B. G., Muthanna, T. M., & Braskerud, B. C. (2018). Detention and Retention Behaviour of Four Extensive Green Roofs in Three Nordic Climate Zones. *Water* 10(6), 671. <https://doi.org/10.3390/w10060671>
- Kabisch, M., Korn, H., Stadler, J., & Bonn, A. (2017). Nature based Solutions to Climate Change Adaptation in Urban Areas. Cham: SpringerOpen. https://doi.org/10.1007/978-3-319-56091-5_1
- Kang, S., van Iersel, M. W., Kim, J. (2019). Plant root growth affects FDR soil moisture sensor calibration, *Scientia Horticulturae* 252, 208-211, <https://doi.org/10.1016/j.scienta.2019.03.050>
- Kapetas, L., Fenner, R. (2020). Integrating blue-green and grey infrastructure through an adaptation pathways approach to surface water flooding. *Philosophical Transaction of the Royal Society A* 378(2168). <https://doi.org/10.1098/rsta.2019.0204>
- Kizito, F., Campbell, C.S., Campbell, G.S., Cobos, D.R., Teare, B.L., Carter, B., Hopmans, J.W. (2008). Frequency, electrical conductivity and temperature analysis of a low-cost capacitance soil moisture sensor. *Journal of Hydrology* 352 (3-4), 367-378. <https://doi.org/10.1016/j.jhydrol.2008.01.021>
- La Loggia, G., Puleo, V., Freni, G. (2020). Floodability: A New Paradigm for Designing Urban Drainage and Achieving Sustainable Urban Growth. *Water Resources Management* 34 (10), 3411-3424. <https://doi.org/10.1007/s11269-020-02620-6>
- La Loggia, G., Fontanazza, C.M., Freni, G., Notaro, V., Olivieri, E., Puleo, V. (2012). Urban drainage and sustainable cities: how to achieve flood resilient societies? *Urban Water* 122, 203-2014. <https://doi.org/10.2495/UW120181>
- Larsen, T. A., Hoffman, S., Luthi, C., Truffer, B., & Maurer, M. (2016). Emerging solutions to the water challenges of an urbanizing world. *Science* 352(6288), 928-933. <https://doi.org/10.1126/science.aad8641>
- Larson, L. W., Peck, E. L. (1974). Accuracy of precipitation measurements for hydrologic modeling. *Water Resources Research* 10(4), 857-863. <https://doi.org/10.1029/WR010i004p00857>
- Lashford, C., Rubinato, M., Cai, Y., Hou, J., Abolfathi, S., Coupe, S., Charlesworth, S., Tait, S. (2019). SuDS & Sponge Cities: A Comparative Analysis of the Implementation of Pluvial Flood Management in the UK and China. *Sustainability* 11(1), 213. <https://doi.org/10.3390/su11010213>
- Lee, E. H., Lee, Y. S., Joo, J. G., Jung, D., Kim, J. H. (2016). Flood Reduction in Urban Drainage Systems: Cooperative Operation of Centralized and Decentralized Reservoirs. *Water* 8(10), 469. <https://doi.org/10.3390/w8100469>
- Li, P., Liu, J., Fu, R., Liu, X., Zhou, Y., Luan, M. (2015). The performance of LID (low impact development) practices at different locations with an urban drainage system: a case study of Longyan, China. *Water Practice and Technology* 10 (4), 739-746. <https://doi.org/10.2166/wpt.2015.090>
- Li, Q., Wang, F., Yu, Y., Huang, Z., Li, M., Guan, Y. (2019). Comprehensive performance evaluation of LID practices for the sponge city construction: A case study in Guangxi, China. *Journal of Environmental Management* 231, 10-20. <https://doi.org/10.1016/j.jenvman.2018.10.024>
- Liuzzo, L., Bono, E., Sammartano, V., Freni, G. (2016). Analysis of spatial and temporal rainfall trends in Sicily during the 1921-2012 period. *Theoretical Applied Climatology* 126, 113-129 (2016). <https://doi.org/10.1007/s00734-016-0671-1>

org/10.1007/s00704-015-1561-4

Longobardi, A., D'Ambrosio, R., Mobilia, M. (2019). Predicting Stormwater Retention Capacity of Green Roofs: An Experimental Study of the Roles of Climate, Substrate Soil Moisture, and Drainage Layer Properties. *Sustainability* 11(24), 6956. <http://dx.doi.org/10.3390/su11246956>

Longobardi, A., Diodato, N., Mobilia, M. (2016). Historical storminess and hydro-geological hazard temporal evolution in the solofrana river basin—Southern Italy. *Water* 8(9), 398. <https://doi.org/10.3390/w8090398>

Luino, F., Turconi, L., Petrea, C., Nigrelli, G. (2012). Uncorrected land-use planning highlighted by flooding: the Alba case study (Piedmont, Italy). *Natural Hazards and Earth System Sciences* 12, 2329-2346. <https://doi.org/doi:10.5194/nhess-12-2329-2012>

Madsen, H., Lawrence, D., Lang, M., Martinkova, M., Kjeldsen, T.R. (2014). Review of trend analysis and climate change projections of extreme precipitation and floods in Europe. *Journal of Hydrology* 519 (D), 3634-3650. <https://doi.org/10.1016/j.jhydrol.2014.11.003>

Mazzoleni, M., Bacchi, B., Barontini, S., Di Baldassarre, G., Pilotti, M., Ranzi, R. (2014). Flooding Hazard Mapping in Floodplain Areas Affected by Piping Breaches in the Po River, Italy. *Journal of Hydrological Engineering* 19(4), 717-731. [https://doi.org/10.1061/\(ASCE\)HE.1943-5584.0000840](https://doi.org/10.1061/(ASCE)HE.1943-5584.0000840)

McDaniel, R., O'Donnell, F. C. (2019). Assessment of Hydrologic Alteration Metrics for Detecting Urbanization Impacts. *Water* 11(5), 1017. <https://doi.org/10.3390/w11051017>

Mobilia, M., Longobardi, A., Sartor, J.F. (2017). Including A-Priori Assessment of Actual Evapotranspiration for Green Roof Daily Scale Hydrological Modelling. *Water* 9(2), 72. <https://doi.org/10.3390/w9020072>

Mobilia, M., Longobardi, A. (2017). Smart Stormwater Management in Urban Areas by Roofs Greening. In: *Computational Science and Its Applications – ICCSA 2017. Lecture Notes in Computer Science* 1046, 455-463. https://doi.org/10.1007/978-3-319-62398-6_32

Mobilia, M., Longobardi, A., Amitrano, D., Ruello, G., (2018). Analisi dei cambiamenti climatici e di uso del suolo in un bacino peri-urbano pronò al rischio idrogeologico. In: *XXXVI Convegno di Idraulica e Costruzioni Idrauliche* 106. ISBN:9788894379907

Mobilia, M., D'Ambrosio, R., Longobardi, A. (2020). Climate, soil moisture and drainage layer properties impact on green roofs in a Mediterranean environment. In: *Frontiers in Water-Energy-Nexus—Nature-Based Solutions, Advanced Technologies and Best Practices for Environmental Sustainability*, 169-171. https://doi.org/10.1007/978-3-030-13068-8_41

Munafò, M. (2017). Consumo di suolo, stato attuale e prospettive. ISPRA- Istituto Superiore per la Protezione e la Ricerca Ambientale.

Nawaz, R., McDonald, A., Postoyko, S. (2015). Hydrological performance of a full-scale extensive green roof located in a temperate climate. *Ecological Engineering* 82, 66-80. <https://doi.org/10.1016/j.ecoleng.2014.11.061>

Palermo, S.A., Talarico, V.C., Turco, M. (2019). On the LID systems effectiveness for urban stormwater management: case study in Southern Italy. In: *IOP Conference Series: Earth and Environmental Science* 410. Sustainability in the built environment for climate change mitigation: SBE19. <https://doi.org/10.1088/1755-1315/410/1/012012>

Palermo, S.A., Talarico, V.C., Turco, M. (2020). On the LID systems effectiveness for urban stormwater

management: case study in Southern Italy. IOP Conference Series: Earth and Environmental Science 410. <https://doi.org/10.1088/1755-1315/410/1/012012>

Palla, A., Gnecco, I. (2015). Hydrologic modeling of Low Impact Development systems at the urban catchment scale. *Journal of Hydrology* 528, 361-368. <https://doi.org/10.1016/j.jhydrol.2015.06.050>

Perales-Momparler, S., Andrés-Doménech, I., Hernández-Crespo, C., Vallés-Morán, F., Martín, M., Escuder-Bueno, I., Andreu, J. (2017). The role of monitoring sustainable drainage systems for promoting transition towards regenerative urban built environments: a case study in the Valencian region, Spain, *Journal of Cleaner Production* 163, 113-124, <https://doi.org/10.1016/j.jclepro.2016.05.153>.

Perini, K., Sabbion, P. (2016). *Urban Sustainability and River Restoration: Green and Blue Infrastructure*. John Wiley & Sons Ltd, London. <https://doi.org/10.1002/9781119245025>

Piervitali, E., Colacino, M. and Conte, M. (1998) Rainfall over the Central-Western Mediterranean basin in the period 1951-1995. Part I: precipitation trends. *Il nuovo cimento C*, 21 C (3). pp. 331-344. ISSN 1826-9885

Pistocchi, A., Calzolari, C., Malucelli, F., Ungaro, F., (2015). Soil sealing and flood risks in the plains of Emilia-Romagna, Italy. *Journal of Hydrology: Regional Studies* 4(B), 398-409. <https://doi.org/10.1016/j.ejrh.2015.06.021>

Qin, H., Li, Z., Fu, G. (2013). The effects of low impact development on urban flooding under different rainfall characteristics. *Journal of Environmental Management* 129, 577-585. <https://doi.org/10.1016/j.jenvman.2013.08.026>

Radinjia, M, Atanasova, N., Corominas, L., Comas, J., (2019). Assessing stormwater control measures using modelling and a multi-criteria approach. *Journal of Environmental Management* 243. 257-268. <https://doi.org/10.1016/j.jenvman.2019.04.102>

Recanatesi, F., Petroselli, A. (2020). Land Cover Change and Flood Risk in a Peri-Urban Environment of the Metropolitan Area of Rome (Italy). *Water Resources Management*, 34(5). <https://doi.org/10.1007/s11269-020-02567-8>

Rodríguez-Sinobas, L., Zubelzu, S., Perales-Momparler, S., Canogar, S. (2018). Techniques and criteria for sustainable urban stormwater management. The case study of Valdebebas (Madrid, Spain), *Journal of Cleaner Production* 172, 402-416. <https://doi.org/10.1016/j.jclepro.2017.10.070>

Rossi F., Villani P. (1994). A project for regional analysis of floods in Italy. In: Rossi G., Harmancioglu N., Yevjevich V. (eds). *Coping with Floods*. NATO ASI Series (Series E: Applied Sciences), 257. Springer, Dordrecht. https://doi.org/10.1007/978-94-011-1098-3_11

Samouei, S., Ozger, M. (2020). Evaluating the performance of low impact development practices in urban runoff mitigation through distributed and combined implementation. *Journal of Hydroinformatics*, 22 (6), 1506–1520. <https://doi.org/10.2166/hydro.2020.054>

Sartor, J., Mobilia, M., Longobardi, A. (2018). Results and findings from 15 years of sustainable urban storm water management. *International Journal of Safety and Security Engineering* 8(4), 505-514.

Schultz, I., Sailor, D., Starry, O. (2018). Effects of substrate depth and precipitation characteristics on stormwater retention by two green roofs in Portland OR. *Journal of Hydrology* 18, 110–118.

Scholz, M., (2015). *Sustainable Drainage Systems*. Water special issue 7. <https://doi.org/10.3390/w7052272>

- Semadeni-Davies, A., Hernebring, C., Svensson, G., Gustafsson, L. G. (2008). The impacts of climate change and urbanisation on drainage in Helsingborg, Sweden: Suburban stormwater, *Journal of Hydrology* 350 (1–2), 114–125. <https://doi.org/10.1016/j.jhydrol.2007.11.006>
- Semadeni-Davies, A. (2012). Implications of climate and urban development on the design of sustainable urban drainage. *Journal of Water and Climate Change* 3 (4), 239–256. <https://doi.org/10.2166/wcc.2012.043>
- Simmons, M. T., Gardiner, B., Windhager, S., Tinsley, J. (2008). Green roofs are not created equal: the hydrologic and thermal performance of six different extensive green roofs and reflective and non-reflective roofs in a sub-tropical climate. *Urban Ecosystems* 11(4), 339–348. <https://doi.org/10.1007/s11252-008-0069-4>
- Sims, A.W., Robison, C. E., Smart, C. C., Voogt, J. A., Hay, G. J., Lundholme, J. T., Powers, B., O’Carroll, D. M. (2016). Retention performance of green roofs in three different climate regions. *Journal of Hydrology* 542, 115–124. <https://doi.org/10.1016/j.jhydrol.2016.08.055>
- Soulis, K.X., Ntoulas, N., Nektarios, P. A., Kargas, G. (2017). Runoff reduction from extensive green roofs having different substrate depth and plant cover. *Ecological Engineering* 102, 80–89. <https://doi.org/10.1016/j.ecoleng.2017.01.031>
- Sparkman, S. A., Hogan, D. M., Hopkins, K. G., Loperfido, J.V. (2017). Modeling Watershed-Scale Impacts of Stormwater Management with Traditional versus Low Impact Development Design. *Journal of the American Water Resources Association (JAWRA)*, 1–14. <https://doi.org/10.1111/1752-1688.12559>
- Sperotto, A., Torresan, S., Gallina, V., Coppola, E., Critto, A., Marcomini, A. (2016). A multi-disciplinary approach to evaluate pluvial floods risk under changing climate: The case study of the municipality of Venice (Italy). *Science of the Total Environment* 562, 1031–1043. <http://dx.doi.org/10.1016/j.scitotenv.2016.03.150>
- Stovin, V., Vesuviano, G., Kasmin, H. (2012). The hydrological performance of a green roof test bed under UK climatic conditions. *Journal of Hydrology* 414–415, 148–161. <https://doi.org/10.1016/j.jhydrol.2011.10.022>
- Teegavarapu, R. S. V., Chandramouli, V. (2005). Improved weighting methods, deterministic and stochastic data-driven models for estimation of missing precipitation records. *Journal of Hydrology* 312 (1–4), 191–206. <https://doi.org/10.1016/j.jhydrol.2005.02.015>
- Todeschini, S., Papiri, S., Ciaponi, C. (2012). Performance of stormwater detention tanks for urban drainage systems in northern Italy. *Journal of Environmental Management* 101, 33–45. <https://doi.org/10.1016/j.jenvman.2012.02.003>
- Todorov, D., Driscoll, C. T., Todorova, S. (2018). Long term and seasonal hydrologic performance of an extensive green roof. *Hydrological Processes* 32(16), 2471–2482. <https://doi.org/10.1002/hyp.13175>
- Tutino, J., Melosi, M. V. (2019). *New World Cities, Challenges of Urbanization and Globalization in the Americas*. University of North Carolina Press.
- Vallebona, C., Pellegrino, E., Frumento, P., Bonari, E. (2015). Temporal trends in extreme rainfall intensity and erosivity in the Mediterranean region: a case study in southern Tuscany, Italy. *Climatic Change* 128, 139–151. <https://doi.org/10.1007/s10584-014-1287-9>
- Versini, P.A., Kotelnikova, N., Poulhes, A., Tchiguirinskaia, I., Schertzer, D., Leurent, F. (2018). A

distributed modelling approach to assess the use of Blue and Green Infrastructures to fulfil stormwater management requirements. *Landscape and Urban Planning* 173, 60-63. <https://doi.org/10.1016/j.landurbplan.2018.02.001>

Viero, D. P. Roder, G., Matticchio, B., Defina, A., Tarolli, P. (2019). Floods, landscape modifications and population dynamics in anthropogenic coastal lowlands: The Polesine (northern Italy) case study. *Science of the Total Environment* 651, 1435–1450. <https://doi.org/10.1016/j.scitotenv.2018.09.121>

Vieux, B.E. (2001). Distributed Hydrologic Modeling Using GIS. In: *Distributed Hydrologic Modeling Using GIS*. Water Science and Technology Library 38, Springer. https://doi.org/10.1007/978-94-015-9710-4_1

Thomas M. Walski, T. M. (2000). Model calibration data: the good, the bad, and the useless. *Journal American Water Works Association* 92(1), 94-99.

Wang, X., Tian, Y., Zhao, X., Peng, C. (2017). Hydrological performance of dual-substrate-layer green roofs using porous inert substrates with high sorption capacities. *Water Science Technology* 75 (12), 2829-2840. <https://doi.org/10.2166/wst.2017.161>

Woods Ballard, B., Wilson, S., Udale-Clarke, H., Illman, S., Scott, T., Ashley, R., Kellagher, R. (2015). *The SuDS Manual*. CIRIA.

Xu, C., McDowell, N.G., Fisher, R.A., Wei, L., Sevanto, S., Christoffersen, B.O., Weng, E., Middleton, R.S. (2019). Increasing impacts of extreme droughts on vegetation productivity under climate change. *Nature Climate Change* 9(12), 948-953. <https://doi.org/10.1038/s41558-019-0630-6>.

Zahmatkesh, Z., Karamouz, M., Goharian, E. Burian, S. J. (2014). Analysis of the Effects of Climate Change on Urban Storm Water Runoff Using Statistically Downscaled Precipitation Data and a Change Factor Approach. *Journal of Hydrologic Engineering* 20(7), 05014022. [https://doi.org/10.1061/\(ASCE\)HE.1943-5584.0001064](https://doi.org/10.1061/(ASCE)HE.1943-5584.0001064)

Zhang, K. and Chui, T.F.M. (2019). Linking hydrological and bioecological benefits of green infrastructures across spatial scales—A literature review. *Science of the Total Environment* 646, 1219-1231. <https://doi.org/10.1016/j.scitotenv.2018.07.355>

Zang, W., Liu, S., Huang, S., Li, J., Fu, Y., Sun, Y., Zheng, J. (2019). Impact of urbanization on hydrological processes under different precipitation scenarios. *Natural Hazards* 99, 1-25. <https://doi.org/10.1007/s11069-018-3534-2>

Zhou, Q. , Leng, G., Su, J., Ren, Y. (2019). Comparison of urbanization and climate change impacts on urban flood volumes: Importance of urban planning and drainage adaptation. *Science of The Total Environment* 658, 24-33. <https://doi.org/10.1016/j.scitotenv.2018.12.184>.